

THE UNIVERSITY OF MANITOBA

EFFECTS OF THERMAL GRADIENTS UPON
MASS TRANSPORT IN SOIL

by

CHI CHANG

A THESIS

SUBMITTED TO THE FACULTY OF GRADUATE STUDIES
IN PARTIAL FULFILMENT OF THE REQUIREMENTS FOR THE DEGREE
DOCTOR OF PHILOSOPHY

DEPARTMENT OF SOIL SCIENCE

WINNIPEG, MANITOBA

JANUARY, 1976

"EFFECTS OF THERMAL GRADIENTS UPON
MASS TRANSPORT IN SOIL"

by
CHI CHANG

A dissertation submitted to the Faculty of Graduate Studies of
the University of Manitoba in partial fulfillment of the requirements
of the degree of

DOCTOR OF PHILOSOPHY

© 1976

Permission has been granted to the LIBRARY OF THE UNIVER-
SITY OF MANITOBA to lend or sell copies of this dissertation, to
the NATIONAL LIBRARY OF CANADA to microfilm this
dissertation and to lend or sell copies of the film, and UNIVERSITY
MICROFILMS to publish an abstract of this dissertation.

The author reserves other publication rights, and neither the
dissertation nor extensive extracts from it may be printed or other-
wise reproduced without the author's written permission.

ACKNOWLEDGEMENTS

Sincere appreciation is extended to many organizations and individuals who supported my graduate study. In particular, I would like to express my appreciation to the following:

I am deeply grateful to my advisor, Dr. C.M. Cho, for his help throughout this study. Professor Cho generously shared his ideas and his personal contributions are many more than I am able to acknowledge in this page. Without his guidance and constant encouragement throughout the entire period of my study, helping me with patience and care in other matters than study, this research would not have been possible. Participation in several research projects with Dr. Cho provided excellent opportunities in gaining research experience.

Special thanks are due to my dissertation committee members, Dr. G.J. Racz and Dr. R.A. Hedlin, for their thoroughly and patiently going through from one draft to another and making important suggestions towards improvement. I am deeply indebted to them. Thanks are also due to Dr. C.F. Shaykewich, Associate Professor of Soil Physics, University of Manitoba, Dr. D.E. Elrick, Associate Dean of Graduate Studies, University of Guelph, and Dr. G.K. Yuill, Professor of Mechanical Engineering, University of Manitoba, for their careful reading of the dissertation and valuable suggestions.

Appreciation is also extended to Mr. L. Hordo for his efforts in obtaining field samples especially in the freezing cold winter and to the Provincial Soil Testing Laboratory of Manitoba for the use of their laboratory facilities.

I am grateful to the National Research Council, Faculty of Graduate Studies, University of Manitoba for their financial support, my graduate

study and Computer Centre, University of Manitoba for their providing computer funding.

Finally, a special thanks is extended to my wife, Mei-Huey to whom I am deeply indebted for her alert and excellent work in typing this dissertation and for her help in many other ways throughout this study and to my parents for their sacrifice and encouragement.

ABSTRACT

A field study of the movement of NO_3^- and Cl^- from surface applied $\text{Ca}(\text{NO}_3)_2$ and CaCl_2 was undertaken on Red River clay and Almasippi loamy sand. The downward movement of NO_3^- and Cl^- , the latter serving as a tracer for water movement, was quite small from application of the salt in July until April of the following year when the ground thawed. At that time NO_3^- and Cl^- moved to the water table.

The moisture contents of the soil profiles in the fields were found to be related to the soil temperature. The seasonal variation in the soil temperature at a fixed depth was found to be a typical cosine function. The amplitude of the cosine curve decreased with soil depth.

Laboratory investigations involved the study of water, NO_3^- and Cl^- movement in soil columns of different moisture contents incubated with and without a temperature gradient. Other factors studied included the effect of freezing one end of the column, reversal of temperature gradients, closed versus open columns and continuous columns as compared to those with an air gap.

In a closed continuous soil column with a temperature gradient but without freezing process, the movement of soil moisture was a circulation of soil water as a result of vapor condensation at the cold end and the return flow of liquid to the warm end. As the consequence of this circular movement the moisture accumulated at the cold end and salt concentrated at the warm end. The results obtained with discontinuous columns, in which the return flow of liquid was partially blocked, showed a similar concentration of salt near the warm end as was observed with continuous columns. It seemed, however, that the process of concentration of salt near the warm end of the soil column was due not only to the liquid water movement but also to the

Soret effect.

Both vapor and liquid forms of soil moisture moved to the frozen zone of soil columns. The rate of vapor movement was, however, greater than that of liquid water movement. The relative changes in Cl^- concentration based on soil solution and soil material in the frozen zone as compared to the initial values before subjecting to a temperature gradient were used in order to deduce the relative speed of vapor and liquid movement.

The distribution patterns of soil moisture, Cl^- and NO_3^- after thermal treatment in open soil columns were different from those observed in the closed columns. The position of maximum moisture content in the open column after subjecting to a temperature gradient was not located at the coldest end of the columns as was found in the closed column.

Reversing the direction of the thermal gradient during the period of thermal treatment, in order to simulate the freeze-up of the surface in fall and thawing from the surface in spring, resulted in an increase in salt transport to both ends of the soil column as compared to the column without such reversal treatment. The stability of the soil moisture in a system as governed by the direction of thermal gradients might be the cause of the increased salt transport.

A mathematical formulation for the simultaneous transport of vapor and liquid with condensation and vaporization under a thermal gradient in soil was carried out. Simultaneous partial differential equations for vapor and liquid transport in unsaturated soil columns were presented. Analytical or numerical solution of the differential equations could not be carried out.

TABLE OF CONTENTS

CHAPTER	PAGE
1. INTRODUCTION	1
2. LITERATURE REVIEW.....	4
2.1. Field Observation.....	4
2.2. Laboratory Investigation.....	7
2.2.1. Isothermal Mass Transport.....	7
2.2.2. Nonisothermal Mass Transport.....	17
3. THEORY.....	27
3.1. General Theory of Transport Phenomena.....	27
3.1.1. Equation of Continuity of Mass.....	27
3.1.2. Equation of Motion.....	29
3.1.3. Energy Transport Equation.....	29
3.1.4. Phenomenological relation.....	30
3.1.5. Momentum Transport.....	32
3.1.6. Mass Transport.....	35
3.2. Mathematical Development for Experimental Conditions	39
3.2.1. Equations of Mass Transport.....	39
4. MATERIALS AND METHODS.....	48
4.1. Field Experiment.....	48
4.2. Laboratory Experiment.....	50
4.2.1. Effect of Moisture and Salt Concentration on Mass Transport.....	53
4.2.2. Effect of the Freezing Process on Mass Transport	54
4.2.3. Effect of Different Geometrical Configurations on Mass Transport.....	54

CHAPTER	TABLE OF CONTENTS (Continued)	PAGE
	4.2.4. Effect of Air Gap Length and Position on Mass Transport.....	54
	4.2.5. Simulation of Natural Conditions.....	56
	4.2.6. Open System.....	56
	4.3. Determination of NO_3^- -N, NO_2^- -N, Cl^- and Water Content of Soil.....	58
5.	RESULTS AND DISCUSSION.....	59
5.1	Field Experiment.....	59
5.1.1.	1973 Almasippi Sandy Loam Soil Plot.....	59
5.1.2.	1974 Almasippi Sandy Loam Soil Plot.....	71
5.1.3.	Red River Clay Soil Plot.....	74
5.2.	Laboratory Experiments.....	79
5.2.1.	Effect of Moisture and Salt Concentration on Thermal Mass Transport.....	79
5.2.2.	Effect of Freezing Process on Mass Transport...	100
5.2.3.	Effect of Stability Configurations on Mass Transport.....	105
5.2.4.	Effect of Air Gap Length and Position on Mass Transport.....	110
5.2.5.	Simulation of Natural Conditions.....	121
5.2.6.	Open System.....	123
5.2.7.	General Discussion.....	127
6.	SUMMARY AND CONCLUSIONS.....	131
	BIBLIOGRAPHY.....	135
	APPENDIX A.....	147
	APPENDIX B.....	162
	APPENDIX C.....	166

LIST OF TABLES

TABLE	PAGE
1. Some characteristics of the soils.....	49
2. Some characteristics of Wellwood soil.....	51
3. Amount of precipitation and depth of salt penetration in 1973 Almasippi plot on various sampling dates.....	66
4. Soil temperature (C) of 1973 Almasippi plot at various depths on various sampling dates.....	67
5. Amount of precipitation and depth of salt penetration in 1974 Almasippi plot on various sampling dates.....	72
6. Amount of precipitation and depth of salt penetration in Red River clay plot on various sampling dates.....	77
7. Soil temperature (C) of Red River clay plot at various depths on various sampling dates.....	78
8. Saturated vapor pressure of water at various temperatures.	89
9. Vapor pressure of aqueous solutions of KCl.....	90
B1. Distribution of NO_3^- -N in check soil profile of Almasippi loamy fine sand plots.....	163
B2. Distribution of Cl^- in check soil profile of Almasippi loamy fine sand plots.....	164
B3. Distribution of NO_3^- -N in check soil profile of Red River clay plot.....	165

LIST OF FIGURES

FIGURE		PAGE
1.	Construction of closed soil column and air gap.....	52
2.	Construction of the open soil column.....	57
3.	Moisture, NO_3^- and Cl^- distribution in 1973 Almasippi plot from Oct. 15, 1973 to Nov. 28, 1973.....	60
4.	Moisture, NO_3^- and Cl^- distribution in 1973 Almasippi plot from Dec. 11, 1973 to Mar. 28, 1974.....	61
5.	Moisture, NO_3^- and Cl^- distribution in 1973 Almasippi plot from Apr. 17, 1974 to Jun. 10, 1974.....	62
6.	Moisture, NO_3^- and Cl^- distribution in 1973 Almasippi plot from Jun. 20, 1974 to Aug. 7, 1974.....	63
7.	Moisture, NO_3^- and Cl^- distribution in 1973 Almasippi plot from Aug. 26, 1974 to Dec. 19, 1974.....	64
8.	Moisture, NO_3^- and Cl^- distribution in 1973 Almasippi plot from Feb. 19, 1975 to Apr. 19, 1975.....	65
9.	Moisture, NO_3^- and Cl^- distribution in 1974 Almasippi plot from Jul. 11, 1974 to Aug. 26, 1974.....	73
10.	Moisture, NO_3^- and Cl^- distribution in 1974 Almasippi plot from Oct. 3, 1974 to Feb. 19, 1975.....	75
11.	Moisture, NO_3^- and Cl^- distribution in 1974 Almasippi plot on Apr. 19, 1975.....	76
12.	Moisture and NO_3^- distribution in Red River clay plot from Nov. 14, 1973 to Jun. 20, 1974.....	80
13.	Moisture and NO_3^- distribution in Red River clay plot from Jul. 4, 1974 to Oct. 2, 1974.....	81
14.	Moisture and NO_3^- distribution in Red River clay plot on Oct. 31, 1974.....	82
15.	Moisture and Cl^- distribution in $\text{Ca}(\text{NO}_3)_2$ and KCl -treated columns without temperature gradients (initial $\text{H}_2\text{O} = 27\%$ and $\text{KCl} = 10\%$).....	83
16.	Temperature distribution in soil columns with various initial moisture contents after 4 hours of thermal treatment.....	85

LIST OF FIGURES (Continued)

FIGURE		PAGE
17.	Moisture distribution in soil columns with or without air gap after 10 days of thermal treatment (no salt added)...	86
18.	Moisture characteristic curve of Wellwood clay loam at 22 C.....	88
19.	Moisture and Cl^- distribution in $\text{Ca}(\text{NO}_3)_2$ and KCl-treated columns after 10 days of thermal treatment (initial $\text{H}_2\text{O} = 27\%$).....	91
20.	Moisture and Cl^- distribution in $\text{Ca}(\text{NO}_3)_2$ and KCl-treated soil columns with or without gap after 5 or 20 days of thermal treatment (initial $\text{H}_2\text{O} = 27\%$ and KCl = 10%).....	94
21.	Moisture and Cl^- distribution in $\text{Ca}(\text{NO}_3)_2$ and KCl-treated soil columns with or without gap after 5 or 20 days of thermal treatment (initial $\text{H}_2\text{O} = 27\%$ and KCl = 20%).....	96
22.	Moisture and Cl^- distribution in $\text{Ca}(\text{NO}_3)_2$ and KCl-treated soil columns with or without gap after 10 days of thermal treatment (initial $\text{H}_2\text{O} = 32\%$).....	97
23.	Moisture and Cl^- distribution in $\text{Ca}(\text{NO}_3)_2$ and KCl-treated soil columns with or without gap after 5 or 20 days of thermal treatment (initial $\text{H}_2\text{O} = 32\%$ and KCl = 10%).....	98
24.	Moisture and Cl^- distribution in $\text{Ca}(\text{NO}_3)_2$ and KCl-treated soil columns with or without gap after 5 or 20 days of thermal treatment (initial $\text{H}_2\text{O} = 32\%$ and KCl = 20%).....	99
25.	Temperature distribution in soil columns with temperature gradients of -19 to 22 C (initial moisture contents: 27 and 32%).....	101
26.	Moisture and Cl^- distribution in $\text{Ca}(\text{NO}_3)_2$ and KCl-treated soil columns with a frozen end.....	103
27.	Direction of liquid water flow under the influence of thermal gradient for vertical and horizontal columns.....	106
28.	Moisture and Cl^- distribution in vertical and horizontal columns after 10 days of thermal treatment (initial $\text{H}_2\text{O} = 27\%$ and KCl = 10%).....	107
29.	Moisture and Cl^- distribution in vertical and horizontal columns with one frozen end (initial $\text{H}_2\text{O} = 27\%$ and KCl = 10%).....	109
30.	Moisture, Cl^- and temperature distribution in soil column with an open and frozen top end and with 0.5 cm air gap..	112

LIST OF FIGURES (Continued)

FIGURE		PAGE
31.	Temperature, moisture and Cl^- distribution in a discontinuous column with one frozen end and an 1-cm air gap (4 sections of dry soil).....	113
32.	Temperature, moisture and Cl^- distribution in soil column with an 1-cm air gap and frozen bottom end (initial $\text{H}_2\text{O} = 27\%$ and $\text{KCl} = 10\%$).....	115
33.	Hydraulic conductivity (K) and pF relation curve of Wellwood clay loam.....	117
34.	Pushing process in a closed system.....	118
35.	Pushing process in an open system.....	118
36.	Temperature, moisture and Cl^- distribution in soil column with a 2-cm air gap and a frozen bottom end (initial $\text{H}_2\text{O} = 27\%$ and $\text{KCl} = 10\%$).....	120
37.	Temperature, moisture and Cl^- distribution in soil column with frozen top end for first 10 days and frozen bottom end for second 10 days of thermal treatment.....	122
38.	Temperature, moisture and Cl^- distribution in soil column with an open top after 10 days of thermal treatment.....	124
39.	Temperature, moisture and Cl^- distribution in soil column with a frozen top end and open.....	126
A1.	Nitrate distribution in $\text{Ca}(\text{NO}_3)_2$ and KCl -treated soil columns without temperature gradients (initial $\text{H}_2\text{O} = 27\%$ and $\text{KCl} = 10\%$).....	148
A2.	Nitrate distribution in $\text{Ca}(\text{NO}_3)_2$ and KCl -treated soil columns after 10 days of thermal treatment (initial $\text{H}_2\text{O} = 27\%$).....	149
A3.	Nitrate distribution in $\text{Ca}(\text{NO}_3)_2$ and KCl -treated soil columns with or without gap after 5 or 20 days of thermal treatment (initial $\text{H}_2\text{O} = 27\%$ and $\text{KCl} = 10\%$).....	150
A4.	Nitrate distribution in $\text{Ca}(\text{NO}_3)_2$ and KCl -treated soil columns with or without gap after 5 or 20 days of thermal treatment (initial $\text{H}_2\text{O} = 27\%$ and $\text{KCl} = 20\%$).....	151
A5.	Nitrate distribution in $\text{Ca}(\text{NO}_3)_2$ and KCl -treated soil columns with or without gap after 10 days of thermal treatment (initial $\text{H}_2\text{O} = 32\%$).....	152

LIST OF FIGURES (Continued)

FIGURE		PAGE
A6.	Nitrate distribution in $\text{Ca}(\text{NO}_3)_2$ and KCl-treated soil columns with or without gap after 5 or 20 days of thermal treatment (initial $\text{H}_2\text{O} = 32\%$ and $\text{KCl} = 10\%$).....	153
A7.	Nitrate distribution in $\text{Ca}(\text{NO}_3)_2$ and KCl-treated soil columns with or without gap after 5 or 20 days of thermal treatment (initial $\text{H}_2\text{O} = 32\%$ and $\text{KCl} = 20\%$)	154
A8.	Nitrate distribution in $\text{Ca}(\text{NO}_3)_2$ and KCl-treated soil columns with a frozen end.....	155
A9.	Nitrate distribution in $\text{Ca}(\text{NO}_3)_2$ and KCl-treated soil columns after 10 days of thermal treatment (initial $\text{H}_2\text{O} = 27\%$ and $\text{KCl} = 10\%$).....	156
A10.	Nitrate distribution in vertical and horizontal soil columns with one frozen end (initial $\text{H}_2\text{O} = 27\%$ and $\text{KCl} = 10\%$).....	157
A11.	Nitrate distribution in soil column with an 1-cm air gap and frozen bottom end (initial $\text{H}_2\text{O} = 27\%$ and $\text{KCl} = 10\%$)..	158
A12.	Nitrate distribution in soil column with a 2-cm or 1-cm air gap and a frozen bottom end (initial $\text{H}_2\text{O} = 27\%$ and $\text{KCl} = 10\%$).....	159
A13.	Chloride distribution in soil column with top end frozen for first 10 days and bottom end frozen for second 10 days of thermal treatments.....	160
A14.	Nitrate distribution in soil column with an open top after 10 days of thermal treatment.....	160
A15.	Nitrate distribution in soil columns with an open and frozen top end and with or without gap (initial $\text{H}_2\text{O} = 27\%$ and $\text{KCl} = 10\%$).....	161

1 INTRODUCTION

Joffe (1949) defined soil as a natural body of mineral and organic constituents differentiated into horizons. Soil differs from the material below it in morphology, physical make up, chemical properties and composition, and biological characteristics. The definition fully embraces the non-equilibrium characteristics of soil. The temperature distribution within natural soil systems also follows the non-equilibrium characteristics of chemical composition and soil moisture. Moisture content, the presence of soluble substances and soil temperature are very important in governing plant growth and leaching or accumulation of soluble substances in the soil. These factors vary with plant growth and seasonal or diurnal fluctuations in atmospheric temperature and rainfall.

The soil moisture distribution in natural systems is never in equilibrium. The movement of soil moisture takes place within a soil profile. Movement induced by rainfall or evaporation from the soil surface is well known. The moisture moving downward after rainfall carries with it dissolved substances. The moisture moving upward accumulates the substances on the surface due to evaporation from the soil surface. Thus the direction and magnitude of soil moisture movement directly affects the movement of dissolved substances many of which are valuable plant nutrients. The movement of dissolved substances can also take place under uniform soil moisture conditions. This process is generally called diffusion.

A temperature gradient within a soil profile either directly or indirectly induces mass transport. The mechanism by which mass is

transported under a thermal gradient in soil is not fully understood. However, the mechanism seems different from convective or diffusive transport. Soil water may be present in vapor, liquid and solid phases while the transported substance of interest exists primarily in the liquid phase. The thermal gradient influences the movements of vapor, liquid and dissolved substances in different ways. In addition to influencing movement, the thermal gradient may also result in phase changes in soil moisture depending on local conditions. Because of varying solubilities of a substance in these phases, accumulation, depletion or exclusion of the substance may occur depending upon the magnitude of the phase change. Thus under a thermal gradient the movement of dissolved substances becomes very complicated.

In Manitoba, surface soil temperatures can range from about +30 to -35 C during a period of one year. The surface is the warmest part of the soil profile during the crop growing season. For more than half of the non-growing season, the surface soil is colder than lower horizons and frost may occur as deep as 1.5 meters. The transport phenomena that occur during the frozen period are not fully understood. The differences in NO_3^- -N content of soil profiles sampled in fall and spring indicates that movement of water and dissolved substances does take place in the soil during this period.

In order to investigate the mass transport that occurs during the fall to spring period, field and laboratory experiments were conducted. The field experiment was designed to determine the magnitude of transport of surface-applied $\text{Ca}(\text{NO}_3)_2$ and CaCl_2 both of which contain water soluble anions. The laboratory investigation was initiated in order to determine the relative speed and direction of liquid and vapor flow and the

movement of dissolved salt under a temperature gradient in a soil column.
A mathematical modelling approach was also attempted.

2 LITERATURE REVIEW

2.1 Field Observation

Water is one of the most important materials for crop growth. The amount of water used to produce 1.25×10^3 Kg/ha of wheat is 3.05×10^6 Kg/ha but 99% of this water is lost by evaporation and transpiration (Shaykewich 1974). Water not only supports plant turgidity but also acts as a medium for the transport of essential plant nutrients. The ability of a soil to supply water and nutrients to crops is an important factor in agricultural production.

The direction and magnitude of water and solute movement under natural field conditions is very complicated. This is partly due to the heterogeneous nature of soil, microclimatic change and differences resulting from the presence or absence of a growing crop. Many field investigations have involved the measurement and prediction of water and solute movement under very dry or very wet conditions. Generally Darcy's law or a modified form of Darcy's law was successfully applied to describe the soil moisture transfer process. Diffusion and convective transport equations were used to describe solute transfer in soil. In applying these equations, an isothermal assumption was generally made in order to describe the water and solute transport in soil. Field observations and the theory of mass transport under isothermal conditions have been reviewed by several workers. Infiltration of moisture into soil, the general application of flow theory in the field and the factors affecting the flow were reviewed by Parr and Bertrand (1960), Swartzendruber (1966), Nielsen et al. (1972) and Klute (1973). Solute transport associated with water movement was discussed by Nielsen and Biggar (1973). The presence or absence of a water table upon moisture transport was reviewed

by Raats and Gardner (1972).

Soil under natural conditions is not in a steady state with respect to temperature distribution. Seasonal and diurnal variations in atmospheric temperature affect the surface soil temperature. If the variation in the seasonal atmospheric temperature is expressed as a cosine wave then the soil temperature can be expressed by

$$T = T_0 + T_1 e^{-kx} \cos(\omega t - kx) \quad (1)$$

where T is the soil temperature, T_0 is the average yearly temperature of the soil surface, T_1 is the amplitude of the surface temperature wave, ω is the frequency, $k = (\omega/2\Lambda)^{1/2}$, Λ is the thermal diffusivity, t is time and x is the depth (Carslaw and Jaeger 1959). The equation expresses the fact that the surface temperature wave is transmitted downward with damping. The diurnal temperature change is also expressible by a cosine wave, so that an equation similar to the above can be applied to the diurnal change in soil temperature (Cary 1965). In the latter case, however, the change in soil temperature throughout the horizon due to seasonal variation was taken into account by adding a linear term. Field observations made by Smith (1932) indicated that diurnal fluctuations of soil temperature occurred to a depth of approximately 30 cm and seasonal fluctuations occurred below this depth. The maximum soil temperature gradient due to diurnal temperature variation was found to be 10 C cm^{-1} (Rose 1968a). These temperature variations were known to induce mass transport in soil. Lebedeff (1927) and Edlefsen and Bodman (1941) attributed the upward movement of moisture during the winter season to vapor transfer caused by the temperature gradient associated with the annual wave. Rose (1968 a,b) observed water movement in the field corresponded to the diurnal temperature change. He found that the direction

of liquid movement was upward through the profile even at suctions as low as 200 cm of water during both day and night. Water movement fluctuated in response to the diurnal temperature gradient with vapor moving downward at night time and upward during day time. At suctions greater than 5000 cm of water the predominant flow was in the vapor phase. He postulated a theory of mass transport due to a thermal gradient. However, the theory was found to be inadequate. He attributed this inadequacy to the assistance to vapor flux that can be provided by a discontinuous liquid phase. Jackson et al. (1973), during 16 days of measurement, observed a downward flux of soil moisture below 1 to 3 cm during several hours between sunrise and early afternoon. They concluded that there was soil water flux in the surface zone of a field subjected to diurnal variation. Soluble salts such as Cl^- also followed a diurnal pattern but out of phase with soil water during the first few days after irrigation in the 0 to 0.5 and 0 to 1 - cm depth increments. The diurnal amplitude of Cl^- , however, decreased with time as the soil progressively dried (Nakayama et al. 1973).

There are few field investigations concerning soil moisture transport during the winter period. Willis et al. (1961) detected no upward movement of soil water during the winter in North Dakota. However, in another study Willis et al. (1964) found that water table drop was associated with depth of frost. The drop was accompanied by an increase in soil moisture in the frost zone above the water table. Ferguson et al. (1964) found that an appreciable amount of water moved to the frozen zone in plots in which the unfrozen subsoil water was held at tensions less than about 2 atm.. They also noticed that water held at tensions of less than 5 atm. moved toward the frozen zone whereas soil water held by greater than 5 atm.

tension was not mobile toward the frozen zone. Sartz (1969), on the other hand, speculated that the frost was formed mainly by percolating water from the surface rather than by moisture transported from subsoil. He showed that water could readily infiltrate more than 60 cm of hard-frozen ground. However, he found that the frozen ground impeded percolation during spring melt.

2.2. Laboratory Investigation

Most laboratory studies were initiated to investigate the effects of hydraulic conductivity, soil-water characteristics, soil-salt reaction, salt-water interaction, temperature, temperature gradient and potential gradient upon water and salt movement. Movement under uniform temperature conditions is called isothermal mass transport and movement under the influence of a thermal gradient is known as nonisothermal mass transport.

2.2.1 Isothermal Mass Transport

Under constant temperature conditions, the description of mass transport is relatively simple and many studies have been conducted.

Darcy (1856) was the first scientist to derive an empirical mathematical formula to describe saturated water flow through a porous medium. This simple mathematical formulation is known as Darcy's law and is :

$$J = -KVh \quad (2)$$

where J is the total flux, K is the proportionality constant called the hydraulic conductivity and h is the hydraulic head.

Darcy's law was derived from observation of water flow through a sand. Olsen (1966) showed that this law was obeyed at low water gradients in saturated kaolinite over a wide range of porosities. Other studies (Fireman 1944; Low 1960; Olsen 1962, 1965) also showed support for

the application of Darcy's law to water flow in saturated clays. Lutz and Kemper (1959) showed that while Darcy's law was followed reasonably well for certain hydrogen - and calcium - saturated clays a positive deviation from Darcy's law was observed for other similar clays. It was also found that water flow in kaolinite and 50 per cent montmorillonite closely obeyed Darcy's law but this was not the case for 9, 30, and 40 per cent montmorillonite samples (Miller et al. 1969). Miller and Low (1963) reported the presence of a threshold gradient for water flow in clays. The threshold gradient decreased with decreasing clay content and increasing temperature. Even above the threshold gradient, they found the flow-hydraulic head relationship was curvilinear for samples of a high clay content at low gradients and for samples of a low clay content at any gradient. Swartzendruber (1962) found measured values for water flow exceeded that predicted by Darcy's law when sandy materials contained more than 5 per cent clay. Swartzendruber (1968) recalculated values for hydraulic conductivity, K , cited in the literature and found 2 to 4 fold variations in K to be fairly common with variability as high as 5 to 15 fold.

Factors which may account for differences between measured water flow and that predicted by Darcy's law has been discussed by several authors (Olsen 1966; Swartzendruber 1966,1968). Probable reasons for the deviations are : (1) the presence of a threshold gradient to initiate water flow and (2) increases in the hydraulic conductivity with increasing gradient. The tentative explanations of non-Darcian behavior are (1) quasi-crystalline water or modified water properties (Miller and Low 1963; Low 1961), (2) particle rearrangement (Micheals and Lin 1954; Martin 1962; Mitchell and Younger 1967), (3) electrokinetic effects or streaming

potential effects (Micheals and Lin 1954; Kemper 1960), (4) range in pore sizes (Miller and Low 1963; Olsen 1966), and (5) experimental errors (Olsen 1965,1966).

Most of the processes involving soil-water movement in the field, and in the rooting zone, occur while the soil is in an unsaturated condition. Unsaturated water movement is more complicated and difficult to describe quantitatively than saturated flow. The processes of unsaturated flow change with changing water content, suction, and conductivity, which may be affected by hysteresis. Most studies have been conducted to investigate if Darcy's law would describe unsaturated water flow. Many authors (Richards 1931; Kemper 1960; Miller and Low 1963; Swartzendruber 1963; Olsen 1965; Thames and Evans 1968; Miller et al. 1969) reported unsaturated water movement deviated from Darcy's law. Deviations of 8-fold between measured values and that predicted by Darcy's law have been observed by Abdel-Aziz and Taylor (1965), Rawlins and Gardner (1963) and Swartzendruber (1968). Many factors causing non-Darcian behavior of unsaturated water flow in soil have been suggested, but the extent of the contribution by each factor is not fully understood. Richards (1931) found that K in equation (2) is a function of temperature and moisture tension. Kemper (1960) suggested the resistance to flow caused by a streaming potential affected the value of hydraulic conductivity. Swartzendruber (1963) and Thames and Evans (1968) accounted for some of the discrepancies between theoretical and experimental data by empirically adjusting the theory to account for non-Darcian flow.

Darcy's law was modified by Richards (1931) in an attempt to describe unsaturated water flow. The modification included the provision that the conductivity be a function of the matric suction head. Darcy's

law, as modified by Richards (1931) can be rewritten

$$J = -K(\Gamma)\nabla h \quad (3)$$

where Γ is the matric suction. This formulation did not take into consideration the hysteresis effect of soil water (Miller and Miller 1956). Topp and Miller (1966) pointed out that the relationship between hydraulic conductivity and volumetric water content was affected by hysteresis to a much lesser extent than is the $K(\Gamma)$ function. Thus Darcy's law for an unsaturated soil can be expressed as

$$-J_1 = K(\theta)\nabla h \quad (4)$$

where θ is the volumetric water content of the soil. Many attempts have been made to develop equations for calculating hydraulic conductivity, $K(\theta)$, (Childs and Collis-George 1950; Marshall 1958; Millington and Quirk 1959, 1961; Kunze et al. 1968; Jackson et al. 1965; Green and Corey 1971). Reasonably accurate $K(\theta)$ values can be calculated for water contents as low as the wilting point for a large number of soil types provided that accurate soil water characteristic curves are available.

The concept of treating soil water movement as a diffusion phenomenon was proposed by Childs (1945) and Childs and Collis-George (1950). A partial differential equation describing liquid-phase water movement in a porous medium was proposed by Childs and Collis-George (1950)

$$J_1 = -D(\theta) \frac{\partial \theta}{\partial x} \quad (5)$$

where they defined diffusivity, $D(\theta) = K(\theta) dh/d\theta$. The flux and force relation, equation (5), was then combined with the equation of continuity.

Thus,

$$\frac{\partial \theta}{\partial t} = \frac{\partial}{\partial x} \left(D(\theta) \frac{\partial \theta}{\partial x} \right) \quad (6)$$

was used to describe horizontal water movement and

$$\frac{\partial \theta}{\partial t} = \frac{\partial}{\partial x} \left(D(\theta) \frac{\partial \theta}{\partial x} \right) + \frac{\partial K(\theta)}{\partial x} \quad (7)$$

was used to describe vertical water flow. Later Klute (1952) derived similar equations using a different method of derivation. Equations (6) and (7) are valid only when diffusivity is a unique function of moisture content. Gardner and Mayhugh (1958) found that the relation between $D(\theta)$ and water content could be approximated by the empirical equation

$$D(\theta) = ae^{b\theta} \quad (8)$$

where a and b are constants. The empirical relation equation (8) is known as the exponential diffusivity function. This equation does not adequately estimate diffusivity for very dry soils probably due to the contribution of vapor movement. Hallaire and Henin (1958) questioned the validity of equations (6) and (7) to describe unsaturated flow. Since the diffusivity, D , is not a unique function of moisture content, it exhibits hysteresis which is caused by water hysteresis (Topp and Miller 1966). Diffusivity is also a function of moisture gradient (Swartzendruber 1963), soil texture (Philip 1957), the solute concentration, and ionic composition (Reeve 1960; McNeal and Coleman 1966; Rhoades and Ingvalson 1969; Yaron and Thomas 1968).

The solutions to equations (6) and (7) for infiltration and redistribution have been sought using both analytical and numerical techniques for several boundary and initial conditions. A numerical solution for water infiltration into a loam over a silt loam soil and vice versa was obtained by Hanks and Bowers (1962). Rubin and Steinhardt (1963) obtained a numerical solution for infiltration of rain into soil. Some digital computer solutions for two dimensional transient flows have also been reported (Hornberger et al. 1969; Taylor and Luthin 1968; Rubin 1968). Other

numerical solutions based on different boundary conditions were provided by Klute (1952), Day and Luthin (1956), Rubin and Steinhardt (1964), Whisler and Klute (1965), Freeze (1969), Rubin (1968) and Staple (1966). It is difficult to make general conclusions from these numerical solutions. However, due to the more general availability of high-speed digital, analog and digital-analog computers and improved numerical methods, a more general and practical numerical solution for the equations of flow is likely to be developed. On the other hand analytical solutions, even if they are based upon simplifying assumptions, have the advantage of showing the structure of the flow and its dependence upon parameters characterizing the soil. Approximations such as the use of a weighted mean diffusivity to obtain the inflow or outflow behavior of water in a soil column (Gardner 1969, 1962; Doering 1965) or the assumptions that the water content in a drying soil column is dependent upon time and not on its position (Gardner and Hillel 1962), and the assumption that the soil is uniform and under a unit hydraulic gradient (Black et al. 1969; Davidson et al. 1969) have been successfully used to obtain solutions for particular flow problems. An extensive summary of various solutions based on various boundary conditions has been presented by Kirkham and Powers (1972).

Vapor transfer under isothermal conditions is minimal. However, in relatively dry soil vapor flow is probably the controlling mechanism (Jackson 1964a, 1964b; Rose 1963a, 1963b). Vapor flow can be expressed by Fick's law with the gradient of the water vapor density being the driving force.

$$J_v = - D_v \nabla \rho_v \quad (9)$$

where J_v is the vapor flux, D_v is the diffusivity of vapor and $\nabla \rho_v$ is the

vapor gradient. By assuming that changes in liquid water with time are much greater than vapor density changes with time Jackson (1964a) obtained the equation,

$$\frac{\partial \theta}{\partial t} = \frac{\partial}{\partial x} \left(D_v \frac{\partial \rho_v}{\partial \theta} \frac{\partial \theta}{\partial x} \right) \quad (10)$$

for non-steady vapor transfer in terms of soil water content, θ . Rose (1965) proposed an equation for simultaneous liquid and vapor transfer

$$J_w = -K_w \nabla h \quad (11)$$

where J_w , the total water flux is equal to liquid flux plus vapor flux, $(J_l + J_v)$, the total hydraulic conductivity, K_w , is equal to the vapor hydraulic conductivity plus liquid hydraulic conductivity, $(K_l + K_v)$, and h is the hydraulic head. More recently an equation has been suggested for non-steady state simultaneous liquid and vapor transfer (Nielsen et al. 1972)

$$\frac{\partial \theta}{\partial t} = \frac{\partial}{\partial x} \left(D_{\theta v} \frac{\partial \theta}{\partial x} \right) \quad (12)$$

where the combined diffusion coefficient for liquid and vapor is

$$D_{\theta v} = D_v \frac{\partial \rho_v}{\partial \theta} + D_\theta \quad (13)$$

Dissolved salts tend to move simultaneously with soil water either by diffusion or convection or by both processes. Diffusion is due to a concentration gradient of dissolved salt and convection is caused by mass flow of soil solution. The processes of diffusion and convection can occur simultaneously, either in the same or opposite directions. The magnitude and direction of salt movement are affected by (1) the concentration and concentration gradient of salts in the soil solution, (2) the direction and rate of movement of the soil solution, (3) soil texture and structure (Thomas 1970; Olsen et al. 1965; Kissel et al. 1973), (4) the degree of interaction between salt and soil particles as affected by factors such as soil cation exchange capacity (Thomas and Swoboda 1970;

Dyer 1965) and (5) the rate of net production of the salt.

Diffusion is the predominant process for salt movement if there is no convection. Fick (Crank 1967) quantitatively described the diffusion process by adopting the mathematical equation of heat conduction derived some years earlier by Fourier. The mathematical expression of diffusion in a medium was described by the equation:

$$J_m = - D \frac{\partial C_m}{\partial x} \quad (14)$$

where J_m is the diffusion flux of a substance, D is the diffusion coefficient, C_m is the concentration of diffusive material, and x is the space variable.

Diffusion of dissolved salt takes place mainly in the soil solution. Thus, the rate of diffusion or flux in soil is a function of the degree of saturation of the soil with moisture (Klute and Letey 1958; Porter et al. 1960). Fick's law, modified for moisture content, is

$$J_m = - D\theta \frac{\partial C_m}{\partial x} \quad (15)$$

where θ is the volumetric moisture content. The magnitude of the diffusion coefficient, D , is generally smaller in soil than in bulk water.

Van Schaik and Kemper (1966) introduced the pore width factor, γ , the viscosity factor, α , and the tortuosity factor, $(L_x/L_e)^2$, into the diffusion equation. Equation (15) modified for the above factors, was written as:

$$-J_m = D\theta \left(\frac{L_x}{L_e} \right)^2 \gamma \alpha \frac{\partial C_m}{\partial x} = D_\rho \frac{\partial C_m}{\partial x} \quad (16)$$

where L_x is the distance between two points, L_e is the acute distance through which the ions diffuse and D_ρ is equal to $D(L_x/L_e)^2 \theta \gamma \alpha$ (Porter et al. 1960; Van Schaik and Kemper 1966). Combining equation (16) with equation of continuity resulted in

$$\frac{\partial C_m}{\partial t} = D_\rho \frac{\partial^2 C_m}{\partial x^2} \quad (17)$$

where D_{ρ} , the apparent diffusivity, was assumed to be a constant (Philip and Brown 1964; Olsen and Kemper 1968). Numerous soil properties such as bulk density, water content (Graham-Bryce 1963; Klute and Letey 1958; Romkens 1964; Brown 1953; Kemper et al. 1964; Olsen et al. 1962; Porter et al. 1960; Biggar and Nielsen 1967; Jackson 1973), texture, kind and amount of clay (Lai and Mortland 1961; Olsen and Watanabe 1963), interaction of water and soil particles (Olsen and Watanabe 1963; Olsen et al. 1965), soil compaction (Philip and Brown 1965) tortuosity (Porter et al. 1960; Van Schaik and Kemper 1966), negative adsorption (Van Schaik and Kemper 1966), and ion size and charge (Shainberg and Kemper 1966a,b) were shown to affect D_{ρ} . A detailed review on this topic has been presented by Olsen and Kemper (1968). Due to the requirement of electrical neutrality, diffusion of anions must be accompanied by cations or counter diffused by other anions. Therefore the properties and concentrations of counter diffusing or codiffusing ions also affect the diffusion process. The apparent diffusion coefficient for an ion is the average of the separate diffusion coefficients of two or more ions. Jost (1952) expressed the apparent diffusion coefficient, D_{12} , for a two ion system as:

$$D_{12} = \frac{D_1 D_2 (Z_1 C_1 + Z_2 C_2)}{Z_1 C_1 D_1 + Z_2 C_2 D_2} \quad (18)$$

where Z is the valence of the ions and the subscripts 1 and 2, refer to the ionic species. The solutions for the diffusion equations for various boundary conditions have been given by Jost (1952) and Crank (1967).

Under normal field conditions liquid water always tends to flow. Liquid water moving in soil will carry dissolved salts along with it and diffusion processes may take place simultaneously. The simultaneous

diffusion and convection processes were described by

$$\frac{\partial C_i}{\partial t} = -v \cdot \nabla C_i + D \nabla^2 C_i \quad (19)$$

where C_i is the concentration of component i , v is the center of mass velocity and D is the apparent diffusion coefficient. This equation was presented by Scheidegger (1954) and first introduced into soil literature by Day and Forsythe (1957). Equation (19) can be transformed into a form of a diffusion equation by substitution. This has been shown by Cho (Kirkham and Powers 1972) and the solutions for the equation can be obtained.

The velocity distribution of water flow and the concentration of salt within pores and sequences are not uniform. This nonuniform velocity phenomenon is known as hydrodynamic dispersion. This dispersion process can enhance the diffusion process. The apparent diffusion coefficient, called the dispersion coefficient, is a function of flow velocity and tends to increase with increasing flux (Nielsen and Biggar 1963, 1967; Scheidegger 1963; Taylor 1953). Anion exclusion introduces anisotropy and factors such as ion exchange and hydration also affect the solute dispersion coefficient (Nielsen and Biggar 1961, 1962; Day 1956; Berg and Thomas 1959; Mokady et al. 1958; Mokady and Bresler 1968; Bresler 1973; Krupp et al. 1972).

The dissolved salts are subjected to reactions in soil such as transformation, fixation, plant uptake, exchange, precipitation, and chelation. Some of these reactions are purely chemical reactions and some are the result of biological activities. Some reactions increase the salt concentration in the soil solution whereas some reactions remove salt from the soil solution. The chemistry of ions in soil is a very complicated process. The mathematical formulation for simultaneous processes of diffusion,

convection and chemical reaction of an ion was expressed as:

$$\frac{\partial C_i}{\partial t} = v \cdot \nabla C_i + D \nabla^2 C_i + \phi_i \quad (20)$$

where ϕ_i is the chemistry term used to describe soil-ion interactions (Fitts 1962; de Groot 1952; Crank 1967). Few studies have been done on this subject because the chemistry of ions in soil is not fully understood. The theoretical analysis and the analytical solution of equation (20) for nitrogen movement with nitrification and adsorption has been studied by Cho (1971) using first order reaction kinetics. Other authors (Lapidus and Amundson 1952; Oddson et al. 1970) assumed that the chemistry was a reversible reaction and also obtained solutions for equation (20). Laboratory studies conducted by Musa (1968), Carter et al. (1967), Erh et al. (1971), Overrein (1968, 1969), Meek et al. (1970) and Stewart et al. (1967) showed that nitrogen transformations greatly affected the convective transport of nitrogen in soil.

2.2.2 Nonisothermal Mass Transfer

The first evidence, obtained in laboratory studies, of soil moisture movement induced by a thermal gradient was provided by Bouyoucos (1915). He found a net transfer of moisture from warm to cold regions. The results of numerous observations and investigations of the effects of thermal gradients upon mass transfer have been reported periodically since then (Moore 1940; Smith 1944; Gurr et al. 1952; Taylor and Cavazza 1954; Hutcheon 1958; Anderson and Linville 1960; Jackson et al. 1965; Weeks et al. 1968; Cassel et al. 1969; Westcot and Wierenga 1974; Field-Ridley 1975).

Soil moisture may flow in either liquid or vapor phase or simultaneously in both phases under nonisothermal conditions. Various methods have been employed to study the relative magnitude of water transfer in the

liquid and vapor phases. One such method consists of inserting an air gap and labelling the liquid with inert ions. Bouyoucos (1915) was the first to attempt to segregate liquid and vapor flow characteristics by dividing a soil column into two parts with an air gap. He found that water flow was largely in the liquid phase. Winterkorn (1947) also considered that film flow of liquid water from the warm to the cold end was a more important mechanism than vapor flow. Smith (1940) criticized Bouyoucos' work on the basis that the temperature gradient affected only a small part of a soil column with an air gap. Maclean and Gwatkin (1946) and Jones and Kohnke (1952) showed that thermal transport of moisture occurred largely in the vapor phase. Smith (1944) conducted an experiment and found that moisture movement under the influence of a temperature gradient was due to a cyclical process of vapor condensation and local capillary flow.

Gurr et al. (1952) assumed that the movement of the Cl^- ion in soil was due solely to liquid water convection. They labelled the soil column uniformly with a small amount of Cl^- salt to evaluate the magnitude of liquid flow by measuring the redistribution of Cl^- after having subjected the soil column to a thermal gradient. It was found that there was a net transfer of moisture from the warmer to the colder end and Cl^- moved from the colder end to the warmer end. They concluded that water from the warmer region moved as vapor into the colder end where it condensed and then returned as liquid to the warmer region. By using the Cl^- ion as a liquid flow indicator Weeks et al. (1968), Jackson et al. (1965) and Hutcheon (1955) also concluded that soil moisture movement in a closed container under a thermal gradient was a circular convection process. Taylor and Cavazza (1954) employing a segment technique and

Rollins et al. (1954) also arrived at the same conclusion as Gurr et al. (1952) for a closed soil column. Thermal diffusion of Cl^- in soil, if any, was neglected in arriving at the above conclusion since the magnitude of thermal diffusion of many Cl^- salts in pure water was very small (Fitts 1962 and de Groot 1952). The magnitude of soil water movement was found to be dependent upon initial water content, bulk density, temperature gradient and mean temperature. An initial soil water content of one third of moisture equivalent was found to have maximum moisture transfer (Gurr et al. 1952; Hutcheon 1955). Studies by MacLean and Gwatkin (1946) and Hutcheon (1955) showed that the net movement of moisture was markedly influenced by the bulk density of soil. The net movement of soil moisture tends to increase with increasing temperature gradient and increasing average temperature.

Various theoretical analyses have been proposed to describe moisture transfer under the influence of a thermal gradient. All of these theories can be divided into two groups. The first group can be represented by the studies conducted by Philip and de Vries (1957) and Dirksen (1969). The second group is based on the theory of irreversible thermodynamics (Taylor and Cary 1960, 1964; Cary and Taylor 1962a,b; Cary 1965; Bolt and Groenevelt 1967; Joshua and de Jong 1973; Kay and Groenevelt 1974; Groenevelt and Kay 1974).

Philip and de Vries (1957) developed a theory for simultaneous heat and water transfer in porous media under a temperature gradient. They considered that vapor and liquid water movement were independent and that there was no interaction between the two during the course of movement. Vapor and liquid movement were treated separately. They modified the simple vapor transfer theory by considering the vapor density to be a

function of saturated vapor density and relative humidity. The vapor density gradient was expressed as

$$\nabla \rho = H \nabla \rho_0 + \rho_0 \nabla H \quad (21)$$

where ρ is the vapor density, H is the relative humidity and ρ_0 is the saturated vapor density. Furthermore, they assumed that the saturated vapor density was a function only of temperature (T) and that the relative humidity was a function only of volumetric moisture content, (θ).

Thus,

$$\nabla \rho = H \frac{d\rho_0}{dT} \nabla T + \rho_0 \frac{dH}{d\theta} \nabla \theta \quad (22)$$

By using this relation and the simple vapor diffusion equation they obtained

$$J_{\text{vap}} \frac{\rho}{\rho_w} = - D_{T \text{ vap}} \nabla T - D_{\theta \text{ vap}} \nabla \theta \quad (23)$$

where J_{vap} is the vapor flux, ρ_w is the water density, $D_{T \text{ vap}}$ is the thermal vapor diffusivity and $D_{\theta \text{ vap}}$ is the ordinary vapor diffusivity. Thus vapor flux was separated into two components, that due to the temperature gradient and that due to the moisture gradient. Considering that the water potential was a function of temperature and water content they obtained liquid flux as

$$\frac{J_{\text{liq}}}{\rho_w} = - D_{T \text{ liq}} \nabla T - D_{\theta \text{ liq}} \nabla \theta \quad (24)$$

where J_{liq} is the liquid flux and $D_{T \text{ liq}}$ and $D_{\theta \text{ liq}}$ are the thermal liquid diffusivity and ordinary diffusivity of water, respectively. They derived the total flux of water by summing the individual fluxes. The equation, after substitution into the continuity relation was:

$$\frac{\partial \theta}{\partial t} = \nabla \cdot (D_T \nabla T) + \nabla \cdot (D_\theta \nabla \theta) \quad (25)$$

where D_T , the thermal water diffusivity, is equal to $D_{T \text{ vap}} + D_{T \text{ liq}}$ and D_θ , the ordinary diffusivity, is equal to $D_{\theta \text{ vap}} + D_{\theta \text{ liq}}$. The heat conduction equation was:

$$C \frac{\partial T}{\partial t} = \nabla \cdot (\lambda \nabla T) - LV \cdot (D_{\theta \text{ vap}} \nabla \theta) \quad (26)$$

where C is the volumetric heat capacity of the soil, λ , the thermal conductivity, is equal to $D_{\text{vap}} L \rho_w$, L is the latent heat of water vaporization and T is the temperature.

Philip and de Vries (1957) attributed the high apparent vapor transfer to the contribution of 'liquid islander' to the vapor movement and to a higher average temperature gradient in pores than the apparent thermal gradient. It is interesting to note that they did not consider the rate of vaporization nor condensation in developing the liquid transport equation.

Taylor and Cary (1960) attempted to develop a theory of soil water movement under a thermal gradient based on the theory of irreversible thermodynamics. Their application of the theory was rudimentary. Later, Taylor and Cary (1964) applied the theory of irreversible thermodynamics to a closed soil system under a continuous thermal gradient. They assumed that the center of mass of the system was fixed with the solid matrix which was used as a reference for measuring flow velocities. A set of equations was obtained for describing simultaneous heat and mass transport:

$$J_i = \sum_{k=1}^n \Omega_{ik} \left\{ \chi_k - T \left(\frac{d(\frac{\mu_k}{T})}{dz} \right)_T \right\} - \Omega_{iq} \frac{d \ln T}{dZ} \quad (27)$$

$$J_q = \sum_{k=1}^n \Omega_{qk} \left\{ \chi_k - T \left(\frac{d(\frac{\mu_k}{T})}{dz} \right)_T \right\} - \Omega_{qq} \frac{d \ln T}{dZ} \quad (28)$$

where J is the flux, Ω is the phenomenological coefficient, μ is the

chemical potential, i and k are for components i and k , q is the heat and X is the external force. Furthermore they assumed that water was the only flowing matter, that the chemical potential of water was a single valued function of water content and that gravitational force was the only external force. Under isothermal conditions equation (27) was expressed as:

$$J_w = - \Omega_{ww} \frac{d\psi}{dz} \quad (29)$$

where ψ is the total water potential. They claimed that equation (29) is similar to Darcy's law (4). Nielsen et al. (1972) have extensively reviewed the work done by Taylor and Cary (1960, 1964), Cary and Taylor (1962a,b) and Cary (1963, 1964, 1965, 1966) on the application of irreversible thermodynamics to mass and heat transfer in soil. In most of the studies the authors claimed that the Onsager's reciprocal relationship held in their system. Cary and Taylor (1962a) showed the Onsager's reciprocal relation held for vapor and heat transfer but that the vapor flux equation was not adequate to describe moisture movement in their system. In a later paper Cary and Taylor (1962b) extended the flux equation to describe both liquid and vapor transfer. The rate equations were then tested and found to give reliable predictions of water and energy flow through soil. The interaction coefficient also agreed with the Onsager's reciprocal relation. Cary (1965) separated the flow into liquid and vapor flow components and further divided the liquid component into that flowing due to pressure and thermal differences. His flow equation, based on irreversible thermodynamics, predicted fluxes in agreement with his experimental observations. Joshua (1971) and Joshua and de Jong (1973) showed that the Onsager's reciprocal relation held for their system. Kay and Groenevelt (1974) and Groenevelt and Kay (1974) derived heat and water

transport equations in frozen and unfrozen soil for both vapor and liquid phases and they claimed that they had theoretically proved the Onsager's reciprocal relation. Cassel and his co-workers (1969), on the other hand, calculated their data by using the theory of Philip and de Vries (1957), Fick's law, and the theory of Taylor and Cary (1964). They found that the theory of Philip and de Vries gave the best agreement with their observations. Fick's law and Taylor-Cary's equations underestimated the observed flux. Matthes and Bowen (1963) modified Fick's first law by substituting the relationship between temperature and vapor pressure for the pressure gradient. They used the equation to predict vaporization and condensation at various points in the soil column during the course of vapor transfer under a temperature gradient. They assumed that the relative humidity was near 100 per cent throughout the soil column.

The term 'thermo-osmosis' is frequently used to describe liquid flow under a thermal gradient. For saturated Na-kaolinite thermo-osmosis was found to increase with increasing temperature gradient and compact pressure (Dirksen 1969). In the case of saturated Na-bentonite thermo-osmosis decreased with increasing average temperature but did not change with changes in thermal gradient (Dirksen 1969). He also observed that thermal water flow occurred from the warm to the cold side.

According to the experimental results obtained by various workers, liquid, vapor, and solute all moved from the warm to the cold end during the early stages of thermal treatment. After the hydraulic pressure was built up liquid water along with solute returned to the warm end while vapor continued to move to and condense at the cold end in a closed soil column.

The presence of the ice phase in a porous medium greatly increases

the amount of mass transfer under temperature gradients and alters considerably the process of moisture and solute movement. Water moves from unfrozen soil into frozen soil (Dirksen and Miller 1966; Hutcheon 1958; Field-Ridley 1975; Globus 1962; Hoekstra and Chamberlain 1964; Hoekstra 1966, 1969) and the solute is transmitted in the same direction (Field-Ridley 1975). In a completely frozen soil column, Cary and Mayland (1973) found that both water and solute moved from warmer to cooler ends. Dirksen and Miller (1966) and Hoekstra (1966) showed that a great deal of water accumulated in the frozen zone and the accumulation increased with time. The change in the moisture content within the frozen soil was too great and too rapid to be explained by thermal vapor diffusion alone. They suggested that liquid moved through an adsorbed continuous unfrozen water film. The existence of continuous unfrozen water phase in frozen soil has been established by many workers (Anderson 1966, 1967; Anderson et al. 1973; Bouyoucos 1916; and Williams 1964a,b). The thickness of such a film in frozen soil evidently decreases with temperature (Anderson et al. 1973). Thus the rate of flow of liquid water decreases rapidly with a decrease in temperature below 0 C.

Water moves toward the region where ice is forming because the ice phase serves as a sink for liquid water present in the frozen soil, which then imbibes water from the unfrozen soil. This in turn produces a water content gradient in the unfrozen soil. The results obtained by Hoekstra (1966) showed a sharp decrease in water content of unfrozen soil toward the frozen soil. Dirksen and Miller (1966) believed that the flow in the unfrozen soil was not a direct consequence of the temperature gradient in the unfrozen soil but was mainly a result of the events taking place in the frozen part of the column, which created a hydraulic gradient in the

unfrozen soil. They also believed that when ice ceases to form and a steady state has been attained the temperature gradient is responsible for any further movement of water in the unfrozen soil. Cary and Mayland (1972) reported that in frozen soil, moisture flow in the liquid phase followed Darcy's law. However, Anderson and Hoekstra (1965) found liquid transport in frozen soil was due to electrical potential gradients.

Hoekstra (1966) discussed the forces that drive the water into frozen soil in terms of thermodynamic theory. In an unfrozen soil the chemical potential of soil water is a direct function of moisture content, and decreases with water content. Thus if a temperature gradient is placed across a soil column and the temperature of the cold plate is higher than the freezing temperature, a steady state moisture content will be reached. On the other hand, in a frozen soil the chemical potential of ice is independent of the presence of soil. Thus the amount of ice can increase without affecting the amount of unfrozen water and no equilibrium moisture content can be reached.

Ice crystals freeze out of a solution in a relatively pure state. The majority of soluble salts are excluded from frozen water and concentrated in the unfrozen water films and may form relatively high-concentration brines. A twofold concentration difference over a 24 cm distance was found in Cary and Mayland's (1972) experiment. Their results suggested that mass flow of dissolved salts in a liquid film of water was the principal transfer mechanism even vapor and salt diffusion were sometimes significant. They believed that during the frozen period, the salt and water may have moved somewhat independently.

The effects of initial water content and soil texture upon mass

transfer under a temperature gradient with the cold end below freezing temperature was studied by Field-Ridley (1975). She found initial soil water content affected moisture redistribution in a clay soil. The wetter soil columns (above field capacity) showed a moisture content gradient in the unfrozen portion which was not present in the drier soil columns (field capacity). Ice accumulation in the frozen zone appeared to be smaller at higher than at lower moisture contents. The percentage of moisture transferred from unfrozen to the frozen zone was also smaller at the higher moisture content. Nitrate was used as a tracer in this study. In the frozen zone she found a high NO_3^- concentration on a dry soil basis but a low NO_3^- concentration in the soil solution. The high NO_3^- concentrations on a soil weight basis was attributed to liquid transport whereas the low concentration in the soil solution was due to vapor transport. This dilution was greatest at the point of maximum ice accumulation, indicating that the contribution of vapor transport was in excess of that of liquid transport. Internal convection of soil moisture was demonstrated by some of her results.

The mathematical formulation and a numerical solution of heat and mass transport for a partially frozen soil have been attempted by Harlan (1973).

3 THEORY

3.1 General Theory of Transport Phenomena

Pure isothermal viscous flow can be described by the equations of mass and momentum transport. In the case of nonisothermal fluid flow an additional equation is needed to describe the transport of energy.

Consider any extensive property B of a system, for example, the mass, the momentum, the energy, etc. Associated with the quantity B is a specific quantity b, defined as B per unit mass. The general conservation equation is developed by balancing any property B over a stationary volume element, dV , through which the fluid is flowing.

$$\left[\begin{array}{c} \text{rate of B} \\ \text{accumulation} \end{array} \right] = \left[\begin{array}{c} \text{Rate of B} \\ \text{influx} \end{array} \right] - \left[\begin{array}{c} \text{Rate of B} \\ \text{outflux} \end{array} \right] + \left[\begin{array}{c} \text{Rate of B} \\ \text{production} \end{array} \right] \quad (30)$$

The mathematical expression of equation (30) is

$$\int_V \frac{\partial}{\partial t} (\rho b) dv = - \int_A \vec{J}_b \cdot d\vec{A} + \int_V \phi_b dv \quad (31)$$

where ρ is the mass density, V is the volume, A is the area, J_b , the flux of B, is equal to $\rho v'b$, ϕ_b is the production of B and v' is the velocity of the flow medium. After applying the Gauss theorem equation (31) can be written as:

$$\int_V \left\{ \frac{\partial}{\partial t} (\rho b) + \nabla \cdot J_b - \phi_b \right\} dv = 0 \quad (32)$$

where ∇ is the gradient operator. Equation (32) is valid only when

$$\frac{\partial}{\partial t} (\rho b) + \nabla \cdot J_b - \phi_b = 0 \quad (33)$$

This is the general conservation equation.

3.1.1 Equation of Continuity of Mass

Equation (33) can now be applied to obtain the mass continuity equation for component i in the fluid system. Thus the equation of continuity of mass for component i is

$$\frac{\partial \rho_i}{\partial t} + \nabla \cdot (\rho_i v_i) = \phi_i \quad \text{or} \quad \frac{\partial \rho_i}{\partial t} + \nabla \cdot J_i = \phi_i \quad (34)$$

where ρ_i is the density of component i , v_i is the linear velocity of component i , J_i is the flux of component i and is equal to $\rho_i v_i$, and ϕ_i is the rate of internal production of component i in a volume element. By summing all the mass components, we obtain the equation of continuity for the total mass of the system.

$$\frac{\partial \rho}{\partial t} + \nabla \cdot (\rho v) = 0 \quad \text{or} \quad \frac{\partial \rho}{\partial t} + v \cdot \nabla \rho + \rho \nabla \cdot v = 0 \quad (35)$$

where ρ , the mass density, is equal to $\sum_{i=1}^n \rho_i$ and v , the centre of mass velocity, is equal to $(\sum_{i=1}^n \rho_i v_i) / \rho$. The sum of total internal production of mass is equal to zero, i.e.

$$\sum_{i=1}^n \phi_i = 0 \quad (36)$$

If the time derivative is changed to the substantial derivative, equation (35) becomes

$$\frac{d\rho}{dt} + \rho \nabla \cdot v = 0 \quad (37)$$

The diffusive flux, j_i , of component i with respect to the centre of mass velocity is

$$j_i = \rho_i (v_i - v) = J_i - \rho_i v$$

and equation (34) can be rewritten

$$\left. \begin{aligned} \frac{\partial \rho_i}{\partial t} + v \cdot \nabla \rho_i + \rho_i \nabla \cdot v + \nabla \cdot j_i &= \phi_i \\ \text{or} \\ \frac{d\rho_i}{dt} + \nabla \cdot j_i + \rho_i \nabla \cdot v &= \phi_i \end{aligned} \right\} (38)$$

For incompressible viscous flow

$$\nabla \cdot v = 0 \quad (39).$$

The equation of continuity of mass for component i under incompressible flow becomes

$$\frac{\partial \rho_i}{\partial t} + \nabla \cdot j_i = \phi_i \quad (40).$$

For total mass flow it becomes

$$\frac{d\rho}{dt} = 0 \quad (41).$$

3.1.2 Equation of Motion

If the property B represents the total momentum, equation (33) can be used to describe the momentum transfer.

$$\frac{\partial(\rho v)}{\partial t} = -\nabla \cdot (\rho v v) + \rho \chi + \nabla \cdot \sigma \quad (42)$$

where χ is the external forces and σ is the stress tensor. Substitution of equation (35) into equation (42) gives

$$\rho \frac{dv}{dt} = \rho \chi + \nabla \cdot \sigma \quad (43).$$

3.1.3 Energy Transport Equation

The general continuity equation can be used to write the equation of conservation of energy as

$$\frac{\partial}{\partial t} \{ \rho (E + \frac{1}{2} v \cdot v) \} = -\nabla \cdot \{ \rho (E + \frac{1}{2} v \cdot v) v + j_E \} + \rho v \cdot \chi + \nabla \cdot (v \cdot \sigma) \quad (44)$$

where E is the internal energy and j_E is the energy flux which is composed of two terms. One term is due to diffusion flux of fluid and the other is due to conduction of energy.

Equations (38), (44), (45) are the equations of conservation of

mass, momentum, and energy, respectively. There are several unknowns in these equations.

They are

- 1) j_i and ϕ_i for the equation of continuity of mass
- 2) σ for the equation of motion
- 3) j_E for the equation of energy transport.

If these quantities are known, equations of continuity can be solved depending on the boundary and initial conditions. For a non-equilibrium system, these unknowns can be obtained from the theory of irreversible thermodynamics.

3.1.4 Phenomenological Relation

There are three postulates in the theory of irreversible thermodynamics. The first postulate is the 'assumption of local equilibrium'. It states that the thermodynamic relationships within a microscopic volume of an irreversible system are the same as those of equilibrium thermodynamics, i.e. all irreversible processes for a microscopic volume can be described by equilibrium thermodynamic relationships. Gibbs equation can be expressed in terms of local variables for each volume, dv , as

$$dE = Tds - Pd\left(\frac{1}{\rho}\right) + \sum_{i=1}^n \mu_i dX_i \quad (45)$$

where s is the specific entropy, T is the temperature, P is the pressure and μ_i is the chemical potential of component i and the equation is limited to fluids. The Gibbs-Duhem equation,

$$-sdT + \frac{1}{\rho}dP = \sum_{i=1}^n X_i d\mu_i \quad (46)$$

may be applied to a nonequilibrium system. It is generally accepted that if the gradients of the thermodynamic functions in a system are small, the theoretical consequences of postulate I are valid for the system.

The diffusive energy flux can be separated as

$$j_E = q + \sum_{i=1}^n j_i \bar{E}_i + \sum_{i=1}^n j_i P \bar{V}_i \quad (47)$$

where q is the second law heat flux, \bar{E}_i is the specific internal energy of component i , and \bar{V}_i is the specific volume of component i . The energy transport equation can be rewritten as

$$\rho \frac{dE}{dt} = \sigma : \nabla v - \nabla \cdot q - \nabla \cdot \sum_{i=1}^n j_i \bar{H}_i + \rho v \cdot \chi \quad (48)$$

where \bar{H}_i is the specific enthalpy of component i . The equation of continuity of entropy from the general equation (33) is

$$\left. \begin{aligned} \frac{\partial(\rho s)}{\partial t} &= -\nabla \cdot (s \rho v + j_s) + \frac{\phi_s}{T} \\ \rho \frac{ds}{dt} &= -\nabla \cdot j_s + \frac{\phi_s}{T} \end{aligned} \right\} \quad (49)$$

where j_s is the diffusive entropy flux and ϕ_s/T is the rate of entropy production. Substitution of the relations expressed by equations (33), (44), (45) and (47) into equation (49) results in the explicit expression for the entropy production, ϕ_s . The term, $\phi_s = \phi_s/T$ is made up of four terms, ϕ_1 , ϕ_2 , ϕ_3 and ϕ_4 . ϕ_1 , ϕ_2 and ϕ_3 are

$$\left. \begin{aligned} \phi_1 &= (\sigma + P I) : \nabla v \\ \phi_2 &= -\sum j_i \cdot (\nabla_T \mu_i - \chi_i) \\ \phi_3 &= -q \cdot \nabla \ln T \end{aligned} \right\} \quad (50)$$

where I is the unit tensor. The last term ϕ_4 , the chemical production

term, is not presented. Each of the terms ϕ_1 , ϕ_2 and ϕ_3 is regarded as the product of a flux and force, and is written as:

$$\phi = \sum_i G_i F_i \quad (51)$$

where G_i is the flux and F_i represents the driving forces.

Postulate II is a phenomenological relation. It implies that if the internal entropy production can be defined in the form of equation (51), the fluxes or current, G_i , is a linear homogeneous function of the driving forces, F_i . Thus,

$$G_i = \sum_j \Omega_{ij} F_j \quad (52)$$

where Ω_{ij} , the phenomenological coefficient, is independent of the forces.

Postulate III states that if ϕ can be denoted by equation (51) and if G_i is expressed as the linear homogeneous function of F_i , the resulting matrix of phenomenological coefficients is symmetric,

$$\Omega_{ij} = \Omega_{ji} \quad (53)$$

This equation is known as the Onsager's reciprocal relation.

The validity of postulate III has been shown by Fitts (1962) and de Groot (1952). A great deal of caution is required in applying Onsager's reciprocal relation. Even if a set of fluxes and forces, satisfies equations (50) and (52), the Onsager's reciprocal relation may not hold (Fitts 1962).

3.1.5 Momentum Transport

There is no theoretical relation between the stress tensor and ∇v . The generally accepted relationship is that of Newton, and is

$$\sigma + PI = - \frac{2}{3} \eta \text{IV} \cdot v + 2\eta (\nabla v)_s + \psi \text{IV} \cdot v \quad (54)$$

where η is the shear viscosity coefficient, $(\nabla v)_s$ is the symmetrical

part of the tensor and ψ is the bulk viscosity coefficient. If the relationship expressed by equation (54) is used, then

$$\nabla \cdot \sigma = -\nabla P + \left(-\frac{1}{3} \eta + \psi\right) \nabla(\nabla \cdot v) + \eta \nabla^2 v \quad (55)$$

Normally the bulk viscosity coefficient, ψ , is very small. Substituting equation (55) without a ψ term into equation (43), the Navier-Stokes equation,

$$\rho \frac{dv}{dt} = -\nabla P + \rho \chi + \eta \nabla^2 v + \frac{1}{3} \eta \nabla(\nabla \cdot v) \quad (56)$$

is obtained.

Saturated water flow in a porous medium is generally a steady state flow, so that

$$\frac{dv}{dt} = 0 \quad \text{and} \quad \nabla \cdot v = 0 \quad (57)$$

If gravitation is the only external force acting on the system the Navier-Stokes equation becomes

$$\rho g \nabla h = \eta \nabla^2 v \quad (58)$$

where ∇h , hydraulic head, is equal to $\nabla p - \rho g l$ (Hillel 1971) and l is the height of soil column.

Viscous liquid flow through a capillary tube can be expressed by equation (58) in cylindrical coordinates. If the external force is due only to gravitation without any applied pressure, then

$$\frac{1}{r} \left\{ \frac{d}{dr} \left(r \frac{dv}{dr} \right) \right\} = - \frac{\rho g}{\eta} \nabla h \quad (59)$$

where r is the distance from the centre of the tube. Integration of equation (59) results in the velocity profile. The profile is parabolic in the tube,

$$v = \frac{\rho g}{4\eta} \nabla h (R^2 - r^2) \quad (60)$$

where R is the radius of the capillary tube. The rate of the volumetric flow of fluid, Q , through the tube is

$$Q = 2\pi \int_0^R v r dr \quad (61)$$

By using equation (60) and integrating equation (61), the Hagen-Poiseuille equation

$$Q = - \frac{\pi}{8} \frac{R^4 \rho g}{\eta} \nabla h$$

is obtained. The Hagen-Poiseuille equation expressing the relation between the volumetric liquid flux and external force can be applied to water flow in soil. By applying the parallel pipe model (Scheidegger 1963) to a soil, the total flux is obtained by summing the individual fluxes, as

$$\sum_{i=1}^n Q_i = - \sum_{i=1}^n \frac{\pi R_i^4 \rho g}{8\eta} \nabla h \quad (62)$$

If equation (62) is divided by the total area, A , of the soil column then the average velocity or flux is

$$J_w = - \left(\frac{\sum_{i=1}^n R_i^4 \rho g}{8\eta} \right) / A \nabla h = - K \nabla h \quad (63)$$

where $(\sum_{i=1}^n R_i^4 \rho g / 8\eta) / A$ is equal to K , the hydraulic conductivity. This equation (63) is similar to Darcy's law. J_w is the flux of the water and is not the diffusion flux with respect to the centre of mass as shown by Taylor and Cary (1964) and Nielsen et al. (1972). It is seen from equation (63) that K , the hydraulic conductivity is a function of pore size

and viscosity of the liquid.

For an unsaturated soil K is a function of water content. The change in mass within a volume element without chemical reactions can be described by the equation of continuity of mass

$$\frac{\partial \rho_w}{\partial t} = - \nabla \cdot (\rho_w v) \quad (64)$$

When the average velocity from equation (63) is substituted into equation (64) the rate of change in moisture content becomes

$$\frac{\partial \theta}{\partial t} = - \nabla \cdot (K \nabla h) = - \nabla \cdot \left(K \frac{\partial h}{\partial \theta} \nabla \theta \right) = - \nabla \cdot (D(\theta) \nabla \theta) \quad (65)$$

Where $D(\theta)$, the diffusivity, is equal to $K \partial h / \partial \theta$. Equation (65) is commonly used for describing unsaturated water flow. It should be emphasized here that the derivation of equation (65) is based on Navier-Stokes' equation (Equation (56) and (59)) rather than using the relation

$$\phi_2 = - \sum_{i=1}^n j_i \cdot (\nabla_T \mu_i - \chi_i)$$

of equation (50), which is commonly employed by many soil scientists (Taylor and Cary 1964; Neilsen et al. 1972; and Cary 1965, 1966).

3.1.6 Mass Transport

Dissolved solutes tend to move simultaneously with the soil solution. The equation of conservation of mass of component i , equation (38), is employed. The unknown quantities of equation (38) are v and j_i . The centre of mass velocity, can be obtained from equation (63). The diffusion flux j_i can be obtained using postulate II. Thus

$$-j_i = \Omega_{i0} \nabla \ln T + \sum_{j=1}^n \Omega_{ij} \nabla_T \mu_j \quad (66)$$

where ∇_T is the gradient operator at uniform temperature. A more commonly observable quantity such as concentration gradient, can be substituted for the chemical potential gradient in equation (66) as:

$$\nabla_T \mu_j = \sum_{k=1}^{n-1} \frac{\partial \mu_j}{\partial \rho_k} \nabla_T \rho_k$$

A working equation of the form

$$-j_i = \Omega_{i0} \frac{1}{T} \nabla T + \sum_{j=1}^{n-1} \sum_{k=j+1}^n \Omega_{ij} \frac{\partial \mu_j}{\partial \rho_k} \nabla_T \rho_k$$

is obtained. The diffusion coefficient D_{ik} and thermal diffusion coefficient β_i can be defined as :

$$D_{ik} = \sum_{j=1}^n \Omega_{ij} \frac{\partial \mu_j}{\partial \rho_k} \quad \text{and} \quad \beta_i = \Omega_{i0} / T$$

The diffusion flux becomes

$$-j_i = \rho_i \beta_i \nabla T + \sum_{k=1}^{n-1} D_{ik} \nabla \rho_k \quad (67)$$

A general mass transport equation of component i in an incompressible fluid can be obtained by substituting equation (66) into equation (38),

$$\frac{\partial \rho_i}{\partial t} = -v \cdot \nabla \rho_i + \nabla \cdot (\beta_i \nabla T) + \nabla \cdot \left(\sum_{k=1}^{n-1} D_{ik} \nabla \rho_k \right) + \phi_i$$

If $D_{ik} = 0$ when $i \neq k$ and $D_{ii} \neq 0$, the above equation becomes

$$\frac{\partial \rho_i}{\partial t} = -v \cdot \nabla \rho_i + \nabla \cdot (\beta_i \nabla T) + \nabla \cdot (D_{ii} \nabla \rho_i) + \phi_i \quad (68)$$

This equation means that the concentration change within a volume element is due to convection, $v \nabla \rho_i$, thermal diffusion, $\nabla \cdot (\beta_i \nabla T)$, ordinary

diffusion, $\nabla(D_{ii}\nabla\rho_i)$, and chemical production, ϕ_i .

Special cases of physical situations regarding equations (66) and (67) will be analyzed. When there is no temperature gradient, no interaction between components, no convection and no chemical reactions, equations (67) and (68) become

$$j_i = -D_{ii}\nabla\rho_i \quad \text{and} \quad \frac{\partial\rho_i}{\partial t} = \nabla\cdot(D_{ii}\nabla\rho_i)$$

and they are Fick's first and Fick's second laws of diffusion, respectively. Equations (13), (18), (19) and (5) are all special cases of equation (68).

The diffusion flux with respect to solvent, r, is

$$j'_i = \rho_i(v_i - v_r) = J_i - \frac{\rho_i}{\rho_r} J_r = j_i - \frac{\rho_i}{\rho_r} j_r \quad (69)$$

Thus equation (67) becomes

$$-j'_i = \rho_i\beta'_i\nabla T + \sum_k^{n-1} D'_{ik}\nabla\rho_k \quad (70)$$

where β'_i is equal to $\beta_i(\Omega_{ij} - \rho_i/\rho_v \Omega_{rj})/\rho_i$ and D'_{ik} is equal to $D_{ik}(\Omega_{ij} - \rho_i/\rho_r \Omega_{rj} - \rho_i/\rho_r \Omega_{ir} + \rho_i\rho_j/\rho_r \Omega_{rr})$. For steady state conditions in a closed system

$$j'_i = j'_j = j'_k = \dots = 0$$

and equation (70) becomes

$$\rho_i\beta'_i\nabla T = -\sum_k^{n-1} D'_{ik}\nabla\rho_k$$

$$-\left(\frac{\nabla\rho_k}{\nabla T}\right)_{j1} = -\left(\frac{\nabla\rho_k}{\nabla T}\right)_{j2} = \dots = \kappa_k = \text{constant.}$$

Thus

$$\rho_i \beta'_i = \sum_k^{n-1} D'_{ik} \kappa_k.$$

Substituting this relationship into the flux equation results in

$$-j'_i = \sum_k^{n-1} D'_{ik} (\nabla \rho_k + \rho_k S_k \nabla T)$$

where S_k , the Soret coefficient, is defined as $-\kappa_k/\rho_k$. For a two component system, the subscripts 1 and 2 represent solute and solvent respectively, and

$$-j'_1 = D'_{11} (\nabla \rho_1 - \rho_1 S_1 \nabla T) \quad (71).$$

Combining this equation with equation (38) and assuming

$$j'_1 \approx j_1, \quad v = 0 \quad \text{and} \quad \phi_1 = 0$$

gives

$$\frac{\partial \rho_1}{\partial t} = D_{11} \nabla^2 \rho_1 - \nabla \cdot (\rho_1 S_1 \nabla T) \quad (72).$$

If ∇T is constant, $\Delta T/\Delta x = \tau/l$, τ is the temperature difference between two points and l is the distance. Equation (72) for a one dimensional system takes the form,

$$\frac{\partial \rho_1}{\partial t} = D_{11} \frac{\partial^2 \rho_1}{\partial x^2} - \frac{\tau}{l} S_1 \frac{\partial \rho_1}{\partial x} \quad (73).$$

If we define

$$\frac{\tau}{l} S_1 = v_1$$

equation (73) can be rewritten as

$$\frac{\partial \rho_1}{\partial t} = D_{11} \frac{\partial^2 \rho_1}{\partial x^2} - v_1 \frac{\partial \rho_1}{\partial x} \quad (74).$$

Equation (74) has the same form as the transport equation under a

convective system. It is thus noticed that the effect of a temperature gradient upon mass transport of component i under a non-convective system can be identically described as convective transport under isothermal conditions (de Groot 1942; Cho 1975*).

3.2 Mathematical Development for Experimental Conditions

A general theory for mass, momentum and energy transport has been discussed in the previous section. In this section the development of theory is confined to mass transport and is restricted to the conditions encountered in the experiments.

3.2.1 Equations of Mass Transport

In an unsaturated porous medium, soil water can exist simultaneously in three phases i.e. vapor, liquid and solid (ice). In the majority of cases, the transfer of substances in the ice phase is negligible. The movement of moisture in the vapor phase is mainly due to diffusion and the transport of liquid water is caused by diffusion and by convection. The movement of vapor and liquid can occur simultaneously and may be in the same or opposite direction. A phase change may take place in the course of movement. Under a temperature gradient heat transfer also takes place.

A vertical unsaturated soil column with uniform moisture and salt content was selected. This system is closed with respect to mass but is open with respect to heat. The flux of vapor is defined on the unit cross section of air space while flux of liquid is based on unit cross section of soil.

If the chemical potential gradients are expressed as a function of the vapor density, ρ_1 , and volumetric moisture content, θ_2 , then

* C. M. Cho, unpublished work.

$$\left. \begin{aligned}
 -j_1 &= \Omega_{10} \nabla \ln T + \Omega_{11} \left(\frac{\partial \mu_1}{\partial \rho_1} \right) \nabla \rho_1 \\
 -j_2 &= \Omega_{20} \nabla \ln T + \Omega_{22} \left(\frac{\partial \mu_2}{\partial \theta_2} \right) \nabla \theta_2
 \end{aligned} \right\} \quad (75)$$

or, in a workable form,

$$\left. \begin{aligned}
 -\epsilon j_1 &= \rho_1 \epsilon \beta_1 \nabla T + \epsilon D_1 \nabla \rho_1 \\
 -j_2 &= \theta_2 \beta_2 \nabla T + D_2 \nabla \theta_2
 \end{aligned} \right\} \quad (76)$$

In the above equation ϵ stands for porosity and β can be interpreted as the thermal diffusion coefficient.

If the total flux, J , and diffusive flux, j , are assumed to be equal, equation (76) can be directly substituted into the equation of continuity. Thus

$$\left. \begin{aligned}
 \frac{\partial (\epsilon \rho_1)}{\partial t} &= \nabla \cdot (\epsilon \rho_1 \beta_1 \nabla T + \epsilon D_1 \nabla \rho_1) + \epsilon \phi_1 \\
 \frac{\partial \theta_2}{\partial t} &= \nabla \cdot (\theta_2 \beta_2 \nabla T + D_2 \nabla \theta_2) + \phi_2
 \end{aligned} \right\} \quad (77)$$

Solutions of these simultaneous equations under one dimensional steady state conditions (special conditions) have been solved (Cho 1975^{*}). It was assumed that ϵ , β_1 , D_1 , β_2 and D_2 were constant and the temperature profile was a linear distribution. The temperature gradient for one dimension was expressed as:

$$\nabla T = i \frac{T}{l}$$

where i is the unit vector, l is the distance and T is the temperature

* C.M. Cho, unpublished work.

difference. The transport equations of vapor and liquid water were

$$\left. \begin{aligned} \frac{\partial \rho_1}{\partial t} &= \beta_1 \frac{\tau}{l} \frac{\partial \rho_1}{\partial x} + D_1 \frac{\partial^2 \rho_1}{\partial x^2} + \phi_1 \\ \frac{\partial \theta_2}{\partial t} &= \beta_2 \frac{\tau}{l} \frac{\partial \theta_2}{\partial x} + D_2 \frac{\partial^2 \theta_2}{\partial x^2} + \phi_2 \end{aligned} \right\} (78).$$

The reactions of vaporization (ϕ_1) and condensation (ϕ_2) were assumed to be a linear rate law

$$\varepsilon \phi_1 = -k_1 (\rho_1 - \rho_1^0) + k_2 (\theta_2^0 - \theta_2) = -\phi_2 \quad (79)$$

where ρ_1^0 is the saturated vapor pressure corresponding to temperature T. ρ_1^0 was defined in the range of moisture held by soil from saturation to 15 atm. as:

$$\rho_1^0 = \rho_1^0(T) = \rho_1^* + \frac{\partial \rho_1^0}{\partial T} \frac{\tau}{l} x.$$

θ_2^0 is the water holding capacity at equilibrium and is defined as:

$$\theta_2^0 = \theta_2^0(T) = \theta_2^* + \frac{\partial \theta_2^0}{\partial T} \frac{\tau}{l} x$$

and

$$\int_0^l A_c \theta_2^0 dx = \bar{\theta}_2^0 V$$

where A_c is the cross sectional area, l is the length of the column, V is the total volume of the column and $\bar{\theta}_2^0$ is the initial volumetric water content. Therefore equation (79) becomes

$$\varepsilon \phi_1 = -k_1 (\rho_1 - \rho_1^*) + k_2 (\theta_2^* - \theta_2) + (k_1 \frac{\partial \rho_1^0}{\partial T} - k_2 \frac{\partial \theta_2^0}{\partial T}) \frac{\tau}{l} x \quad (80).$$

Substituting equation (80) into equation (78) yields

$$\left. \begin{aligned} \frac{\partial \rho}{\partial t} &= D_1 \frac{\partial^2 \rho}{\partial x^2} + \beta_1 \frac{\tau}{l} \frac{\partial \rho}{\partial x} - \frac{k_1}{\epsilon} \rho + \frac{k_2}{\epsilon} \theta + \frac{k_3}{\epsilon} x \\ \frac{\partial \theta}{\partial t} &= D_2 \frac{\partial^2 \theta}{\partial x^2} + \beta_2 \frac{\tau}{l} \frac{\partial \theta}{\partial x} + k_1 \rho - k_2 \theta - k_3 x \end{aligned} \right\} (81)$$

where

$$\rho = \rho_1 - \rho_1^*$$

$$\theta = \theta_2 - \theta_2^*$$

$$k_3 = \left(\frac{\partial \rho_1^0}{\partial T} - \frac{\partial \theta_2^0}{\partial T} \right) \frac{\tau}{l}$$

For initial conditions where $t = 0$ and $0 \leq x \leq 1$

$$\rho_1 = \rho^0 \quad \text{and} \quad \theta_2 = \theta^0$$

then

$$\rho = \rho^0 - \rho_1^*$$

$$\theta = \theta^0 - \theta_1^*$$

The boundary conditions become

$$\left. \begin{aligned} D_1 \frac{d\rho}{dx} - v_1 (\rho + \rho_1^*) &= 0 \\ D_2 \frac{d\theta}{dx} - v_2 (\theta + \theta_2^*) &= 0 \end{aligned} \right\} \text{at } x = 0 \quad \text{and} \quad x = 1$$

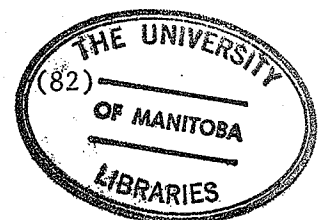
where

$$v_1 = -\beta_1 \frac{\tau}{l}$$

$$v_2 = -\beta_2 \frac{\tau}{l}$$

Salt movement occurs only in the liquid phase. Therefore the flux of salt has to be defined on the basis of liquid water

$$-j_3^I = \Omega_{30} \nabla \ln T + \Omega_{32} \nabla_T \mu_2^I + \Omega_{33} \nabla_T \mu_3^I$$



where subscript 3 is salt. The μ_2' and μ_3' are based on liquid phase. According to the Gibbs-Duhem equation

$$\nabla_T \mu_2' = - \frac{n_3}{1-n_3} \nabla_T \mu_3' \quad (83)$$

where n_3 is the mole fraction of salt and

$$n_2 + n_3 = 1.$$

Substituting equation (83) into equation (82) gives

$$-j_3' = \Omega_{30} \nabla \ln T + \left\{ \Omega_{33} - \Omega_{32} \left(\frac{n_3}{1-n_3} \right) \right\} \frac{\partial \mu_3'}{\partial C_3} \nabla C_3'$$

where C_3' is the concentration of salt based on solution. The equation, modified to a workable form, is

$$-j_3' = C_3' \beta_3 \nabla T + D_3 \nabla C_3' \quad (84).$$

The total flux of salt is

$$J_3 = j_3' \theta_2 + C_3 v \quad (85)$$

where C_3 is the salt concentration based on soil volume, v is the centre of mass velocity and approximately equal to the liquid water velocity i.e.

$$v = J_2 / \theta_2 \quad (86).$$

J_2 is the total flux of water. If the equation of continuity of mass is applied, then

$$\frac{\partial C_3}{\partial t} = - \nabla \cdot J_3 + \phi_3 \quad (87).$$

ϕ_3 is negligible and substituting equations (84), (85) and (86) into equation (87) results in

$$\frac{\partial C_3}{\partial t} = \nabla \cdot (\theta_2 C_3' \beta_3 \nabla T) + \nabla \cdot (\theta_2 D_3 \nabla C_3') - \nabla \cdot (C_3 J_2 / \theta_2) \quad (88).$$

If it is further assumed that β_3 , D_3 and J_2/θ_2 are constant and temperature distribution within the column is assumed to be linear then equation (88) for one dimension can be expressed as:

$$\frac{\partial C_3}{\partial t} = D_3 \frac{\partial^2 C_3}{\partial x^2} + \left(\beta_3 \frac{\tau}{l} - J_2/\theta_2 \right) \frac{\partial C_3}{\partial x} \quad (89)_s$$

By defining

$$v_3 = - \beta_3 \frac{\tau}{l} + J_2/\theta_2$$

and rewriting equation (89), we obtain

$$\frac{\partial C_3}{\partial t} = D_3 \frac{\partial^2 C_3}{\partial x^2} - v_3 \frac{\partial C_3}{\partial x} \quad (90).$$

The initial condition is

$$C_3 = C_3^0 \quad \text{at} \quad t = 0 \quad 0 \leq x \leq 1.$$

The boundary condition becomes

$$D_3 \frac{dC_3}{dx} - C_3 v_3 = 0 \quad \text{at} \quad t > 0, \quad x = 0 \quad \text{and} \quad x = 1.$$

Solution of equation (90) when J_2 was zero and $\beta_3 \tau/l$ was constant under similar boundary and initial conditions as above was shown by de Groot (1942). However, under ordinary experimental conditions the temperature profile within a soil column is usually non-linear and best described by an exponential form of equation. The following form of temperature function

$$T = a - be^{-gx} \quad (91)$$

was chosen. In the above equation a , b and g are constants and x is the distance from the cold end. The chemical terms are chosen as a simple

linear rate law as:

$$\epsilon\phi_1 = -k_1(\rho_1 - \rho_1^0) = -\phi_2 \quad (92)$$

where ρ_1^0 is as defined before. The vapor density has a positive deviation from linearity with temperature. The temperature distribution as shown in equation (91) has a negative deviation from linearity with distance. Therefore the vapor density can be approximated as a linear function of distance and water content,

$$\rho_1^0 = \rho_1^0(T, \theta_2) = \rho_1^0(x, \theta_2) = \rho_1^* + \left(\frac{\partial \rho_1^0}{\partial x}\right)x + \left(\frac{\partial \rho_1^0}{\partial \theta_2}\right)\theta_2 \quad (93).$$

By using this relation equation (92) becomes

$$\epsilon\phi_1 = -k_1\rho + k_2\theta_2 + k_3x \quad (94)$$

where

$$\begin{aligned} \rho &= \rho_1 - \rho_1^* \\ k_2 &= k_1 \left(\frac{\partial \rho_1^0}{\partial \theta_2}\right) \\ k_3 &= k_1 \left(\frac{\partial \rho_1^0}{\partial x}\right). \end{aligned}$$

This equation has the same form as equation (80). The equation of transport of vapor and liquid water can be obtained by substituting equations (91) and (94) into equation (77). If it is assumed that β_1 , D_1 , β_2 and D_2 are constant, the one dimensional transport equations are

$$\left. \begin{aligned} \epsilon \frac{\partial \rho_1}{\partial t} + \rho \frac{\partial \epsilon}{\partial t} &= \left(K_1 \rho_1 e^{-gx} + D_1 \frac{\partial \rho_1}{\partial x}\right) \frac{\partial \epsilon}{\partial x} + K_1 \epsilon e^{-gx} \frac{\partial \rho_1}{\partial x} \\ &+ D_1 \epsilon \frac{\partial^2 \rho_1}{\partial x^2} - K_1 g \rho_1 \epsilon e^{-gx} - k_1 \rho + k_2 \theta_2 + k_3 x \end{aligned} \right\} \quad (95a)$$

$$\frac{\partial \theta_2}{\partial t} = K_2 e^{-gx} \frac{\partial \theta_2}{\partial x} - K_2 g \theta_2 e^{-gx} + D_2 \frac{\partial^2 \theta_2}{\partial x^2} + k_1 \rho - k_2 \theta_2 - k_3 x \quad (95b)$$

where $K_1 = \beta_1 gb$, and $K_2 = \beta_2 gb$.

ϵ can be expressed as:

$$\epsilon = \theta_s - \theta_2$$

where θ_s is the saturated water content. Therefore equation (95) becomes

$$\left. \begin{aligned} (\theta_s - \theta_2) \frac{\partial \rho_1}{\partial t} - \rho_1 \frac{\partial \theta_2}{\partial t} = & - (k_1 e^{-gx} \rho_1 + D_1 \frac{\partial \rho_1}{\partial x}) \frac{\partial \theta_2}{\partial x} + K_1 e^{-gx} \\ & (\theta_s - \theta_2) \frac{\partial \rho_1}{\partial x} + D_1 (\theta_s - \theta_2) \frac{\partial^2 \rho_1}{\partial x^2} \\ & - K_1 g \rho (\theta_s - \theta_2) e^{-gx} - k_1 \rho + k_2 \theta_2 + k_3 x \end{aligned} \right\} (96).$$

$$\frac{\partial \theta_2}{\partial t} = K_2 e^{-gx} \frac{\partial \theta_2}{\partial x} - K_2 g \theta_2 e^{-gx} + D_2 \frac{\partial^2 \theta_2}{\partial x^2} + k_1 \rho - k_2 \theta_2 - k_3 x$$

The initial conditions are

$$\left. \begin{aligned} \rho_1 &= \rho^0 \\ \rho &= \rho^0 - \rho_1^* \end{aligned} \right\} \text{at } t = 0 \text{ and } 0 \leq x \leq 1.$$

The boundary conditions are

$$\left. \begin{aligned} D_1 \frac{d\rho_1}{dx} + K_1 (\rho + \rho_1^*) &= 0 \\ D_2 \frac{d\theta_2}{dx} + K_2 \theta_2 &= 0 \end{aligned} \right\} \text{at } x = 0$$

and

$$\left. \begin{aligned} D_1 \frac{d\rho}{dx} + K_1 (\rho + \rho_1^*) e^{-gl} &= 0 \\ D_2 \frac{d\theta_2}{dx} + K_2 \theta_2 e^{-gl} &= 0 \end{aligned} \right\} \text{at } x = 1$$

$$\left. \begin{aligned} & \\ & \end{aligned} \right\} t \geq 0.$$

The analytical solutions of equation (96) have not been obtained.

For salt movement the exponential temperature distribution model was chosen. The transport equation of salt becomes

$$\frac{\partial C_3}{\partial t} = D_3 \frac{\partial^2 C_3}{\partial x^2} + (K_3 e^{-gx} - J_2/\theta_2) \frac{\partial C_3}{\partial x} - C_3 k_3 g e^{-gx} - C_3 \frac{\partial}{\partial x} (J_2/\theta_2) \quad (97)$$

where $K_3 = \beta_3 g b$. The initial condition is

$$C_3 = C_3^0 \quad \text{at} \quad t = 0 \quad \text{and} \quad 0 \leq x \leq 1.$$

The boundary conditions are

$$\left. \begin{aligned} D_3 \frac{dC_3}{dx} - C_3 v_3' &= 0 & \text{at} & \quad x = 0 \\ D_3 \frac{dC_3}{dx} - C_3 v_3' e^{-g} &= 0 & \text{at} & \quad x = 1 \end{aligned} \right\} \text{at} \quad t \geq 0$$

where $v_3' = J_2/\theta_2 - K_3$. The analytical solutions of equation (97) was attempted, but was not obtained.

Mathematical models for soil columns with ice phase, semi-open or open systems were not attempted in this study.

4 MATERIALS AND METHODS

4.1 Field Experiment

Two experimental sites were chosen for the study of NO_3^- and Cl^- movement in soil. One site was located on an Almasippi loamy fine sandy close to Haywood, Manitoba. This is a slightly alkaline soil (Table 1). The other site was located on a Red River clay soil at Glenlea, Manitoba.

The dimensions of the experimental plots were 4.5 m x 4.5 m. Two plots were established on the Almasippi loamy fine sand site, one plot was treated with $\text{Ca}(\text{NO}_3)_2$ and CaCl_2 on Oct. 5, 1973 and the other plot was treated on July 3, 1974. A single plot on the Red River clay soil was treated with $\text{Ca}(\text{NO}_3)_2$ and CaCl_2 on Nov. 2, 1973. $\text{NO}_3^- - \text{N}$ and Cl^- were applied at 1681.5 Kg/ha. The Cl^- ion was applied to serve as a tracer for water movement. Since Cl^- is not adsorbed by soil or subject to assimilation by soil organisms to a significant degree, a measurement of Cl^- movement would provide information on NO_3^- movement. Ten thermocouples were inserted in the soil at each site at depths of 2.5, 5, 10, 20, 35, 50, 75, 100, 125 and 150 cm. Soil samples were taken at various times at 15.2 cm intervals to a depth of 182.4 cm or to depth of ground water for the Almasippi loamy fine sand site and to 121.6 cm for the Red River clay soil site. Temperature and rainfall were recorded. The field studies were terminated in April, 1975. Soil samples were taken using a 5.1 cm diameter auger when the soil was not frozen. A Kango electric hammer was used for taking frozen soil samples. Due to sampling difficulties, samples were not taken from the Red River clay soil when frozen. Each sample was stored in a sealed plastic bag and transported to the laboratory in a cooler. The samples were stored at 5 C for one or two days and the moisture content and the Cl^- , $\text{NO}_3^- - \text{N}$ and $\text{NO}_2^- - \text{N}$ concentrations in the samples determined.

TABLE 1 SOME CHARACTERISTICS OF THE SOILS

Soil name	Almasippi	Red River
Texture	Loamy fine sand	Clay
C.E.C. (meq/100g)	15.5	44.7
pH	6.6	8.0
Specific conductance (mmhos/cm)	0.8	0.8
Cl ⁻ (ppm)	10-30	10-400
Organic matter (%)	2.5	2.6

Nitrate, NO_2^- and Cl^- were extracted by shaking 10 g soil with 50 ml distilled water for 30 minutes. The suspension was filtered through whatman No. 42 filter paper and the NO_3^- -N and NO_2^- -N concentrations of the filtrate determined using a Technicon Autoanalyzer (Kamphake et al. 1967). The Cl^- concentration was determined by potentiometric titration using a Radiometer titrator equipped with a combination AgCl-HgSO_4 electrode. Standard AgNO_3 solution was used as titrant.

Gravimetric water content was determined on another portion of soil by drying at 110 C for 48 hours.

4.2 Laboratory Experiments

The soil used for the experiments was taken from the 0 to 15-cm depth of a Wellwood clay loam soil. The soil was air dried, passed through a 2-mm sieve and stored at room temperature. Some characteristics of the soil are shown in Table 2.

An acrylic tube, 3.8 cm inner diameter and 16 cm long, was sectioned into 1 cm lengths and filled with soil. One end of the column was sealed with a copper plate and the other end was attached to a heat exchanger connected to a Haake Model FK* or a Lunar Model RK** constant temperature circulator. The construction of the soil column is shown in Fig. 1. The columns were insulated with fiberglass. In columns with an air gap, two perforated copper plates separated by a 0.5, 1, or 2 cm copper ring were placed in the middle of the column, 6, 4, or 1 cm from the cold end of a column. The air gap served as a semipermeable membrane to vapor but was impermeable to liquid water and solutes. A 0.5-cm air gap was inserted between the middle sections of a soil column when the temperature of the cold end was above the freezing point. For columns with the temperature of the cold end below the freezing point 0.5, 1, and 2 cm gaps were used

* Ployscience Cooperation. ** Brinkmann Instruments.

TABLE 2 SOME CHARACTERISTICS OF WELLWOOD SOIL

pH	5.2
Organic carbon (%)	4.53
Total N (%)	0.37
Specific conductance (mmhos/cm)	1.7
C.E.C. (meq/100g)	28.7
Exchangeable cations (meq/100g)	
Ca	18.4
Mg	6.0
K	1.1
Na	0.1
H	6.6
% Sand	50.3
% Silt	33.4
% Clay	16.3

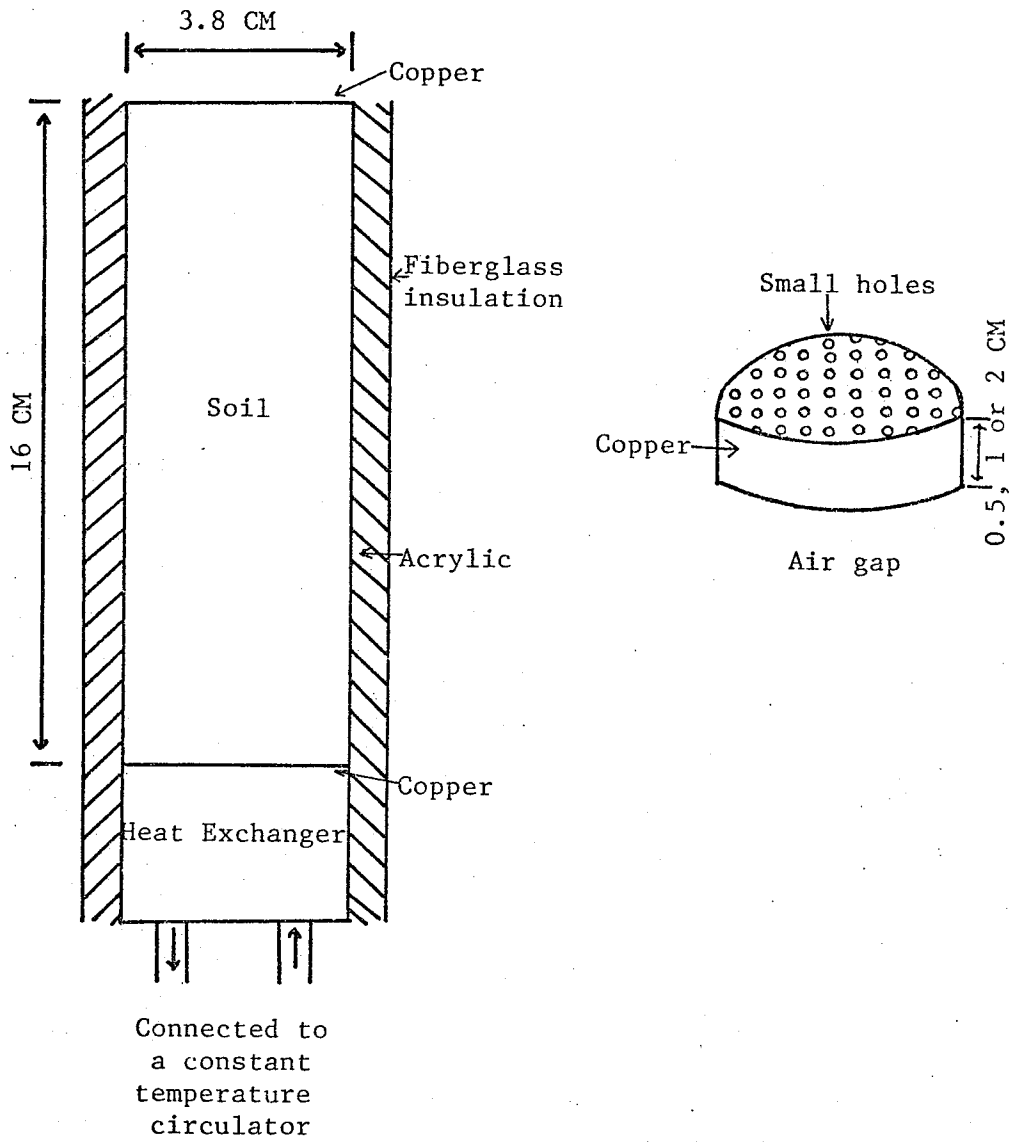


Fig. 1. Construction of closed soil column and air gap

and were placed at 8, 6, 4, or 1 cm from the cold end. The construction of the air gap is also shown in Fig. 1.

The soil was uniformly mixed with water, KCl, and $\text{Ca}(\text{NO}_3)_2 \cdot 4\text{H}_2\text{O}$. The concentration of N was 500 ppm-N for all experiments. The concentrations of KCl were 10 or 20% and water contents were 27 or 32% depending upon the treatments selected. Moisture content (%) and N concentration (ppm-N) were based on dry soil weight and the concentration of KCL (%) was calculated on a soil solution basis. The premixed soil was uniformly packed into the column; the bulk density varied between 1.2 and 1.3 g/cm³. The prepared soil column was immediately subjected to a temperature gradient. The Cl^- served not only as an indicator of liquid flow but also as a solute which depressed the vapor pressure.

The warm end of the soil column was maintained at room temperature which was about 22 C. The heat exchanger at the cold end was maintained at various constant temperatures. Temperatures of the soil columns were measured at 2-cm intervals using thermocouples inserted about 0.5 cm into the section through small holes in the walls of the acrylic rings.

Six different experiments were conducted:

1. Effect of moisture and salt concentration on mass transport
2. Effect of the freezing process on mass transport
3. Effect of different geometrical configurations on mass transport
4. Effect of air gap length and position on mass transport
5. Simulation of natural conditions
6. Open system.

4.2.1 Effect of Moisture and Salt Concentration on Mass Transport

In order to study the effect of moisture content upon mass transport, twelve soil columns, six with and six without an air gap, were

used. Several combinations of salt concentration and moisture content, with or without an air gap, were used to study the salt effect. Moisture contents were 27 and 32%, KCl concentrations were 10 and 20% and a 0.5-cm air gap was inserted between the middle sections in some of the soil columns. All columns contained 500 ppm $\text{NO}_3\text{-N}$. The duration of thermal treatment was 5, 10 or 20 days. The temperature on the cold end of the columns was maintained at 0.5 C.

4.2.2 Effect of the Freezing Process on Mass Transport

Soil was mixed uniformly with 10% KCl, 500 ppm $\text{NO}_3\text{-N}$ and water equivalent to 27 or 32% of soil weight and placed into acrylic tubes. Two columns with 27% moisture were treated for 20 days. All other columns were treated for 10 days. The cold end temperature for all the columns was maintained at -19.5 C.

4.2.3 Effect of Different Geometrical Configurations on Mass Transport

All the soil columns used in this experiment contained 10% KCl, 500 ppm-N and 27% moisture. Duration of the thermal treatment was 10 days.

Four columns were placed vertically with the cold end on top. The cold end temperature of two of these columns was -19.5 C and the temperature for the other two columns was 0.5 C. Four other columns were placed horizontally. Temperatures, maintained at the cold end of the columns, were identical to temperatures maintained for the vertical columns. Each of the treatments had columns with and without an air gap.

4.2.4 Effect of Air Gap Length and Position on Mass Transport

This experiment was initiated to determine the length of air gap necessary to stop the return flow of liquid water from the cold end to the warm end after water accumulated at the cold end. All columns were

placed vertically with the frozen end on the bottom and all systems were closed except for two columns which had the cold side on the upper part of the column and were open on the top.

All columns were treated for 10 days. The soil used in this experiment was premixed with 10% KCl and 500 ppm NO_3^- -N and wetted to 27% moisture.

The first study involved the use of a 0.5-cm air gap placed between the 6th and 7th sections (6 to 7 cm) from the top of the soil column with the cold end on the top and open. The purpose of leaving the soil surface open to the air was to create an infinitely large water sink in the frozen portion.

A second study using a 1-cm air gap located at the 5th section of the column was conducted. A closed system was used with the cold end of the column located at the bottom. In order to provide a large sink for soil moisture without much reduction in porosity, the colder region (four sections) was filled with dry soil. There was no moisture, Cl^- or NO_3^- added in the colder chamber at initiation of the thermal treatment.

In a third study, the soil column was prepared by the same method as the second study except that the colder region was filled with premixed soil. A 2-cm air gap was used in the fourth study. The gap was placed at the second and third sections from the coldest end. The frozen compartment had only one section which was filled with air dry soil.

The temperature on the cold end was adjusted so that the temperature of the soil section on the cold side of the air gap was just below the freezing point (-1.0 C) and the temperature on the warm side of the air gap just above the freezing point (0.5 C). In general this method resulted in a large thermal gradient in the unfrozen part of the soil.

4.2.5 Simulation of Natural Conditions

In Manitoba, the surface soil of cultivated land freezes at the beginning of the winter. The frost penetrates downward with time to 150 or 160 cm depending upon soil and temperature conditions. In spring as the surface soil thaws the soil below the surface remains frozen and the soil below the frozen layer continues to freeze. The soil profile is usually free of frost in late spring or in early summer.

The effects of gradually changing the direction and magnitude of the thermal gradient upon mass transport was studied. Soil columns containing 10% KCl, 27% moisture and 500 ppm NO_3^- -N were placed vertically. The top end of the column was frozen during the first 10 days of thermal treatment. During the second 10 days, the bottom end of the column was frozen, the cold treatment on the top end of the column terminated and the soil allowed to warm to room temperature. Water content, Cl^- and NO_3^- -N concentrations of the soil sections were determined.

4.2.6 Open System

One end of the soil column was sealed with a copper plate and the other end was attached to a heat exchanger built to maintain a constant temperature and yet expose the soil surface. Because the top end had to be open and cold, the heat exchanger could not be directly attached to the top end. In order to create a relatively large thermal gradient a hollow heat exchanger 3-cm long was fitted to the external surface of the column. Thus, the top 3 cm of soil column were surrounded by the exchanger. Thus there was no temperature gradient within the top 3-cm section of the column. Another large heat exchanger was placed about 4 cm above the open soil surface (Fig. 2). The large heat exchanger maintained atmospheric temperature near the top of column close to that of

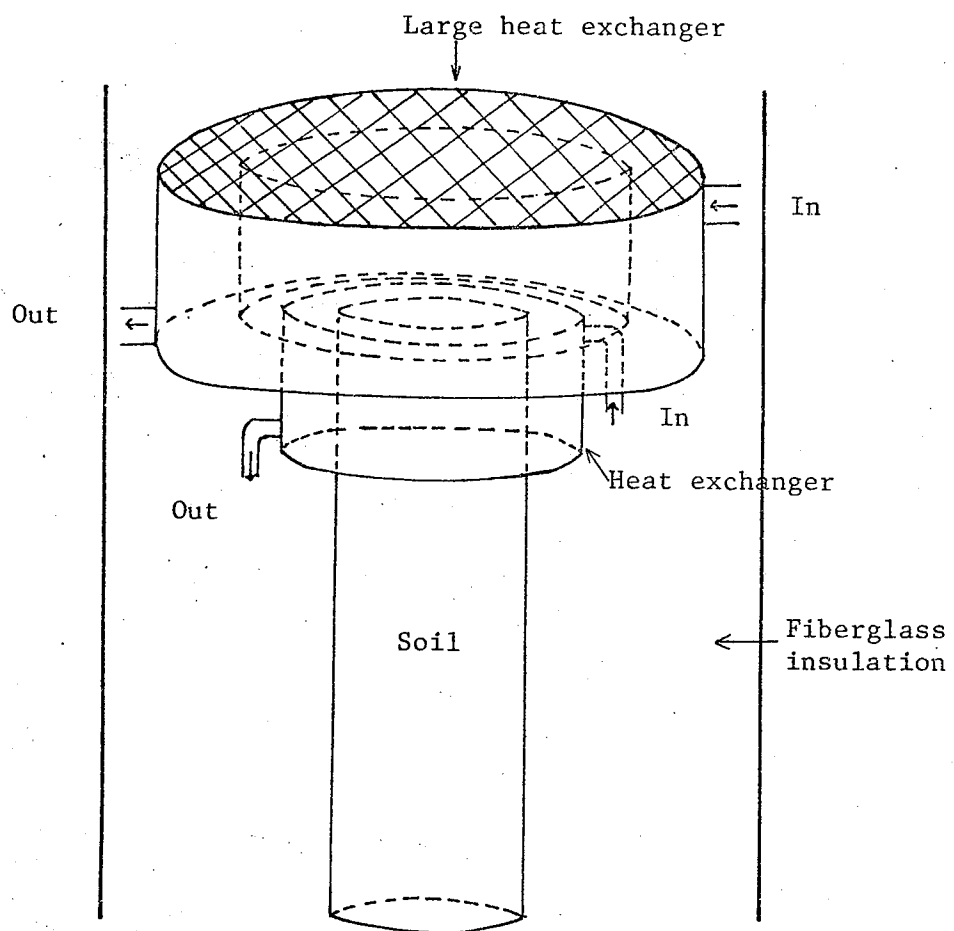


Fig. 2. Construction of the open soil column.

the soil surface. The soil was premixed with 10% KCl, 500 ppm-N and 27% moisture. The duration of the thermal treatment was 10 days. Two temperatures were chosen for the cold side of the column. One, unfrozen treatment, had 0.5 C and the other, frozen treatment, had -19.5 C. On both treatments the warmer part of the column had temperature close to room temperature.

4.3 Determination of NO_3^- -N, NO_2^- -N, Cl^- and Water Content of Soil

At the end of the thermal treatment, the column was removed from the heat exchanger and cut into 1-cm sections. The soil in each section was mixed thoroughly.

The extraction and determination of Cl^- , NO_3^- and NO_2^- was similar to that described in section 4.1 (field experiment). The quantity of soil extracted was reduced to 5g due to the limited quantity of soil in each 1-cm section. Chloride content was determined using a Buchler Digital Chloridometer equipped with Ag and Pt electrodes. The concentrations of Cl^- and NO_3^- -N were expressed as ppm Cl or N based on both dry soil weight and soil solution. The water content of samples was expressed in % based on dry soil weight.

5 RESULTS AND DISCUSSION

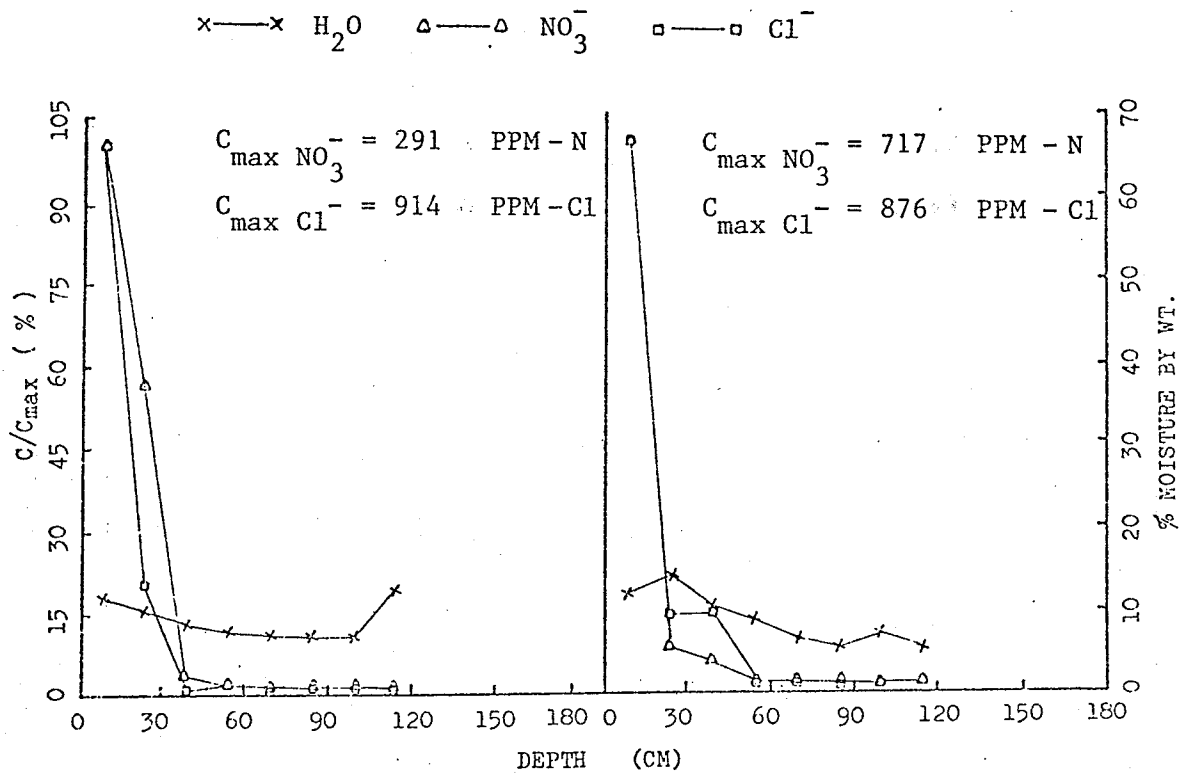
5.1 Field Experiment

5.1.1 1973 Almasippi Sandy Loam Soil Plot

The NO_3^- -N content of the unfertilized Almasippi soil profile varied from 1 to 10 ppm; the Cl^- concentration varied from 10 to 30 ppm. The distribution of NO_3^- , Cl^- and moisture in the unfertilized Almasippi soil at various sampling times are shown in Appendix B. The distribution curves of surface applied NO_3^- and Cl^- and moisture content are shown in Fig. 3 to 8 for the 1973 Almasippi plot. Because of sampling variation and uneven fertilization, the concentrations (C) of NO_3^- -N and Cl^- were expressed as a percentage of the highest concentrations (C_{max}) in the sampling profile i.e. $C/C_{\text{max}} \times 100$. An arbitrary level of 5 to 6 times the concentration in the check soil was chosen as criterion to differentiate between soil samples enriched and not enriched by the added salts. The depth of penetration and the accumulative rainfall between samplings are shown in Table 3.

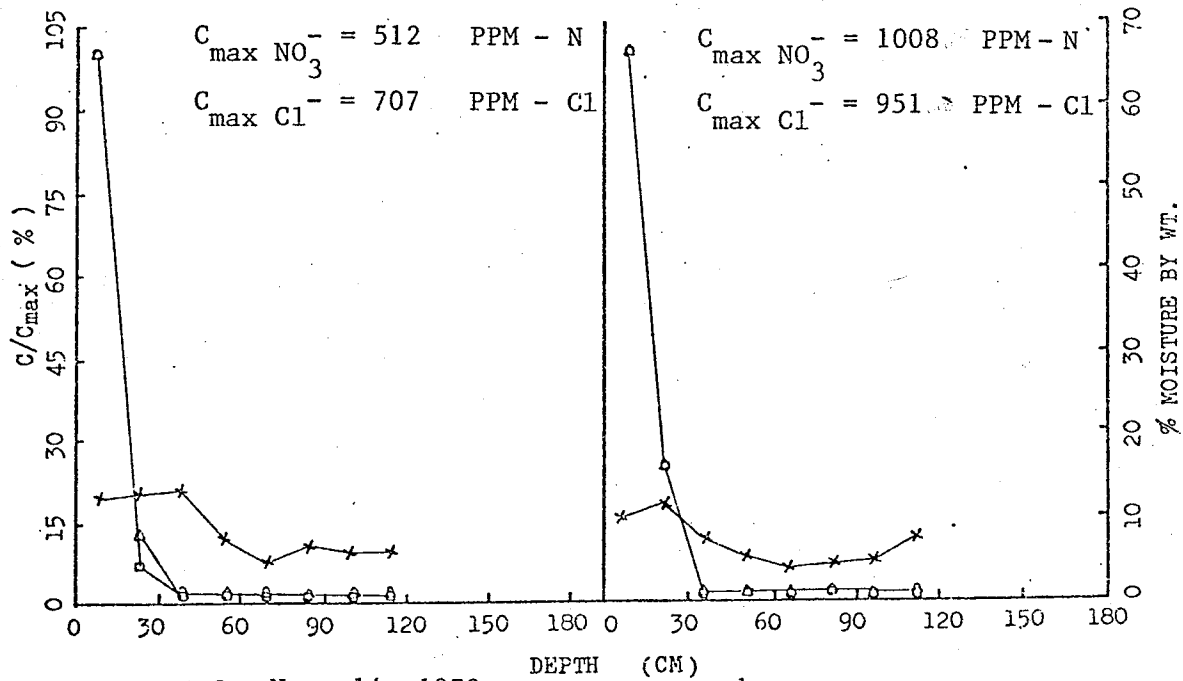
The soil temperatures at various depths for each sampling time are shown in Table 4. The soil temperature increased with increasing depth from October 15, 1973 to March 28, 1974. From April 17 to August 7, 1974, the surface soil temperature increased with time and the temperature decreased with depth. On April 17, 1974, the top 30 cm soil temperature increased to above the freezing point, but the 30-cm zone the soil was still frozen. After August 26, 1974, the temperature of soil profile decreased again. It was clearly shown that the soil temperature was a sine function of time for each depth in a soil profile.

Nitrate and Cl^- both penetrated to depths of 23 cm (Table 3) with most of the salts remaining in the top 15 cm of soil (Fig. 3a) during the



a. Oct. 15, 1973

b. Nov. 2, 1973



c. Nov. 14, 1973

d. Nov. 28, 1973

Fig. 3. Moisture, NO_3^- and Cl^- distribution in 1973 Almasippi plot from Oct. 15, 1973 to Nov. 28, 1973.

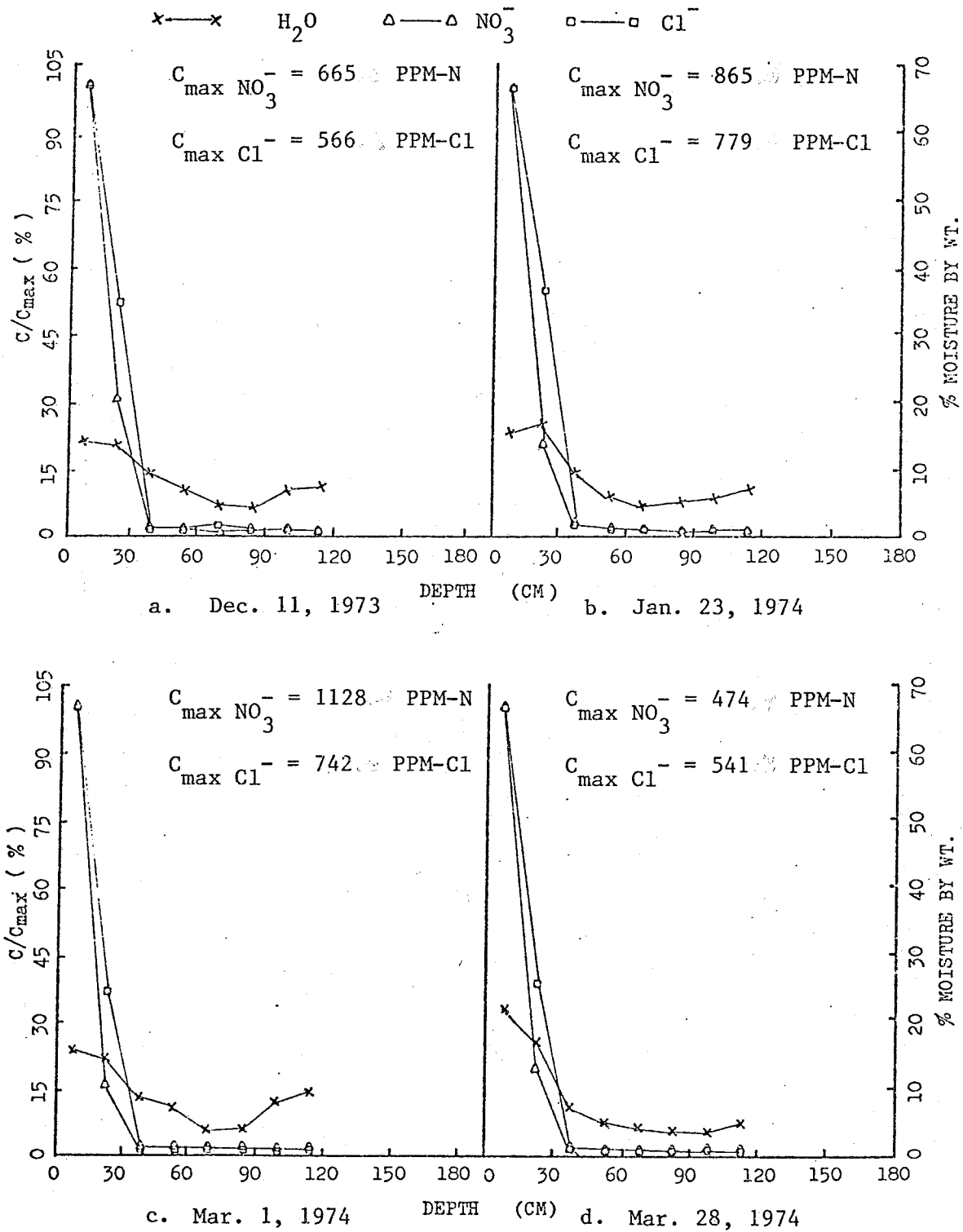


Fig. 4. Moisture, NO_3^- and Cl^- distribution in 1973 Almasippi plot from Dec. 11, 1973 to Mar. 28, 1974.

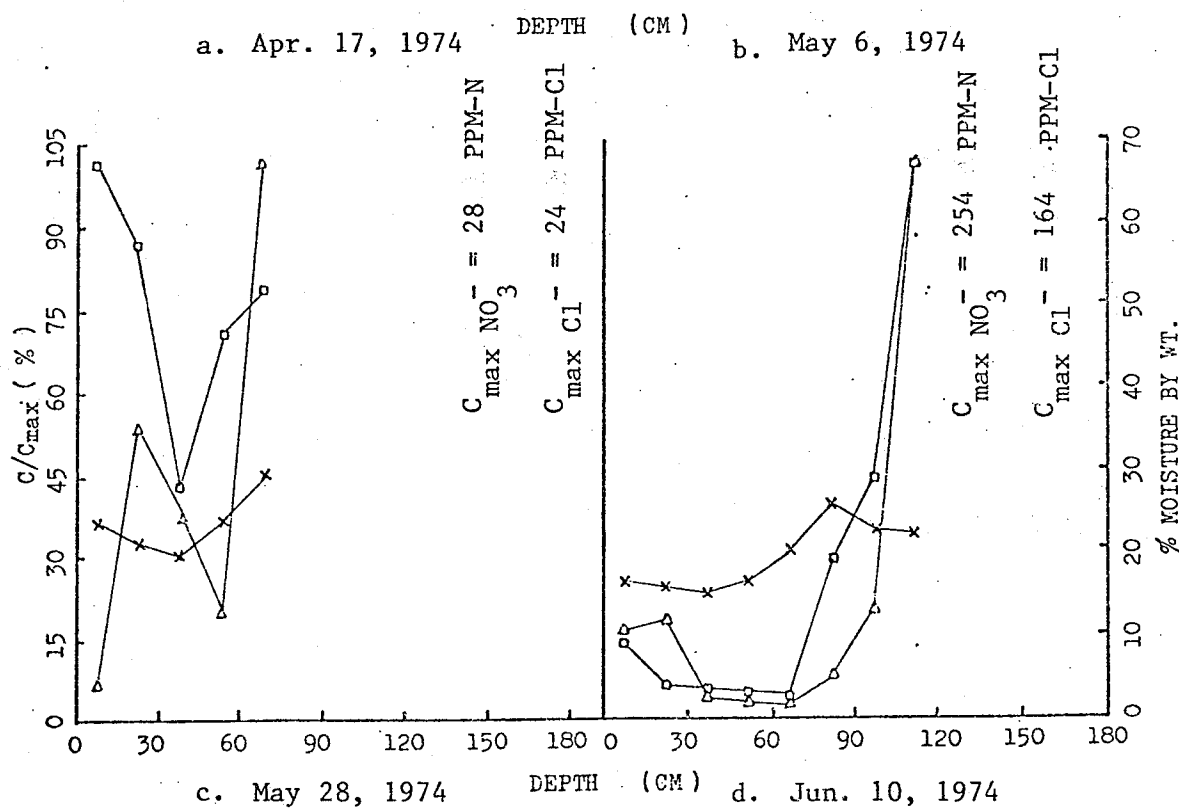
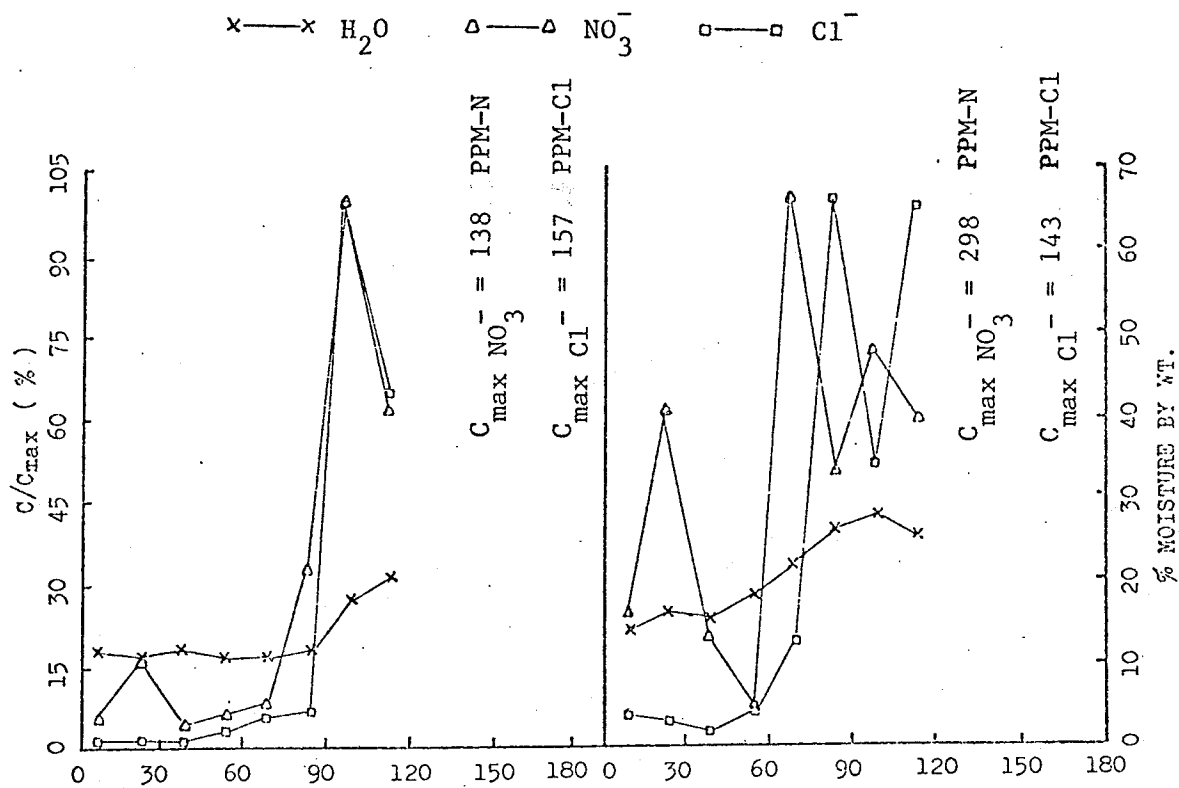


Fig. 5. Moisture, NO_3^- and Cl^- distribution in 1973 Almasippi plot from Apr. 17, 1974 to Jun. 10, 1974.

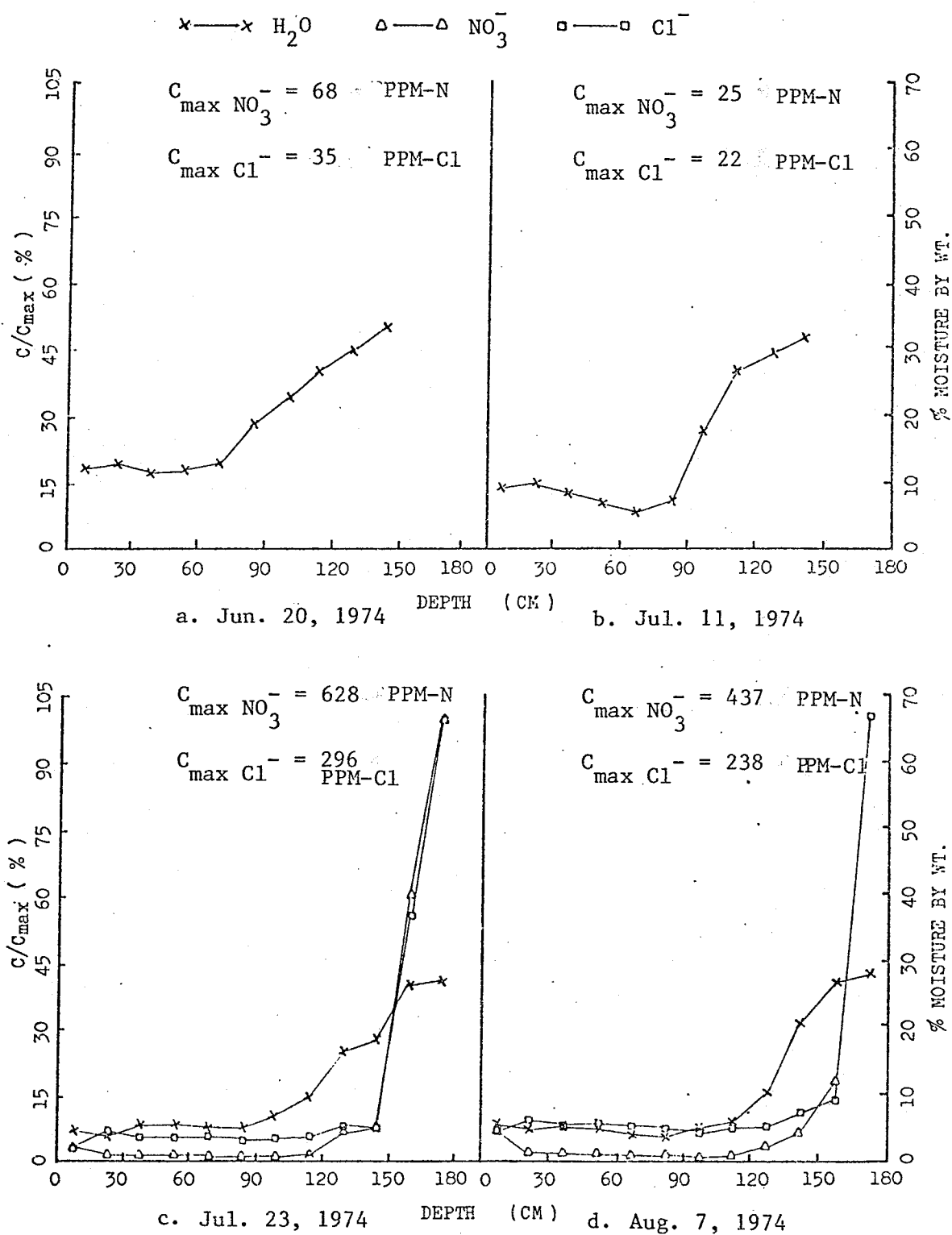


Fig. 6. Moisture, NO_3^- and Cl^- distribution in 1973 Almasippi plot from Jun. 20, 1974 to Aug. 7, 1974.

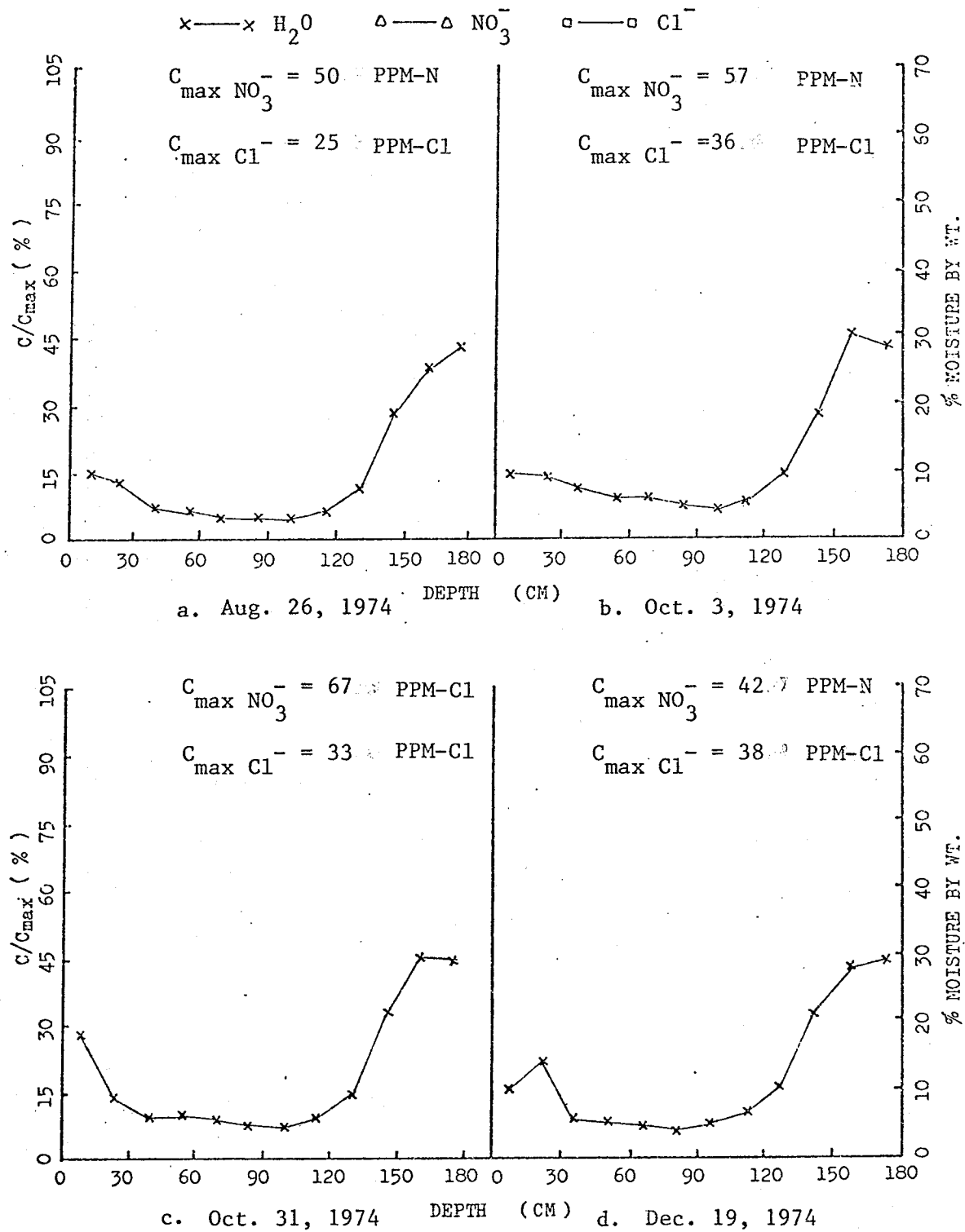


Fig. 7. Moisture, NO_3^- and Cl^- distribution in 1973 Almasippi plot from Aug. 26, 1974 to Dec. 19, 1974.

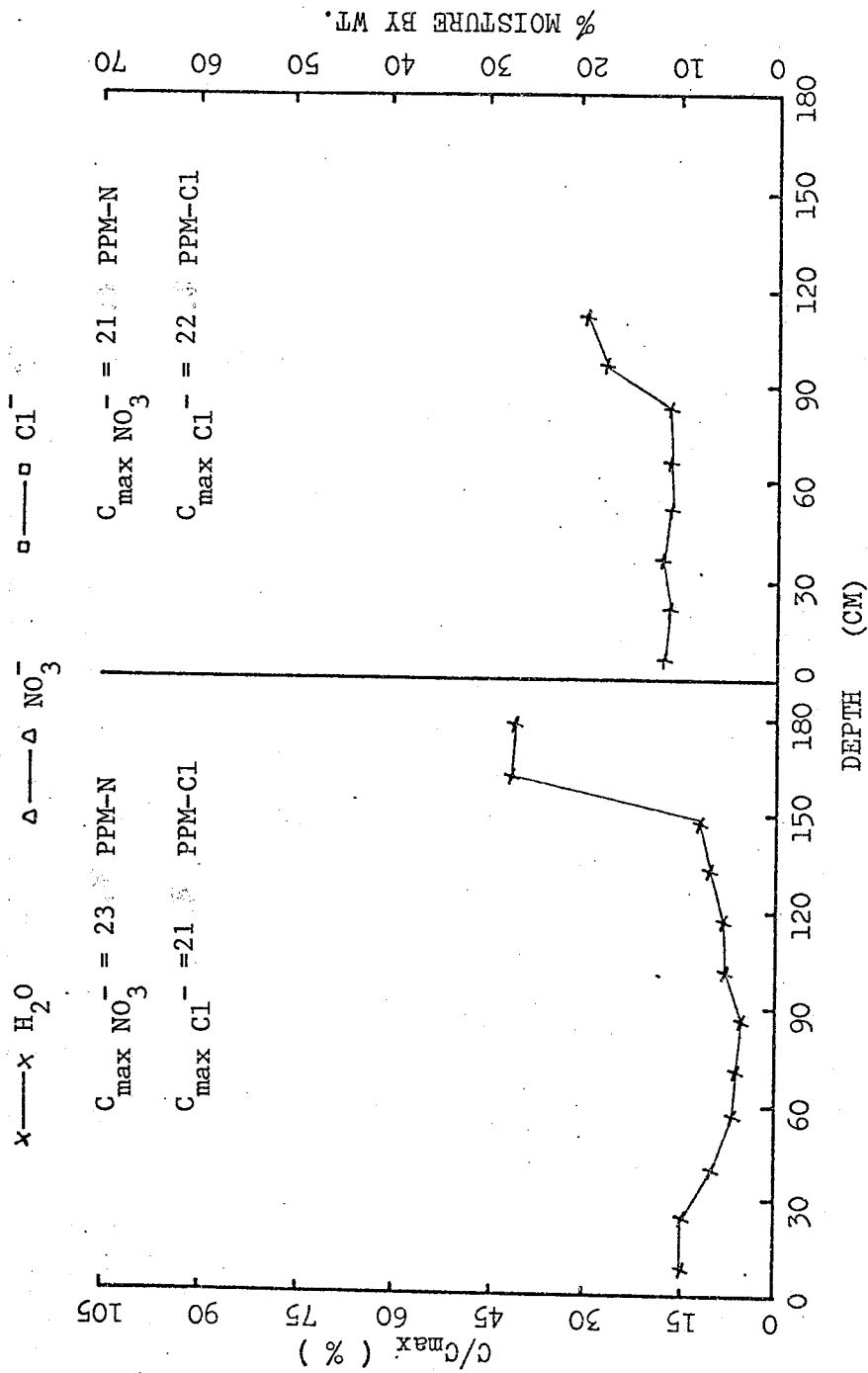


Fig. 8. Moisture, NO_3^- and Cl^- distribution in 1973 Almasippi plot from Feb. 19, 1975 to Apr. 19, 1975.

TABLE 3 AMOUNT OF PRECIPITATION AND DEPTH OF SALT PENETRATION
IN 1973 ALMASIPPI PLOT ON VARIOUS SAMPLING DATES

Sampling Date	Depth of Penetration (cm)		Rainfall (mm)
	NO ₃ ⁻	Cl ⁻	
Oct. 15, 1973	23	23	trace
Nov. 2, 1973	38	38	trace
Nov. 14, 1973	23	23	snow cover
Nov. 28, 1973	23	23	snow cover
Dec. 11, 1973	23	23	snow cover
Jan. 23, 1974	23	23	snow cover
Mar. 1, 1974	23	23	snow cover
Mar. 28, 1974	23	23	snow cover
Apr. 17, 1974	122 ^{**}	122 ^{**}	76.0 [*]
May 6, 1974	122 ^{**}	122 ^{**}	56.0
May 28, 1974	— ^{***}	— ^{***}	107
Jun. 10, 1974	137 ^{**}	137 ^{**}	5.3
Jun. 20, 1974	— ^{***}	— ^{***}	16.0
Jul. 3, 1974	— ^{***}	— ^{***}	trace
Jul. 11, 1974	— ^{***}	— ^{***}	18.0
Jul. 23, 1974	183 ^{**}	183 ^{**}	7.2
Aug. 7, 1974	183 ^{**}	183 ^{**}	6.9
Aug. 26, 1974	— ^{***}	— ^{***}	60.0
to			
Apr. 19, 1975	— ^{***}	— ^{***}	

* Amount of snow thaw equal to the amount of water.

** Applied NO₃⁻ or Cl⁻ appear at water table level.

*** No applied NO₃⁻ or Cl⁻ found above water table level.

TABLE 4 SOIL TEMPERATURE (C) OF 1973 ALMASIPPI PLOT
AT VARIOUS DEPTHS ON VARIOUS SAMPLING DATES

Sampling Date	Depth (cm)									
	2.5	5	10	20	35	50	75	100	125	150
Oct.15, 1973	5.5	5.0	5.0	6.9	—	9.8	—	11.0	—	11.5
Nov. 2, 1973	0.2	1.2	2.6	4.0	5.5	6.8	8.2	9.2	10.5	10.4
Nov.14, 1973	-2.6	-1.6	-0.6	0.0	0.6	1.7	3.4	5.1	6.5	7.5
Nov.28, 1973	-5.2	-3.7	-2.8	-1.4	-0.6	0.2	1.7	2.9	4.2	5.1
Dec.11, 1973	-6.8	-6.1	-5.5	-4.2	-3.2	-2.8	-0.2	1.2	2.3	3.2
Mar. 1, 1974	-4.5	-4.0	-3.8	-3.5	-3.0	-2.6	-1.6	-0.7	0.0	1.0
Mar.28, 1974	-4.5	-3.4	-3.2	-2.7	-2.3	-1.9	-1.0	-0.2	0.2	0.9
Apr.17, 1974	20.2	14.2	7.3	1.4	-0.3	-0.5	-0.5	-0.5	—	-1.1
May 6, 1974	16.0	10.9	5.5	2.2	1.9	1.3	0.0	-1.2	-1.6	-1.2
Jun.10, 1974	17.6	15.5	13.4	11.6	11.4	11.3	10.7	9.5	8.2	6.9
Jun.20, 1974	26.0	21.5	20.0	19.0	17.0	14.5	14.5	13.0	11.0	10.0
Jul.11, 1974	35.8	33.1	28.6	24.1	22.8	21.8	19.3	16.8	15.0	13.2
Jul.23, 1974	35.3	32.8	28.1	25.1	24.7	23.6	21.4	19.4	17.5	15.5
Aug. 7, 1974	37.8	33.5	27.2	24.3	23.8	23.0	21.2	19.1	17.9	16.1
Aug.26, 1974	18.0	16.2	14.8	14.8	16.5	17.2	16.8	16.0	15.2	14.5
Oct.31, 1974	4.5	4.3	4.3	5.7	7.0	7.7	8.0	7.8	8.0	8.3
Dec.19, 1974	-3.5	-4.5	-5.0	-4.6	-3.6	-2.4	0.0	1.4	2.6	3.5
Feb.19, 1975	-3.0	-3.5	-3.7	-3.6	-3.1	-1.6	-0.4	0.4	0.6	1.1
Apr.19, 1975	22.0	20.0	15.0	7.0	2.8	1.9	1.9	1.9	2.8	3.0

first 10 days after application of the salts. The salts penetrated to a depth of 38 cm 18 days after application. However, most of the applied NO_3^- and Cl^- remained in the surface 23 cm of soil. The surface soil started to freeze after November 2, 1973, and the frost front penetrated to 20 cm by November 14, 1973. The salt penetration front seemingly moved upward to the 23-cm depth (Table 3) which was the approximate depth to which frost had penetrated. Samples obtained on November 14, 1973 showed that the majority of the salts remained in the surface soil (Fig. 3). During the period when the surface soil was frozen (November 14, 1973, to March 28, 1974) the concentration, distribution or penetration of NO_3^- and Cl^- in the soil profiles did not change (Fig. 3c,d and Fig. 4).

The water input was about 76.2 cm snow which was equivalent to 7.6 cm rainfall during the spring thaw. After the snow melted and the surface soil started to thaw NO_3^- and Cl^- moved down beyond 122-cm depth even though the soil still had frost between the 75-cm and 150-cm depths on April 17 and May 6, 1974 (Fig. 5a,b). There was about 5.6 cm rainfall between April 17 and May 6, 1974. The recoveries for both Cl^- and NO_3^- were very low and amounted to only about 20-30% of the amount applied. The salt front did not appear to move between April 17 to May 6, 1974. The water table was very high and was located at the 64-cm depth on May 28, 1974. The amount of rainfall was 10.7 cm, during the May 6 to May 28, 1974 period. This rise of the water table may have been due to the lateral movement of ground water. The high Cl^- and NO_3^- concentrations in the deeper profile (the location of depth varied with sampling time) of the check soil (Shown in Appendix B) also suggested that lateral movement of ground water had occurred. The applied salts could not be found

in the soil profile above the water table on May 28, 1974 (Fig. 5c). Fig. 6c shows the distribution curves of NO_3^- and Cl^- in the soil profile on June 10, 1974. The water table moved down to the 122-cm depth and the applied NO_3^- and Cl^- were located just above the water table.

The level of water table was at the 152-cm depth on June 20 and July 11, 1974. The applied NO_3^- and Cl^- was not found in the soil above the water table (Fig. 7a,b). As the water table dropped the applied NO_3^- and Cl^- was found in the soil profiles at the 168-cm depth on July 23, 1974 and at 183 cm on August 7, 1974 (Fig. 7c,d). From August 26, 1974 to the end of this experiment, February 19, 1975, the NO_3^- and Cl^- concentrations in the soil profile were less than one tenth of the amount applied. The maximum concentrations of NO_3^- and Cl^- for every sampling profile from August 27, 1974 to February 19, 1975 are shown in Fig. 8. It was concluded that the applied NO_3^- and Cl^- were lost completely from the soil profile.

The moisture distribution in the soil profile also changed with seasons. The surface soil was colder than the subsoil from time of application of salt to March 28, 1974 and the moisture content of the top 38 cm soil was higher than that of lower horizons (Fig. 3 and 4). The average volumetric moisture content of the top 30 cm soil was about 12% which was the field capacity of this soil and the average moisture content of the subsoil was about 4%. After the spring thaw the temperature decreased with increasing depth and the temperature gradient was very great during the period April 17 to June 10, 1974. The total input of water into the soil was about 76.0 mm. The moisture content of the top 46 cm soil was almost uniform and was higher than the moisture content of the soil profile during the winter period. The moisture content of the soil

profile increased with depth to about 33% at the top of the water table.

The temperature on the surface soil continuously increased during June 20 to August 7, 1974. Due to only trace amounts of rainfall during this period the moisture content of the soil profile decreased except near the water table. The surface soil temperature reached a high of 37.8 C and the moisture content decreased to 3 or 4% (Fig. 7). The low moisture content in the top part of the soil profile might have caused the upward movement of moisture which might account for the reappearance of some of the applied salt in the soil profile at the July 23, 1974 sampling dates (Fig. 7c,d).

On August 26, 1974 the temperature was almost uniform throughout the soil profile from 0 cm to 150 cm. The increase in the moisture content for the surface soil on August 26, 1974 was mainly due to the 5.5 cm of rainfall between August 7 and August 26, 1974. When the surface soil temperature decreased the temperature increased with depth. The moisture content of the top soil was higher than that of the subsoil except near the water table (Fig. 8).

The salts, $\text{Ca}(\text{NO}_3)_2$ and CaCl_2 , applied on the soil surface in the fall penetrated down to the 23 cm depth before the soil froze. Between freeze-up and the spring thaw, the distribution of NO_3^- and Cl^- did not change. The major portion of the applied NO_3^- and Cl^- moved out of the soil profile during the spring thaw. On the basis of the total input of the water (Table 3) during the spring thaw period, the average of volumetric moisture content (12.7%) before the snow melt and the soil water holding capacity of this soil (21% by volume) the water front could reach a depth of 92.2 cm under isothermal conditions. The downward movement of water alone did not seem to account for the salt movement. Thermal

gradients might be another possible driving force for salt movement. The moisture content of the surface soil was a function of rainfall and soil temperature. When the surface soil temperature was lower than the subsoil temperature the moisture content of surface soil was about 12%. As the temperature of surface soil increased the moisture content of surface soil decreased to 3%. It was not known whether the decrease in the moisture content was solely due to thermal effects or due to the combined effects of thermal forces and evaporation. The movement of Cl^- and NO_3^- was similar in this study.

5.1.2 1974 Almasippi Sandy Loam Soil Plot

The salts were applied on the plot on July 3, 1974. The criteria for determining the depth of the salt penetration front and the soil temperature distribution of the soil profile at all sampling times were the same as in the previous study. The depth of penetration and the accumulative amount of rainfall are shown in Table 5. Fig. 9 shows the distribution of Cl^- and NO_3^- in the soil profile on July 11, July 23, August 7, and August 26, 1974. Salts moved down to 23 cm during the first 8 days after application. The rainfall between July 3 and July 11, 1974 was 1.8 cm. Moisture content of the surface soil decreased from July 11 to August 7, 1974. However, the depth of penetration of Cl^- and NO_3^- remained unchanged (Table 5). The majority of the applied salts remained in the top 15 cm of soil during this period. On August 26, 1974 the majority of the Cl^- remained in the surface soil, although, most of the NO_3^- moved down to 38 cm. Rainfall from August 7 to August 26 was 55.0 mm. This amount of rainfall might be responsible for the movement of salts.

As the surface soil temperature decreased the surface moisture increased. This has been discussed in section 5.1.1. The major portions

TABLE 5 · AMOUNT OF PRECIPITATION AND DEPTH OF SALT PENETRATION
IN 1974 ALMASIPPI PLOT ON VARIOUS SAMPLING DATES

Sampling Date	Depth of Penetration (cm)		Rainfall (mm)
	NO ₃	Cl	
Jul. 11, 1974	23	23	18.0
Jul. 23, 1974	23	23	7.2
Aug. 7, 1974	23	23	6.9
Aug. 26, 1974	38	38	55
Oct. 3, 1974	53	53	trace
Oct. 31, 1974	53	53	4.6
Dec. 19, 1974	53	53	snow cover
Feb. 19, 1975	53	53	snow cover
Apr. 19, 1975	122*	122**	70.0*

* Amount of snow thaw equal to the amount of water.

** Applied NO₃⁻ or Cl⁻ appear at water table level.

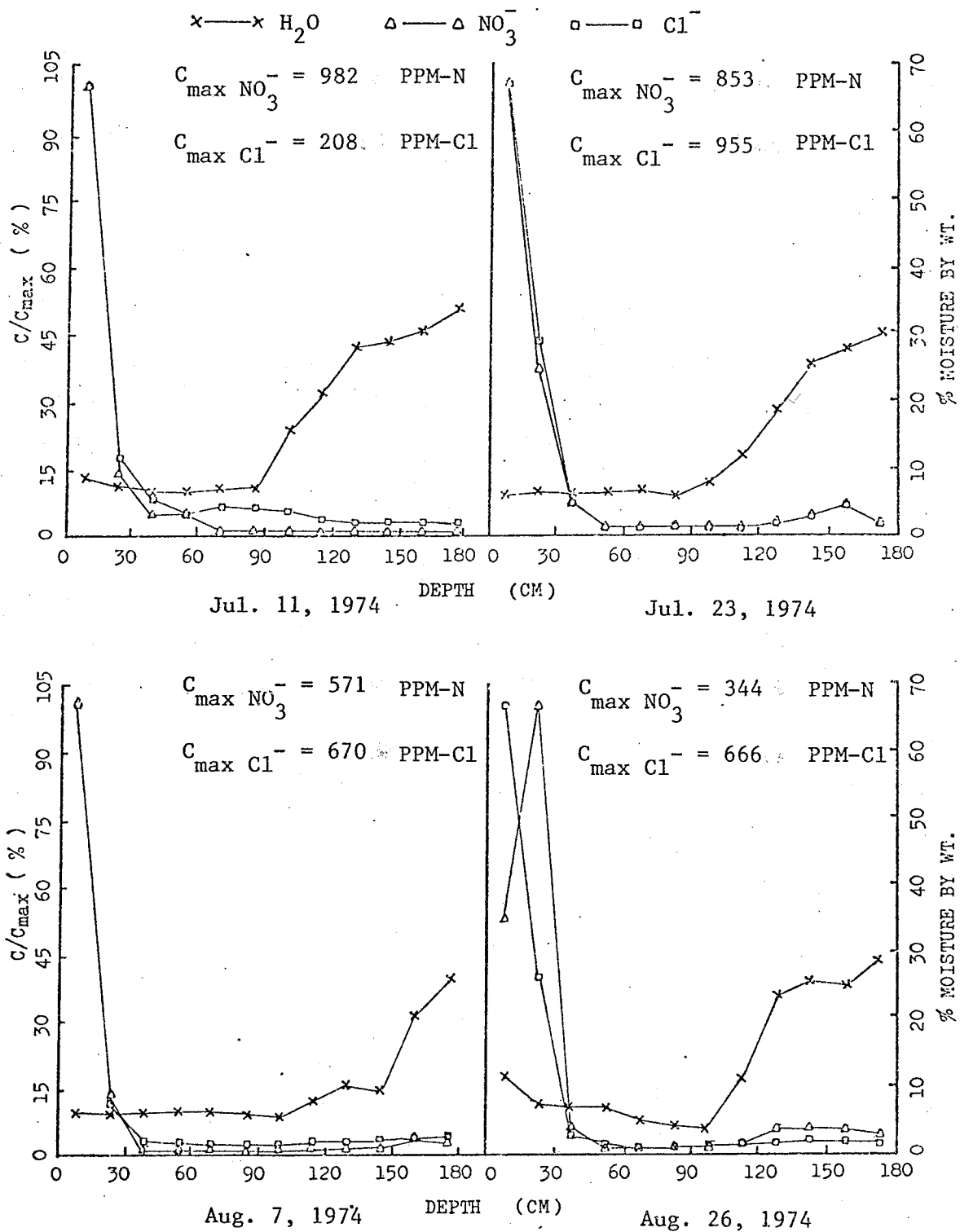


Fig. 9. Moisture, NO_3^- and Cl^- distribution in 1974 Almasippi plot from Jul. 11, 1974 to Aug. 26, 1974.

of both Cl^- and NO_3^- were located at the 23-cm depth but the penetration front of both Cl^- and NO_3^- moved down to 53 cm on October 3, 1974 (Fig. 10) even though trace amounts of rainfall were recorded. Fig. 10b,c and d show that the locations for both salt penetration fronts and C_{max} 's were unchanged during the winter period. This result was similar to that obtained in the previous study (Section 5.1.1) i.e. the concentration profiles of Cl^- and NO_3^- did not change during the winter. Again after the spring thaw both Cl^- and NO_3^- disappeared from the soil profile (Fig. 11).

The results indicate that summer-applied salt remains close to the surface until the next spring thaw. Some local movement occurs due to occasional precipitation. However, during spring thaw the salts are rapidly transported downward in the soil profile.

5.1.3 Red River Clay Soil Plot

The Cl^- content of the Red River clay was very high and variable (Table 1). This high initial Cl^- content obscured measurements of the movement of applied Cl^- . Therefore the results of movement of applied Cl^- are not presented. The concentration of NO_3^- in this soil prior to addition of NO_3^- was also higher than that of the Almasippi sandy loam. Because of the high initial NO_3^- -N concentration in the soil profile, the criterion for determining the depth of applied NO_3^- penetration was chosen to be twice the concentration of the check soil. The depth of NO_3^- penetration and the accumulative amount of rainfall between two sampling times are shown in Table 6. The soil temperature profiles at each sampling time are listed in Table 7. The only winter soil temperature measurement was conducted on November 14, 1973. Soil temperatures increased then decreased with time for each depth from May 6 to Oct. 31, 1974. The soil temperature decreased with depth from May 6 to August 26, 1974 but

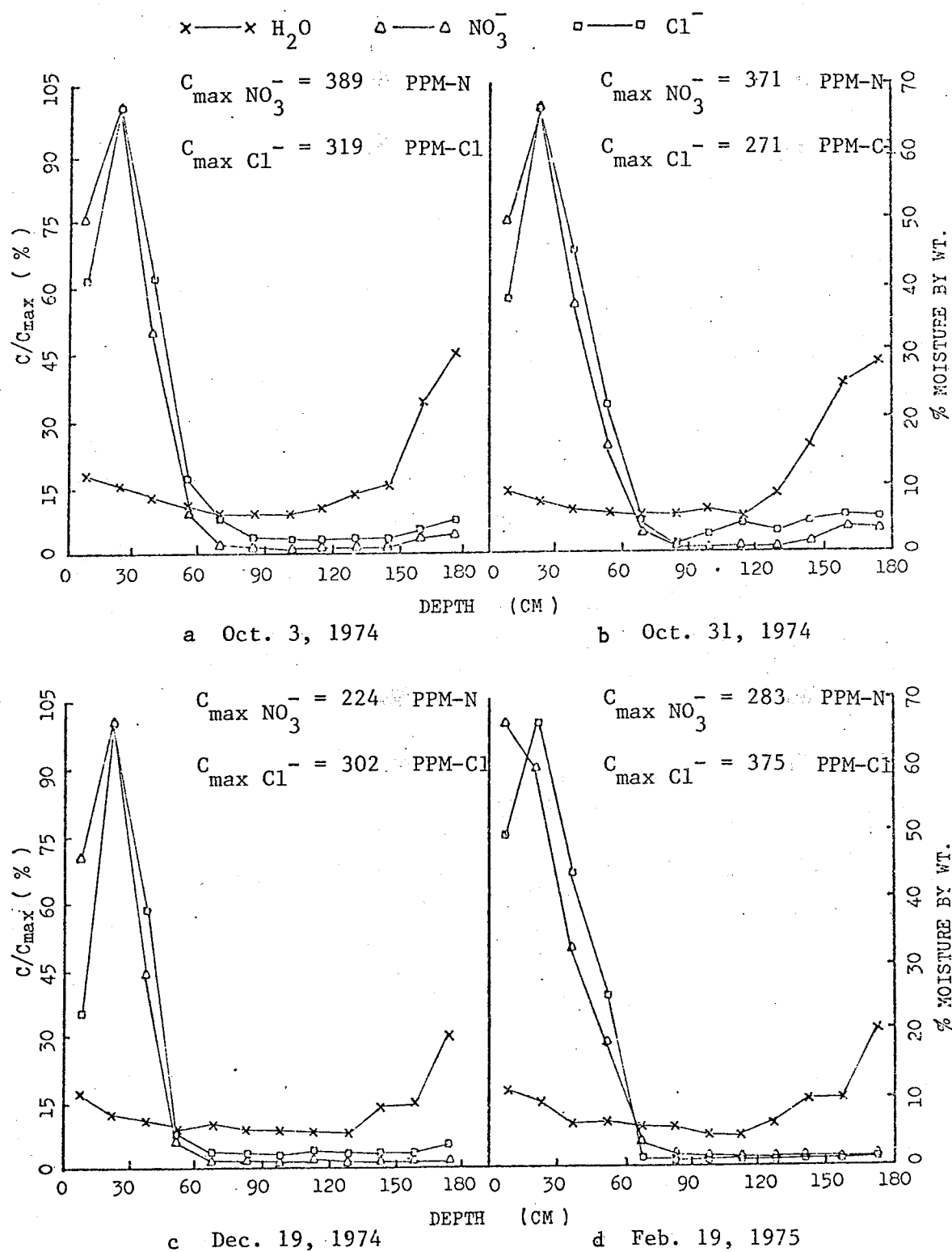


Fig. 10. Moisture, NO_3^- and Cl^- distribution in 1974 Almasippi plot from Oct. 3, 1974 to Feb. 19, 1975.

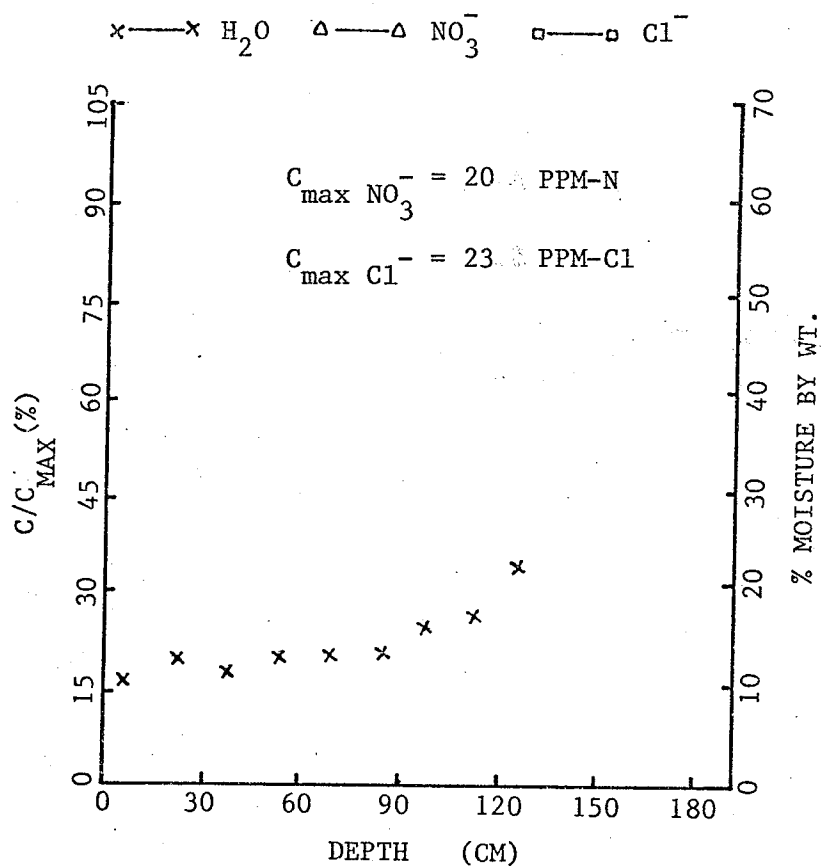


Fig. 11. Moisture, NO_3^- and Cl^- distribution in 1974 Almasippi plot on Apr. 19, 1975.

TABLE 6 AMOUNT OF PRECIPITATION AND DEPTH OF SALT PENETRATION
IN RED RIVER CLAY PLOT ON VARIOUS SAMPLING DATES

Sampling Date	Depth of Penetration (cm) NO_3^-	Rainfall (mm)
Nov. 14, 1973	23	snow cover
May 6, 1974	23	132*
Jun. 20, 1974	23	178
Jul. 4, 1974	23	4.3
Aug. 7, 1974	23	37.0
Aug. 26, 1974	23	65.0
Oct. 2, 1974	23	53.0*
Oct. 31, 1974	23	13.0*

* total precipitation in terms of rainfall.

TABLE 7 SOIL TEMPERATURE (C) OF RED RIVER CLAY PLOT
AT VARIOUS DEPTHS ON VARIOUS SAMPLING DATES

Sampling Date	Depth (cm)								
	2.5	5	10	20	35	50	75	100	150
Nov. 14, 1973	-2.0	-1.2	-0.1	1.0	2.0	4.2	5.5	6.5	8.3
May 6, 1974	12.6	11.3	7.5	2.5	0.3	-1.5	-2.0	-2.1	-1.7
Jun. 20, 1974	35.5	27.0	20.5	12.5	14.5	12.0	10.5	9.2	7.5
Jul. 4, 1974	34.2	31.2	24.7	19.2	18.2	16.6	13.4	9.6	7.7
Aug. 7, 1974	33.4	31.8	27.4	22.9	20.8	19.3	17.6	14.9	12.7
Aug. 26, 1974	25.2	23.3	19.4	16.9	16.9	17.3	16.1	14.2	13.2
Oct. 31, 1974	5.8	5.8	5.7	6.2	6.8	6.9	6.9	7.4	7.5

increased with depth on November 14, 1973 and October 31, 1974.

The salts were applied on November 2, 1973. There were no winter samples obtained as sampling of the frozen clay soil was very difficult. Fig. 12, 13 and 14 show the results of moisture content and NO_3^- distribution from November 14, 1973 to October 31, 1974. The applied NO_3^- penetrated to a depth 23 cm but most of the applied NO_3^- stayed in the surface zone 12 days after application. The pattern of NO_3^- distribution and the depth of NO_3^- penetration did not change appreciably from November 14, 1973 until October 31, 1974.

The movement of applied NO_3^- in sandy loam soil was different from that in clay for the fall surface-applied salts. The applied NO_3^- moved mainly downward during the period of spring thaw in the sandy loam soil. Nitrate did not move down at all over the period of a year in the clay soil. A clay soil has a higher porosity than a sandy soil. However, the average pore size of a clay soil is smaller than that of a sandy soil. The continuity of air space under field conditions in a clay may be almost non-existent. These physical characteristics could have contributed to the retention of the applied salt near the soil surface in the clay soil.

5.2 Laboratory Experiments

The distribution of moisture and Cl^- in vertical soil columns with 27% moisture and 10% KCl for 5 and 10 days under isothermal conditions (at room temperature) are shown in Fig. 15. Neither moisture nor the Cl^- ion moved under the influence of gravitational force alone. The existence of an air gap within the soil column also did not affect the distribution of either moisture or the Cl^- ion under isothermal conditions.

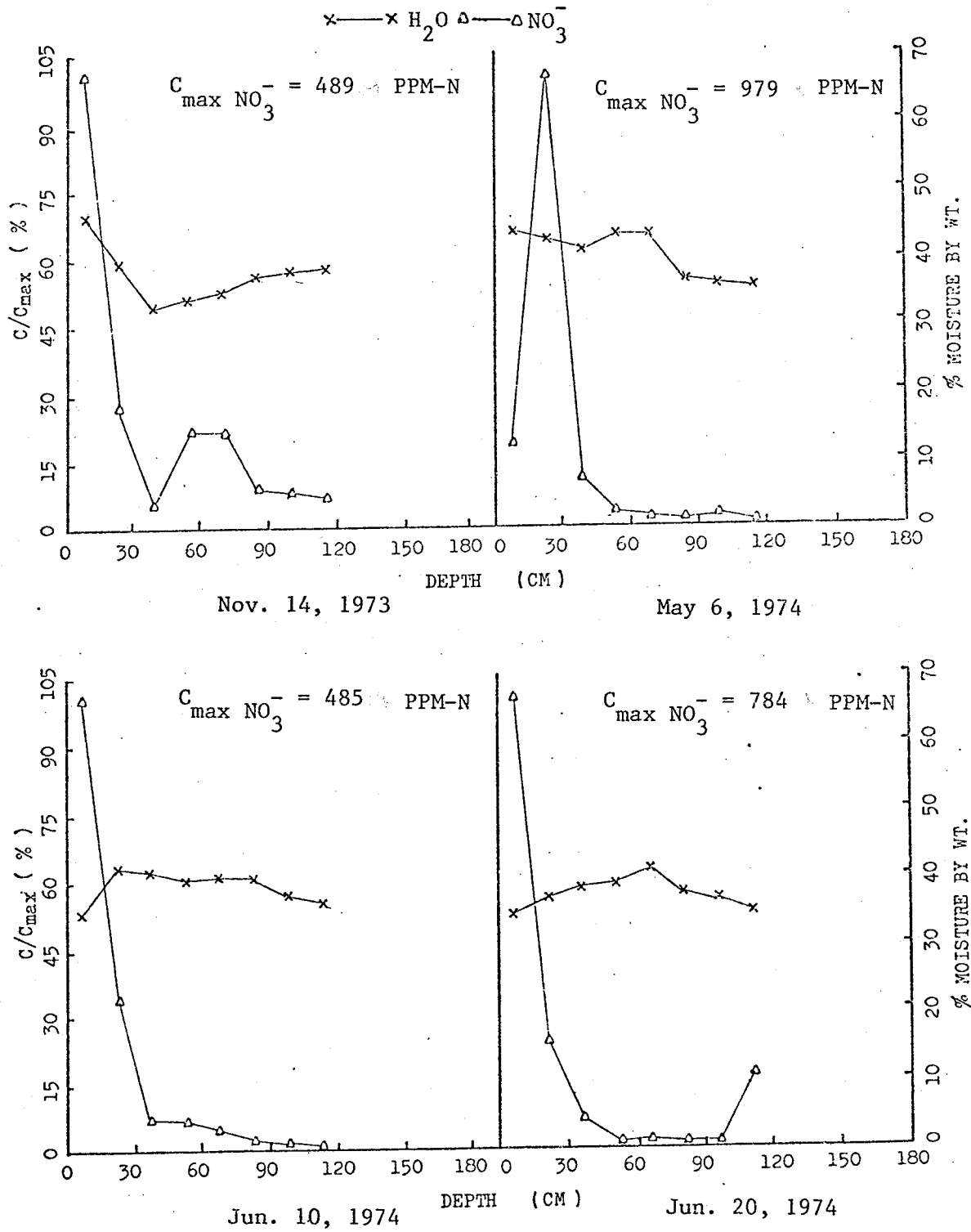


Fig. 12. Moisture and NO_3^- distribution in Red River clay plot from Nov. 14, 1973 to Jun. 20, 1974.

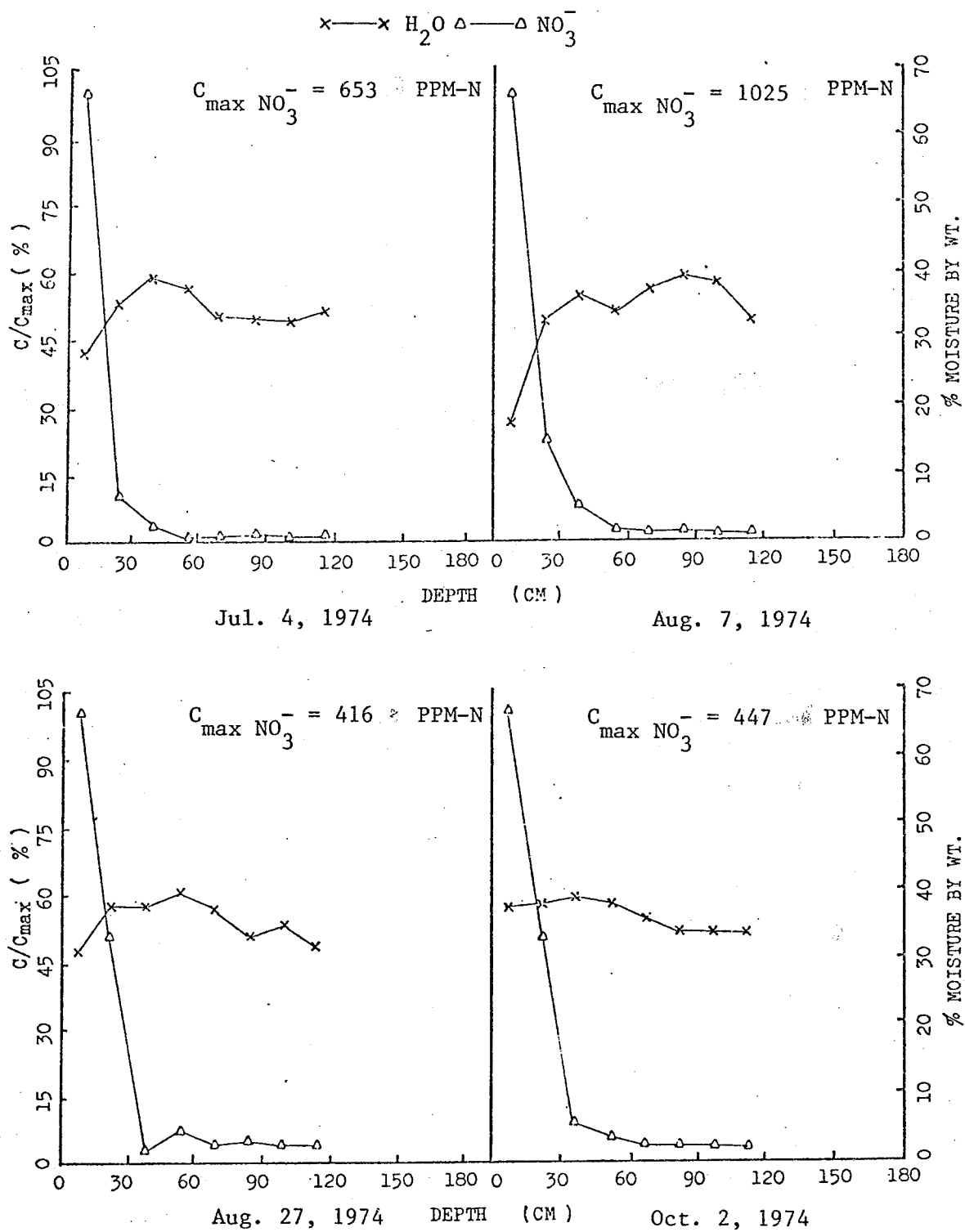


Fig. 13. Moisture and NO_3^- distribution in Red River clay plot from July 4, 1974 to Oct. 2, 1974.

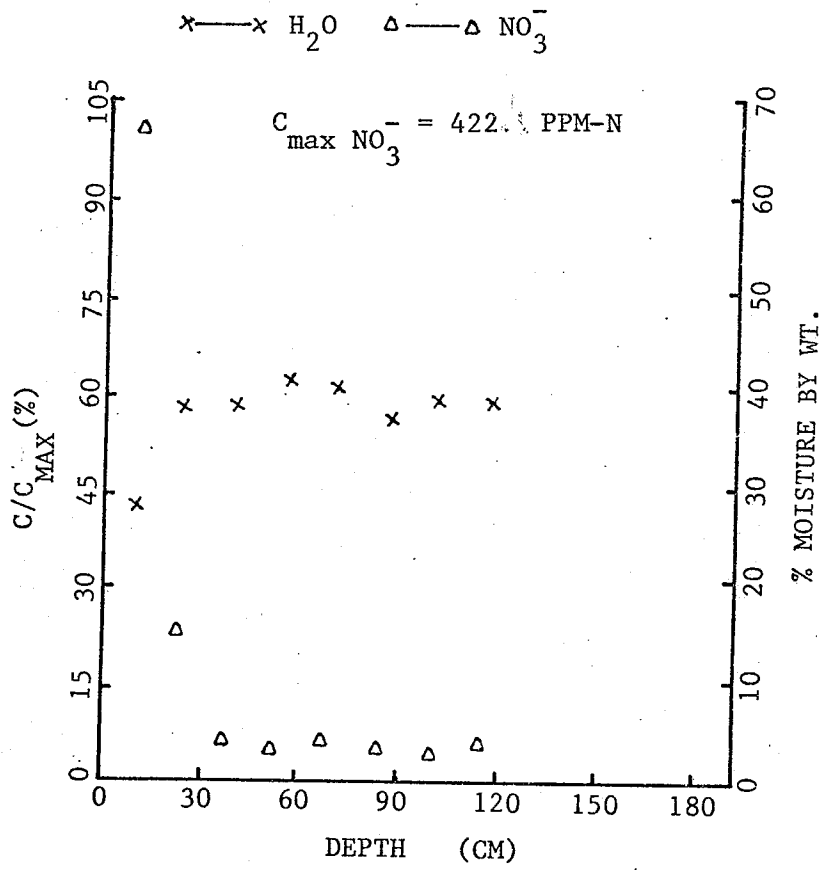


Fig. 14. Moisture and NO₃⁻ distribution in Red River clay plot on Oct. 31, 1974.

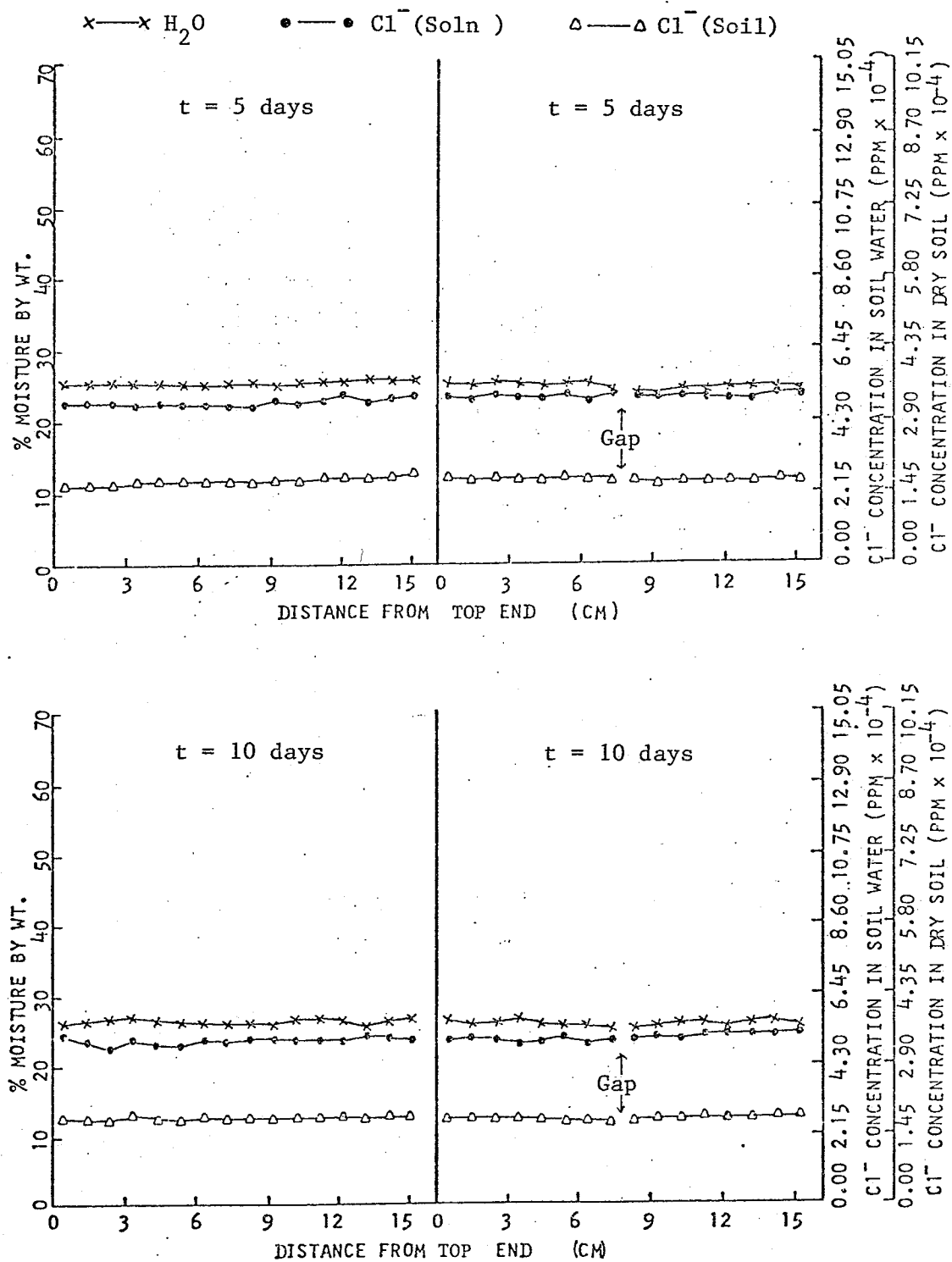


Fig. 15. Moisture and Cl^- distribution in $\text{Ca}(\text{NO}_3)_2$ and KCl -treated columns without temperature gradients (initial $\text{H}_2\text{O} = 27\%$ and $\text{KCl} = 10\%$).

5.2.1 Effect of Moisture and Salt Concentrations on Thermal Mass Transport

All of the soil columns employed for this study were placed vertically with the cold side on the bottom. As far as stability of soil moisture was concerned this geometrical arrangement was the most stable configuration. Initial moisture contents of 23, 27 and 32% were chosen for the study of the effect of moisture content on water movement under a temperature gradient. The temperature distribution of the soil columns reached steady state several hours after the thermal treatment was initiated. The resulting temperature profiles for soil columns with initial moisture contents of 23, 27 and 32% are shown in Fig. 16. The temperature distributions were nonlinear and increased asymptotically with increasing distance from the cold end. This nonlinear temperature distribution was mainly due to incomplete insulation and non-uniform moisture distribution. Even when identical temperatures were imposed on all of the soil columns, the temperature distribution was different. The differences in temperature distribution patterns among the different moisture contents and between the columns with and without an air gap at the same initial moisture content could be due to the effects of moisture content on thermal conductivity.

For the purpose of clarity, soil columns without an air gap will be called continuous soil columns and those with an air gap will be called discontinuous soil columns. The distribution of continuous patterns of moisture in the soil columns 10 days after initiation of the temperature treatment are shown in Fig. 17. There was very little or no net water flow in the soil column with an initial moisture content of 23%. A relatively greater net moisture transport to the cold end was found in the column with 27% moisture content than in the soil column at 32% moisture

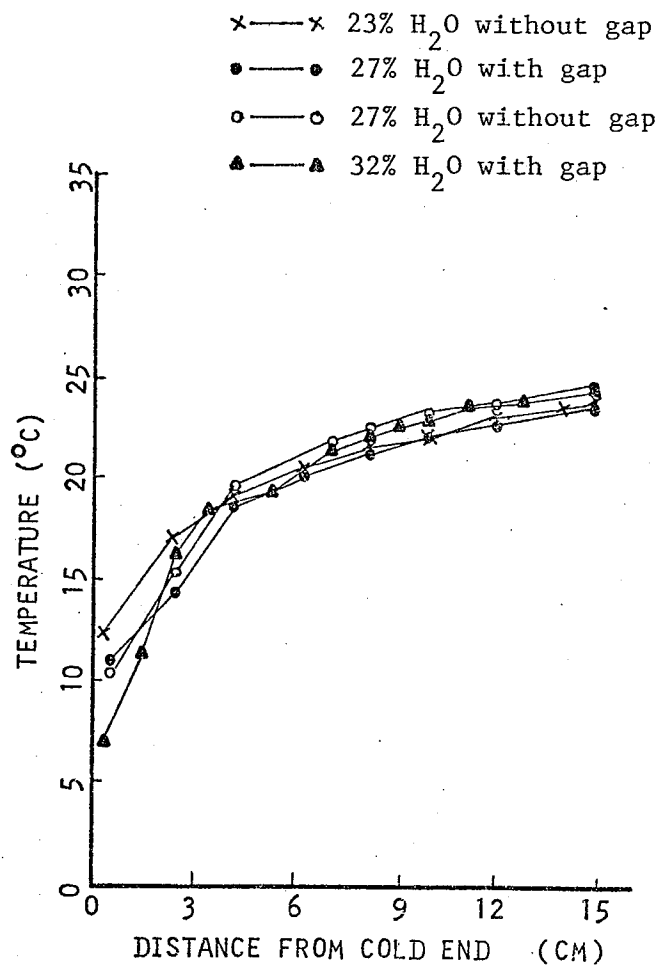


Fig. 16. Temperature distribution in soil columns with various initial moisture contents after 4 hours of thermal treatment.

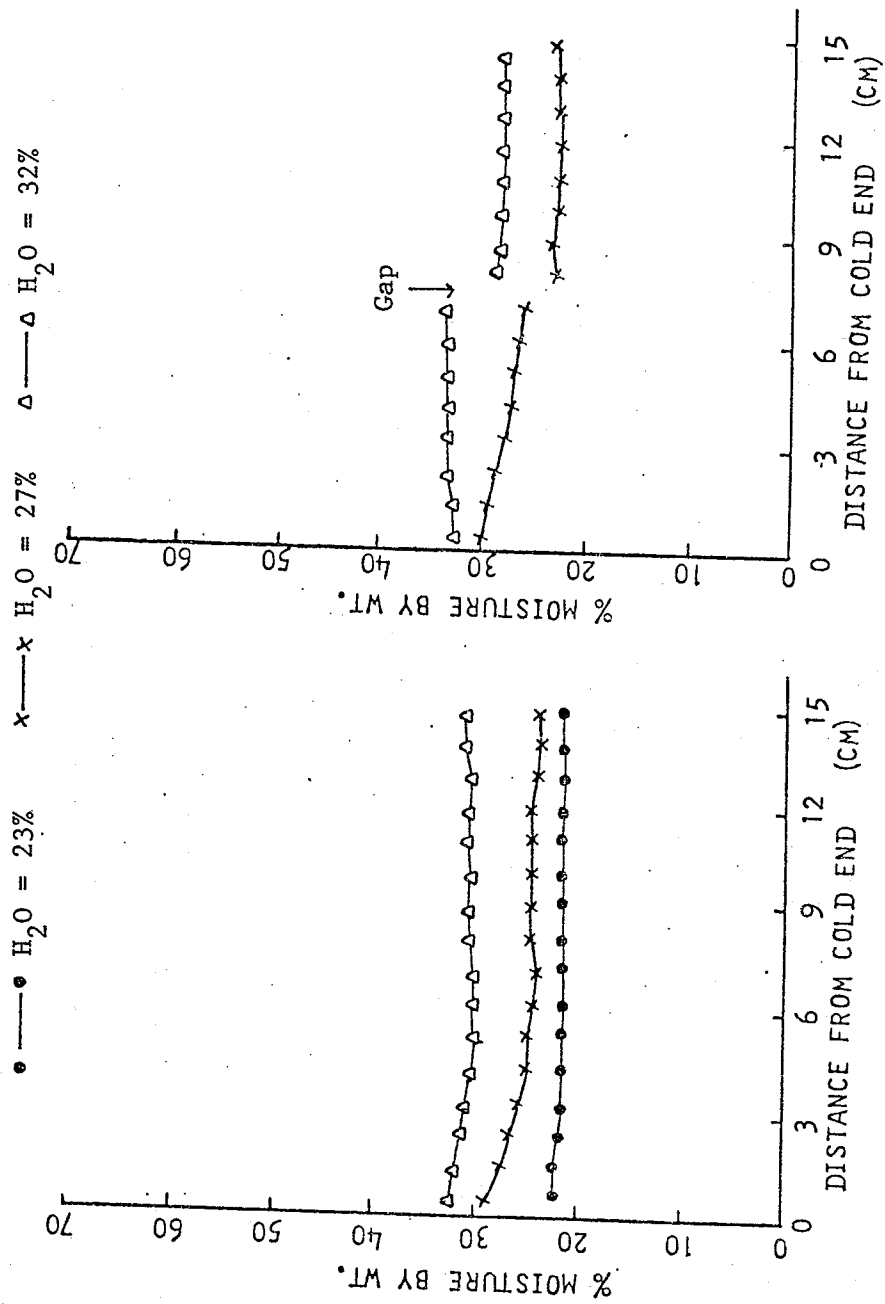


Fig. 17. Moisture distribution in soil columns with or without air gap after 10 days of thermal treatment (no salt added).

content (Fig. 17). Moisture gradients, directed from the cold end to the warmer part, formed in the soil columns. The magnitude of the gradient was greater at 27% moisture than at 32%. Smaller moisture movement in relatively dry and wet soil columns as compared to intermediate moisture content under a temperature gradient was also found by Gurr et al. (1952). The drying moisture characteristic curve (Fig. 18) indicates that at 23, 27 and 32% moisture content soil water was held at tensions of 1732, 565 and 282 cm-H₂O suction, respectively.

Moisture transport to the colder region was greater in the discontinuous soil column (an air gap in the middle of the column) than in the continuous soil column (no air gap) (Fig. 17). The air gap was used as a semipermeable membrane to vapor. The greater water movement in the discontinuous column as compared to the continuous column suggested that the moisture moved to the cold end in the vapor phase and the returning liquid flow did not cross the air gap. If there was no return of liquid flow in the closed soil column the rate of moisture flow should be equal for columns with or without an air gap under the influence of an identical thermal gradient. The higher water transfer in the discontinuous column was explained on the assumption that the gap prevented the return flow of liquid condensed at the cold region. In addition to the above explanation, a slightly higher thermal gradient between the ends of the air gap, more air space (more than 50%) and larger pores for vapor flow at both ends of the air gap than in the soil itself could partially contribute to the greater water movement in the discontinuous soil column as compared to the continuous soil column. Vapor movement in the soil column under a temperature gradient was an important mechanism for soil water movement. The vapor pressure of free water at various temperatures

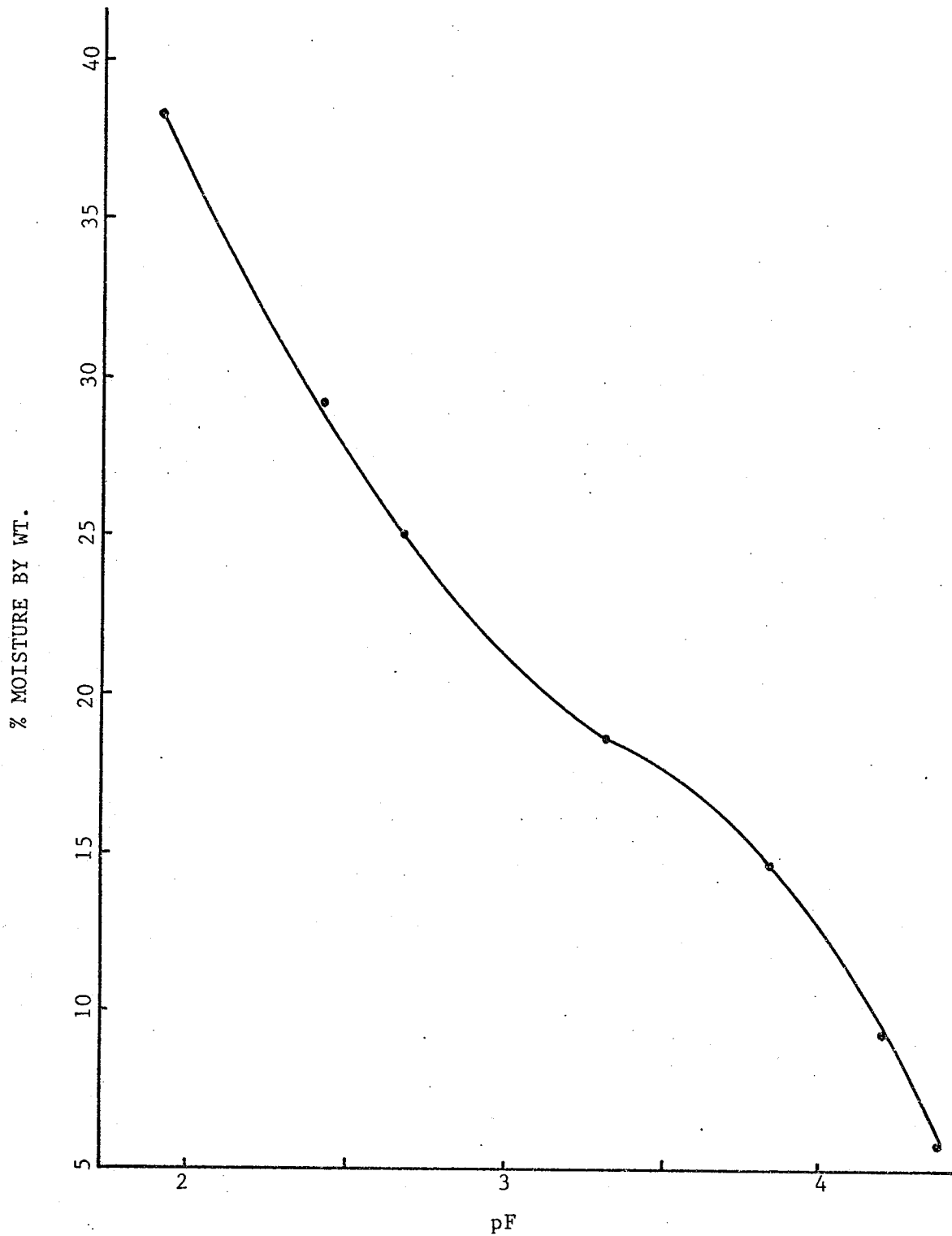


Fig. 18. Moisture characteristic curve of Wellwood clay loam at 22 C.

is shown in Table 8. The relative humidity of the soil atmosphere under suctions of 0 to 15 bar decreases from 100 to 98.8%. Within experimental error, the values in Table 8 could be directly used to describe vapor pressures in the soil column. The vapor pressure changed from 4.715 mm-Hg at the cold end to 21.583 mm-Hg at the warm end for the column with 27% moisture. The average vapor pressure change was about 0.733 mm-Hg per degree in the temperature range of 0.5 to 25 C.

TABLE 8 SATURATED VAPOR PRESSURE OF WATER
AT VARIOUS TEMPERATURES

T C	Pressure mm-Hg
0	4.579
5	6.543
10	9.209
15	12.788
20	17.535
25	23.756

KCl was employed not only as a vapor pressure depressor but also an indicator of liquid water movement. The vapor pressure of an aqueous solution of KCl at various concentrations is listed in Table 9. The change in vapor pressure by the addition of KCl seemed less important than the change in vapor pressure due to a temperature gradient. Because of the possible difference in the behavior of NO_3^- and Cl^- , the behavior of NO_3^- and Cl^- was compared. Chloride concentrations of 0, 10 and 20% based on soil solution were used. The distribution curves of moisture content and Cl^- concentration for columns at 27% initial moisture content and 10 days of thermal treatment are shown in Fig. 19. Moisture movement was only slightly affected by changes in salt concentration for both continuous and discontinuous soil columns (Fig. 17, 19). There was only a 5% difference

TABLE 9 VAPOR PRESSURE OF AQUEOUS SOLUTIONS
OF KCl*

Concentration mole/l	Pressure** mm-Hg
0.0	760.0
0.5	747.8
1.0	735.6
2.0	711.2

* From Smithsonian Tables.

** At temperature 100 C.

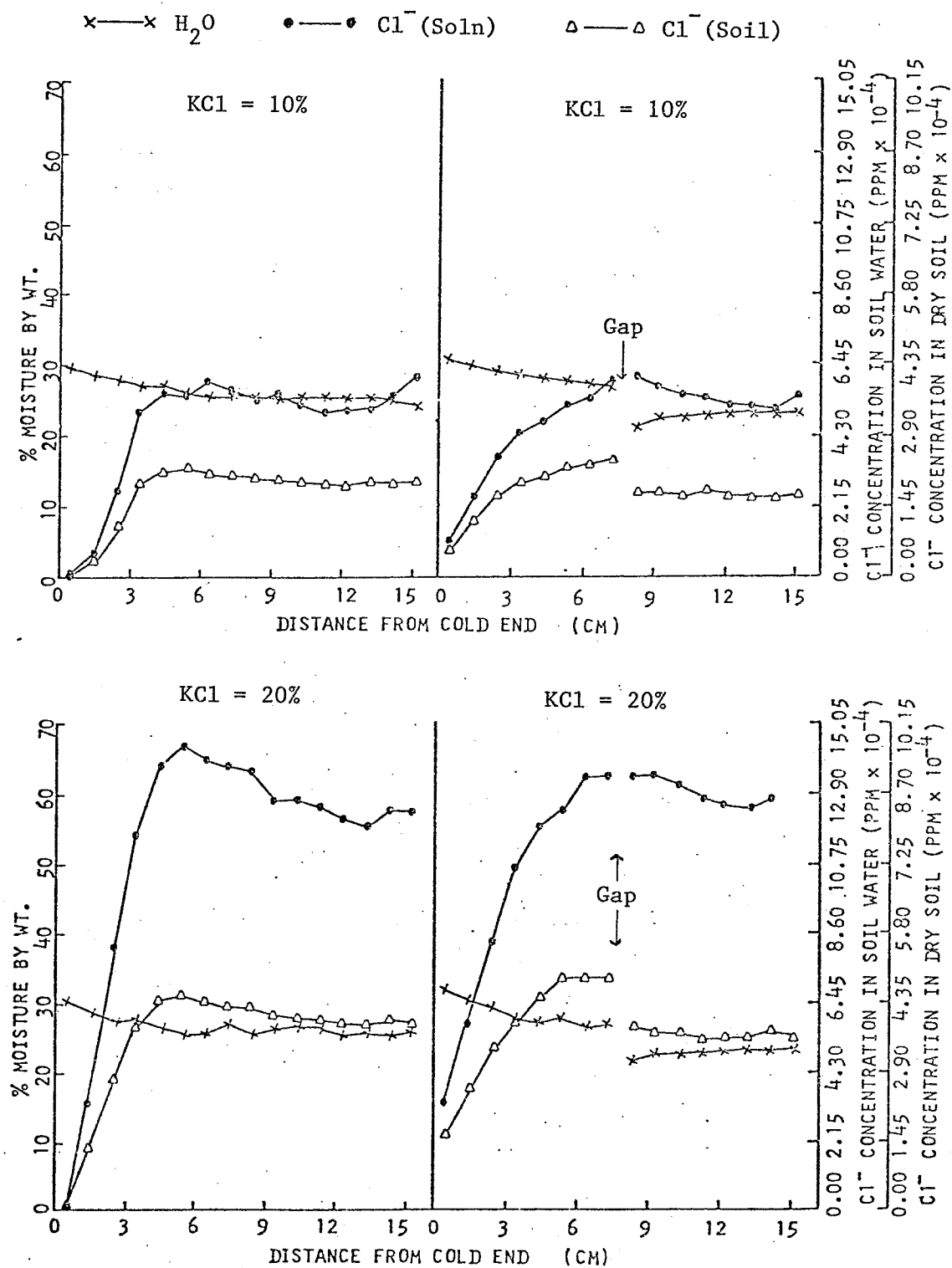


Fig. 19. Moisture and Cl^- distribution in $Ca(NO_3)_2$ and KCl-treated columns after 10 days of thermal treatment (initial $H_2O=27\%$).

in vapor pressure when salt content was varied from 0 to 20% KCl. The effect of temperature upon vapor pressure was much greater than the effect of salt concentration. Therefore there were no observable effects of salt content on water transport. The salt content also had no or very little effect upon the temperature distribution which was the same as the temperature distribution of the soil column without salt (Fig. 16).

The Cl^- ion moved to the warm end. The amount of Cl^- transport was different for the 10 and 20% KCl treatments (Fig. 19). The relative amount (%) of Cl^- moving away from the cold end was the same for columns with different salt content. The difference in the magnitude between the two was caused by the differences in the initial salt content. Consequently the gradient of salt distribution was greater with the 20% than with the 10% KCl treatment. The salt was almost depleted at the coldest end and transported toward the warm end. It was, however, noticed that the concentration of Cl^- , based on soil weight, at the warmest end of the column was not the highest. The maximum concentration of Cl^- was located at a distance of 4 cm from the cold end in the continuous soil columns treated with 10 and 20% KCl. The Cl^- gradient was very great in the colder portion of the soil column and very small in the warmer part. Chloride distribution was very similar to the distribution of temperature in the column. Thus it is possible that the greater salt gradient was due to a greater temperature gradient.

The results obtained using the discontinuous soil columns showed that the movement of the Cl^- ion was similar to that obtained for continuous columns for both the 10 and 20% KCl treatments. The only difference was that the Cl^- concentration, based on soil weight, was higher at the gap than that observed with continuous columns. This was expected since the

gap behaved as an impermeable barrier to the Cl^- . According to the theory of internal circular water movement and the assumption that the Cl^- moved only with the liquid water, the rate of Cl^- movement should be greater in the cold region of the discontinuous column than in the continuous column. However, Fig. 19 showed that the movement of Cl^- in the colder half of the soil column was smaller in the discontinuous columns than in the continuous column. This result might be due to the higher moisture content in the colder region of the discontinuous soil column than that in the continuous column. Chloride movement could also take place by some other means such as by the Soret effect.

The rate of Cl^- movement expressed on a soil solution basis was greater than when expressed on a dry soil weight basis. This could be due to Cl^- moving to the warmer end and water moving to the cold end. The Cl^- concentration curves based on dry soil weight showed that there was almost no Cl^- movement in the warmer part of the discontinuous column.

The moisture distribution of the continuous soil column did not change when the duration of the thermal treatment was varied (Fig. 19, 20). Thus, water movement under a temperature gradient reached a steady state after 5 days of temperature treatment in a closed soil column. However, a steady state was not attained for a closed soil column with an air gap even after 20 days. The amount of moisture moving to the cold region increased with time. This indicated a circular movement of water in the closed continuous soil columns.

Chloride transport did not reach steady state for either continuous or discontinuous soil columns at the end of 20 days. Chloride continuously moved towards the warmer end with time. The distance from the cold end to the point where the Cl^- concentration was below its initial value

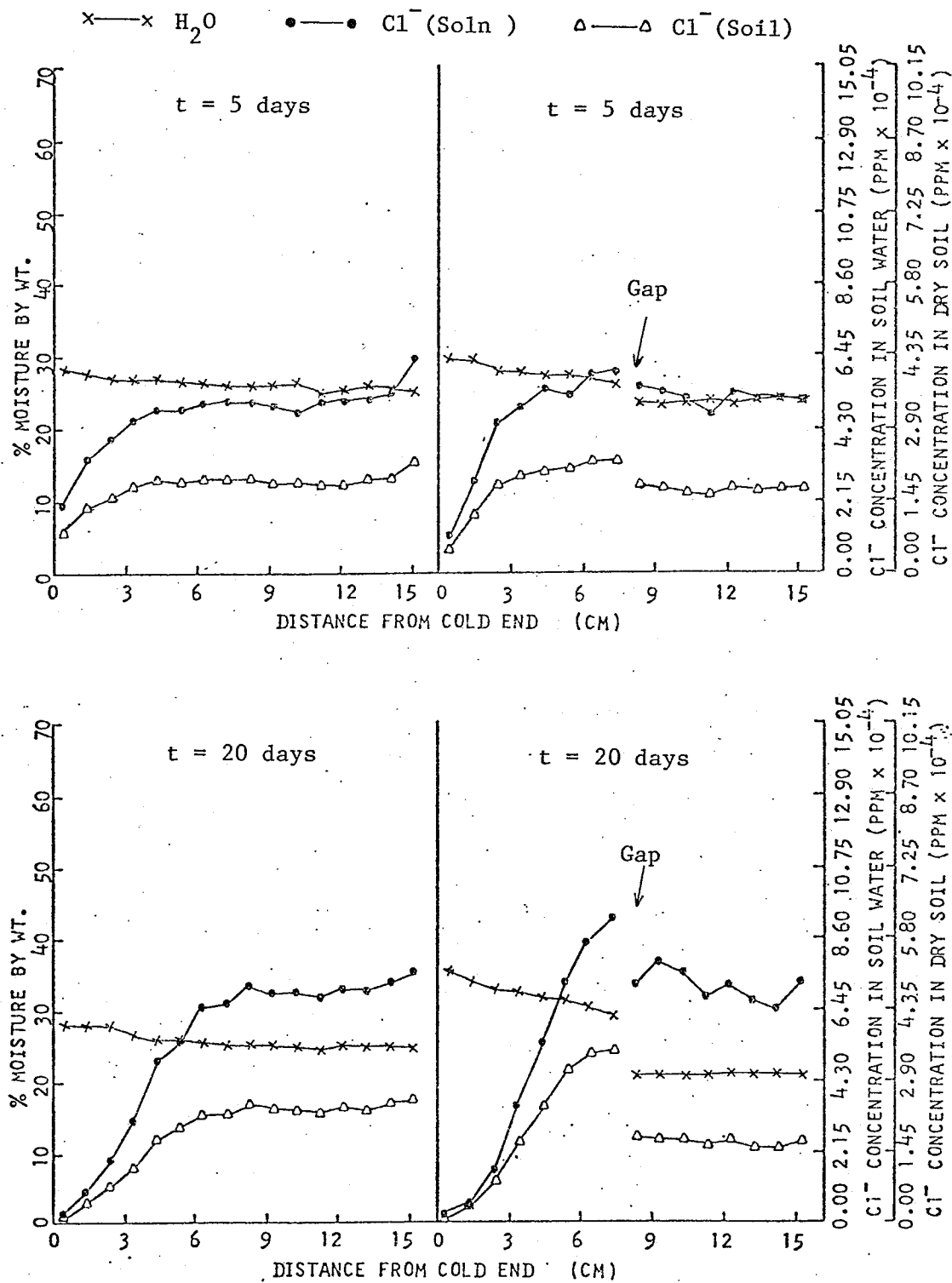


Fig. 20. Moisture and Cl^- distribution in $Ca(NO_3)_2$ and KCl -treated soil columns with or without gap after 5 or 20 days of thermal treatment (initial $H_2O = 27\%$ and $KCl = 10\%$).

or the zone of Cl^- depletion increased with time. For the discontinuous system, the Cl^- also continuously moved to the warmer end in the colder half of the column with time. In the warmer half of the discontinuous system the Cl^- seemed to stay stationary.

In the soil column with 20% KCl similar results (Fig. 19, 21) were obtained for both Cl^- and moisture movement. After 20 days of thermal treatment the point of maximum Cl^- concentration on a dry soil basis was at a point 8 cm from the cold end for the 20% KCl column whereas the zone of maximum Cl^- concentration was found at the warmest end for the column treated with 10% KCl. Therefore, it seemed that the salt concentration did affect salt transport but did not affect net water transport.

As the moisture content increased, the effect of changing salt concentration on the moisture movement was negligible (Fig. 22). However the percentage of moisture transfer decreased as the initial moisture content increased for both continuous or discontinuous soil columns (Fig. 19, 22). Water transfer in the continuous column reached a steady state after 5 days of thermal treatment. For the discontinuous column a steady state for water movement was not attained even at the end of 20 days (Fig. 22, 23, 24).

Chloride movement in the soil column at 10% KCl was different from that of 20% KCl. For the continuous soil columns the concentration of Cl^- on a soil basis was nearly constant from 6 cm onward with 10% KCl. There was a maximum concentration of Cl^- at the warmest end for 20% KCl after 10 days of treatment (Fig. 22). The Cl^- moved continuously to the warm end even at the end of 20 days for both the 10 and 20% KCl treatments. The position of maximum Cl^- concentration did not change but the number of 1-cm soil sections with Cl^- concentration below the initial concentration increased with time for the

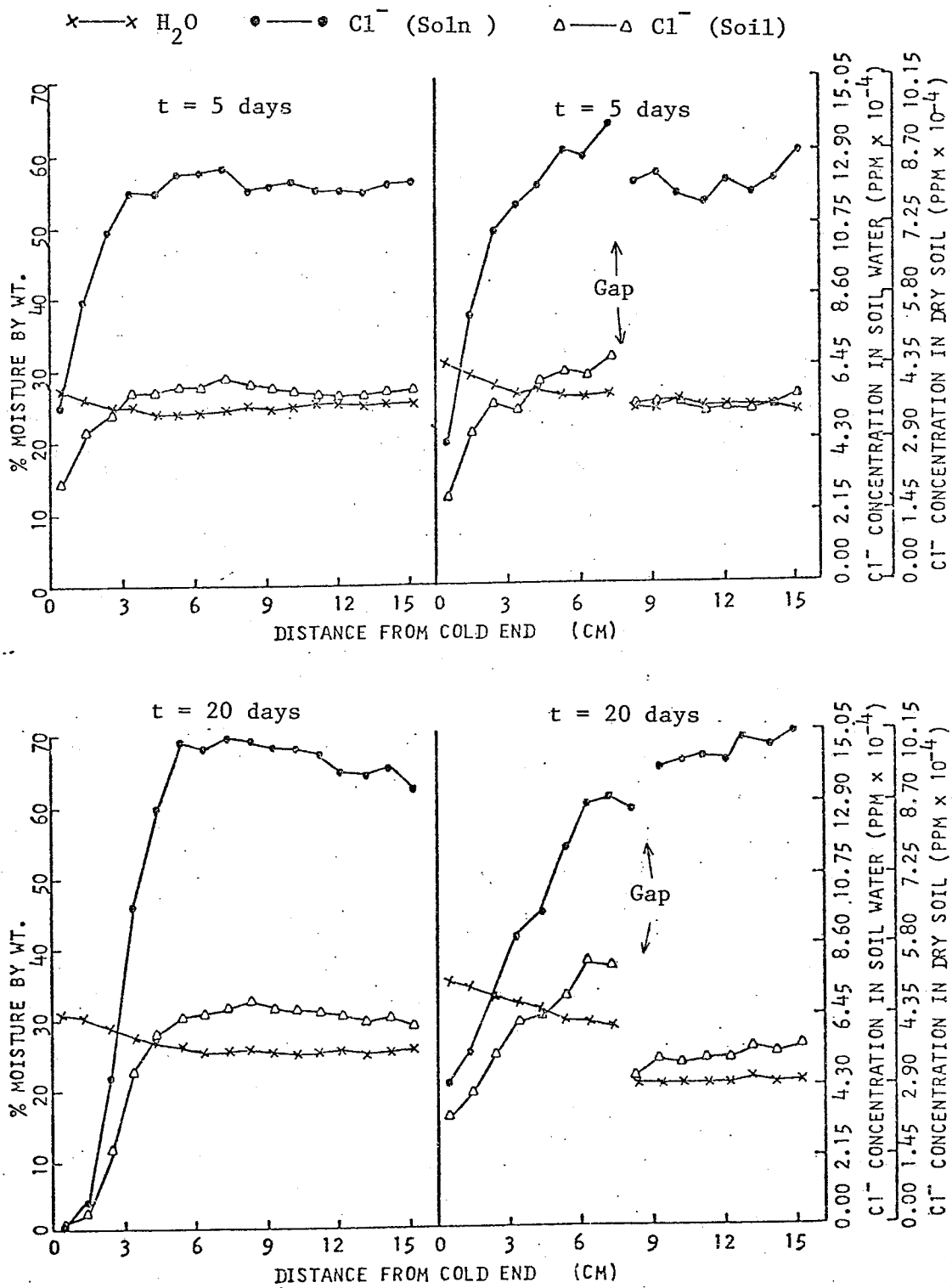


Fig. 21. Moisture and Cl^- distribution in $Ca(NO_3)_2$ and KCl -treated soil columns with or without gap after 5 or 20 days of thermal treatment (initial $H_2O = 27\%$ and $KCl = 20\%$).

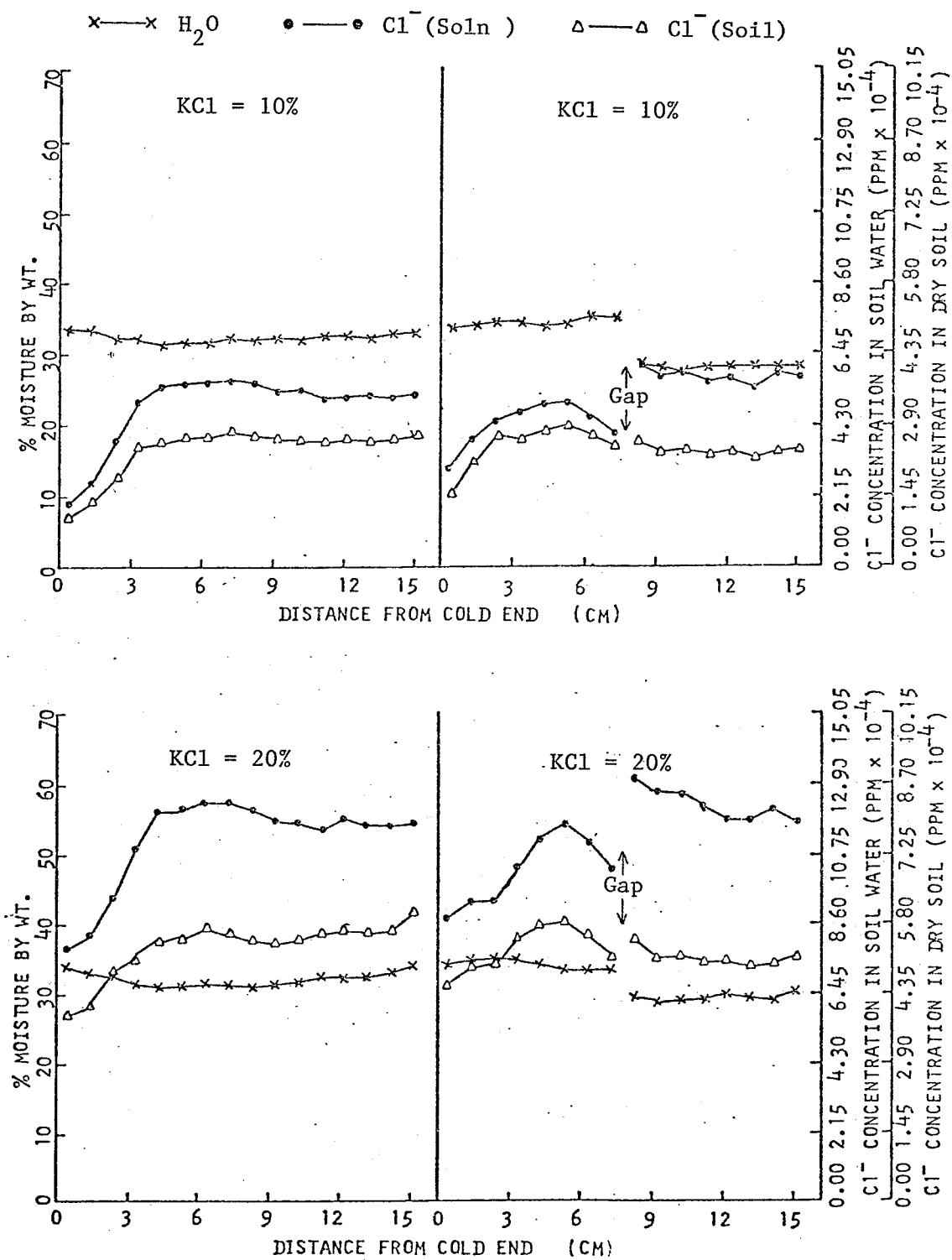


Fig. 22. Moisture and Cl^- distribution in $Ca(NO_3)_2$ and KCl-treated soil columns with or without gap after 10 days of thermal treatment (initial $H_2O = 32\%$).

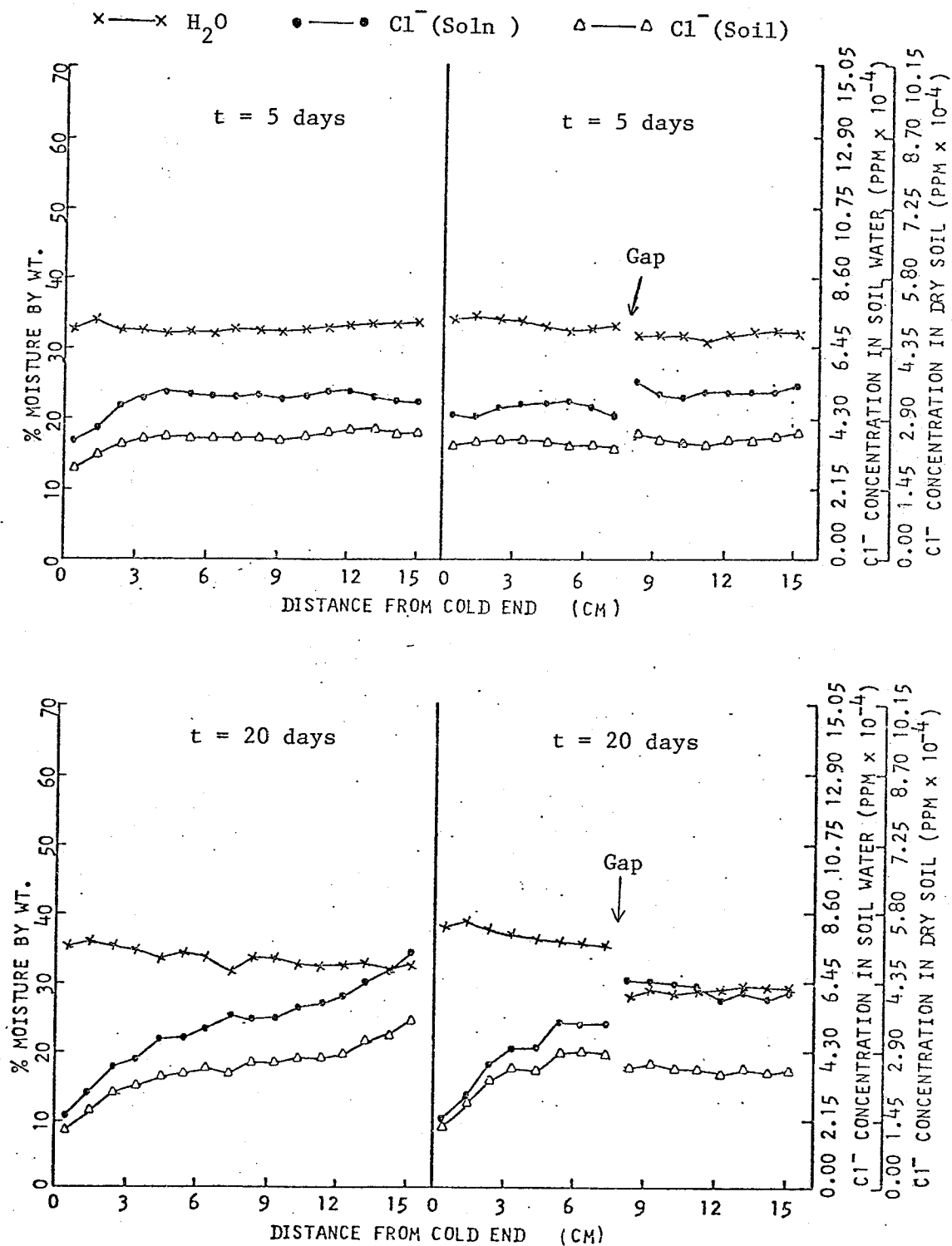


Fig. 23. Moisture and Cl^- distribution in $Ca(NO_3)_2$ and KCl -treated soil columns with or without gap after 5 or 20 days of thermal treatment (initial $H_2O = 32\%$ and $KCl = 10\%$).

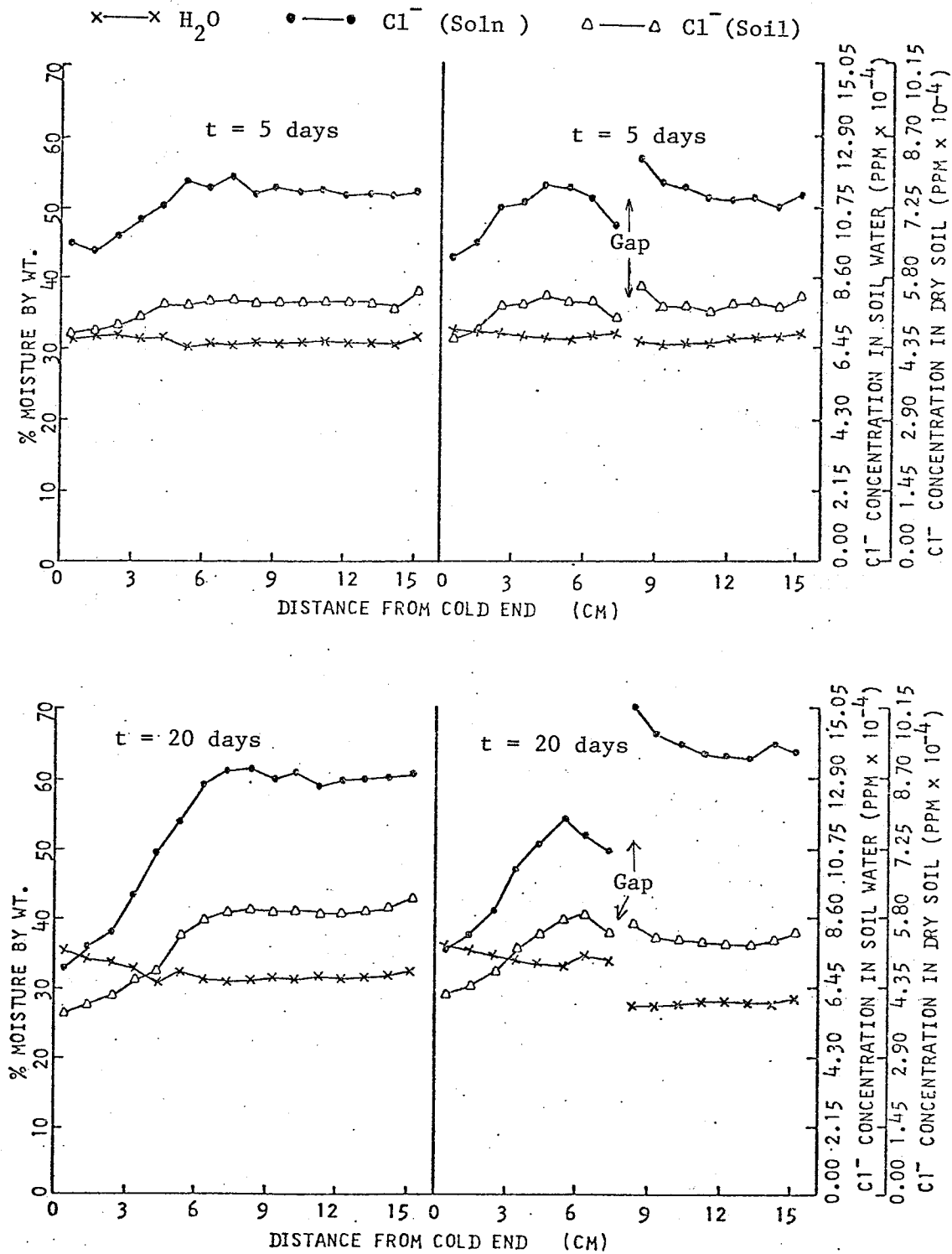


Fig. 24. Moisture and Cl^- distribution in $Ca(NO_3)_2$ and KCl -treated soil columns with or without gap after 5 or 20 days of thermal treatment (initial $H_2O = 32\%$ and $KCl = 20\%$)..

20% KCl treatment. The Cl^- distribution patterns in the discontinuous soil columns at 32% moisture with 10 or 20% KCl were different from that of columns at 27% moisture content (Fig. 20, 21, 22, 23). A maximum Cl^- concentration was always found in the middle of the colder half of the column with 32% moisture content (Fig. 22). The Cl^- concentration on the colder end of the warmer half of the column was found to be higher than that of other parts of the warmer half (Fig. 22, 23). This characteristic was more pronounced in the soil columns with the higher KCl content and persisted in all of the columns regardless of treatment duration. The percentage of Cl^- movement was much smaller in the soil column with the higher moisture content than that with low moisture content for both the 10 and 20% KCl treatments.

5.2.2 Effect of Freezing Process on Mass Transport

In this study, the temperature of the cold end on the bottom of the soil column was -19°C . The temperature distribution curves in soil column at 27 and 32% initial water content 10 days after application of a temperature gradient are shown in Fig. 25. There was some difference in the temperature distribution of the column between the two initial moisture contents. The difference in the thermal gradients was mainly due to the effects of moisture content on soil heat capacity and soil thermal diffusivity and different boundary conditions. The frost penetrated up to 6 cm from the bottom. The 5 to 6-cm section from the bottom was not fully frozen, with frost being present in only the central part of the section. This non-uniform freezing along the cross section of the column was due to insufficient insulation. The temperature gradients in this experiment were much greater than that in the unfrozen columns used in previous experiments. The temperature distribution was curvilinear.

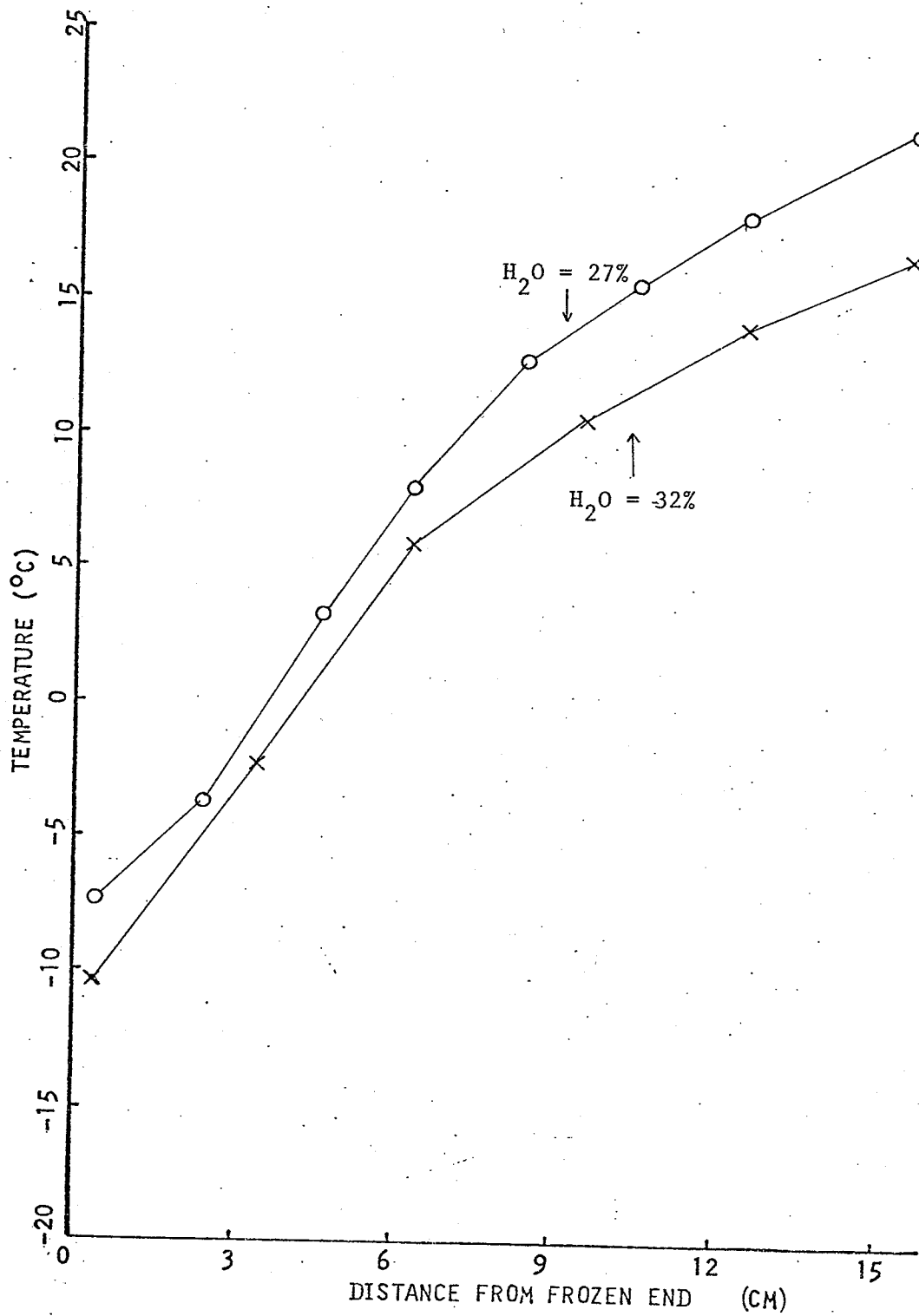


Fig. 25. Temperature distribution in soil columns with temperature gradients of -19 to 22 C (initial moisture contents: 27 and 32%).

The redistribution of moisture in the soil columns with 27 and 32% initial moisture contents 10 and 20 days after frost treatment are shown in Fig. 26. The patterns of moisture distribution were quite different from that of the soil columns without frost. Also the patterns of moisture distribution was not the same in the column with high (32%) initial moisture content as in the column with a lower (27%) initial moisture content. The difference in the moisture distribution between frozen and unfrozen columns was due to higher temperature gradients in the frozen soil column and the retention of water at the frozen end by the freezing process. In the columns with 27% initial water content the maximum moisture content was found at the coldest end, whereas, the position of the highest moisture content was located at the middle of the frozen portion for the columns at the higher (32%) initial moisture content. This difference between the two initial moisture contents could be attributed to the formation of different kinds of frost. A less permeable frost was probably formed in the column with the high moisture content. The moisture content was uniform throughout the unfrozen portion of the soil column at both moisture levels. As the frozen period increased from 10 to 20 days the shape of moisture distribution curves did not change. However, water continuously moved to the frozen zone at both moisture levels (Fig. 26). The frost front also moved upward about 1 cm. The moisture content in the unfrozen zone decreased and a very small moisture gradient was created. Steady state conditions for moisture movement and frost penetration was not attained at the end of 20 days. The relative rate of water movement in the soil column with a high moisture content was smaller than in columns with a low moisture content.

Chloride movement in the soil column with frost formation was

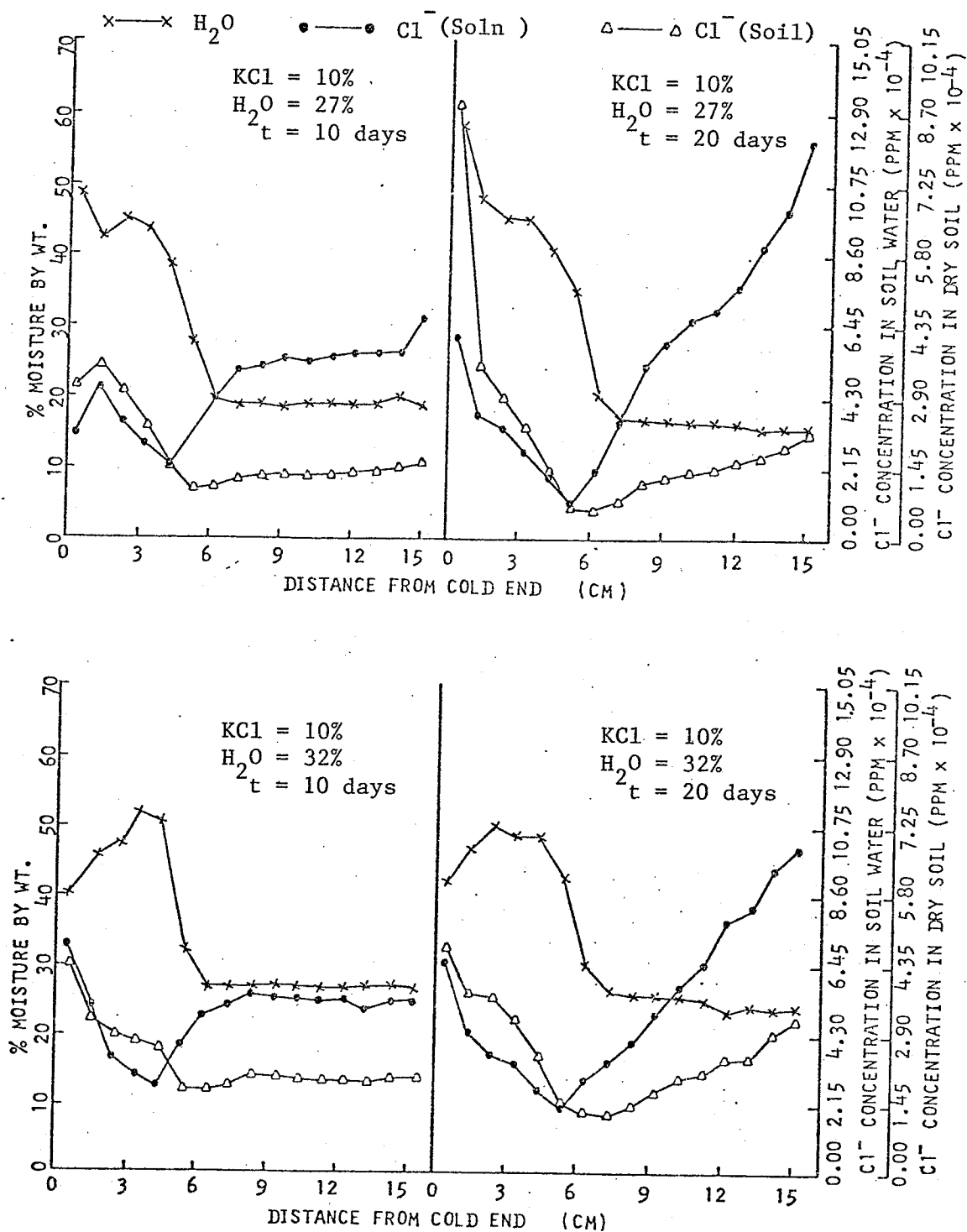


Fig. 26. Moisture and Cl⁻ distribution in Ca(NO₃)₂ and KCl-treated soil columns with a frozen end.

different from that in the soil column without frost (Fig. 19 and 26). The Cl^- ion moved to both cold and warm ends. The amount of Cl^- ion movement to the warm end was much smaller than that to the cold end. The amount of Cl^- ion movement to both ends increased with increasing time of frost treatment. The relative rate of Cl^- movement in the soil column with a low moisture content was greater than that in columns at a high moisture content. The increase in Cl^- concentration on a dry soil basis in the frozen zone indicated that the water moved to the frozen zone in the liquid phase. The Cl^- concentration based on dry soil weight increased towards the coldest end in the frozen zone. This demonstrated that the unfrozen water in the frozen zone moved to the coldest end. The minimum Cl^- concentration on the soil solution basis was found near the frost front. This indicated that water movement was greater than Cl^- movement. The greater movement of water as compared to Cl^- was an indication of the importance of vapor movement in the water transfer. The slope of the Cl^- concentration curve based on the soil solution was greater than that based on dry soil weight in the unfrozen zone i.e. moisture moved out from the unfrozen zone faster than did Cl^- . This result also indicated the presence of water vapor movement.

Little or no moisture gradient existed in the unfrozen zone after 10 days of thermal treatment. Thus the return liquid water flow to the warm end was negligible if it occurred at all. If Cl^- moved with liquid water, Cl^- should not accumulate at the warm end. However, the distribution curve of Cl^- showed there was an accumulation of Cl^- at the warm end. Even in the soil columns incubated for 20 days, the small moisture gradient that was observed could not account for the amount of Cl^- that moved during the thermal treatment between 10 to 20 days. This result seemed

to indicate that Cl^- transport under the influence of a thermal gradient could not be a simple convective process alone.

The magnitude of mass transport induced by a thermal gradient was much greater in the soil column with the cold side temperature below freezing point than in columns without freezing. The greater thermal gradient and the effects of the freezing process in the frozen soil probably account for the difference. The effects of moisture content upon mass transport in the soil column with or without freezing were, however, similar.

5.2.3 Effect of Stability Configuration on Mass Transport

The vertical column with the cold side on the bottom is the most stable geometric configuration because the density of water is maximum at 4 C. Liquid convection due to gravitational force and temperature gradients will not take place in this type of a soil column configuration if the soil was saturated with water. Convection would take place in a vertical soil column with the cold end on the top. The direction of liquid flow is shown in Fig. 27. The liquid water moves upwards near the side and downwards in the middle of the column if it assumed that the soil temperature near the wall was higher than that in the middle of the column due to imperfect insulation. The stability of a horizontal column is much more complicated than that of the vertical column. The liquid water moves downwards on the cold end then flows toward the warm end. On the warm end the water moves upwards then moves to the cold end to complete the circulation.

The redistribution curves of water in these three different configurations of soil columns with or without an air gap were very similar (Fig. 19, and 28). The Cl^- distribution was the same for the vertical column

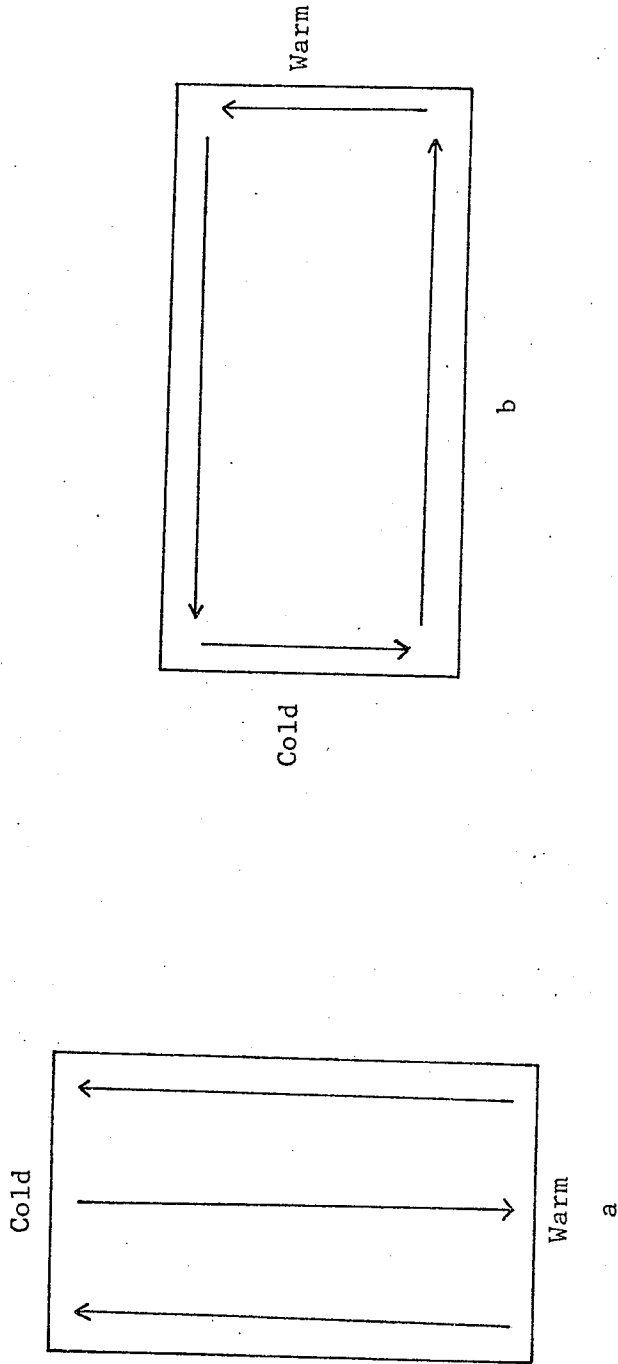


Fig. 27. Direction of liquid water flow under the influence of thermal gradient for vertical and horizontal columns.

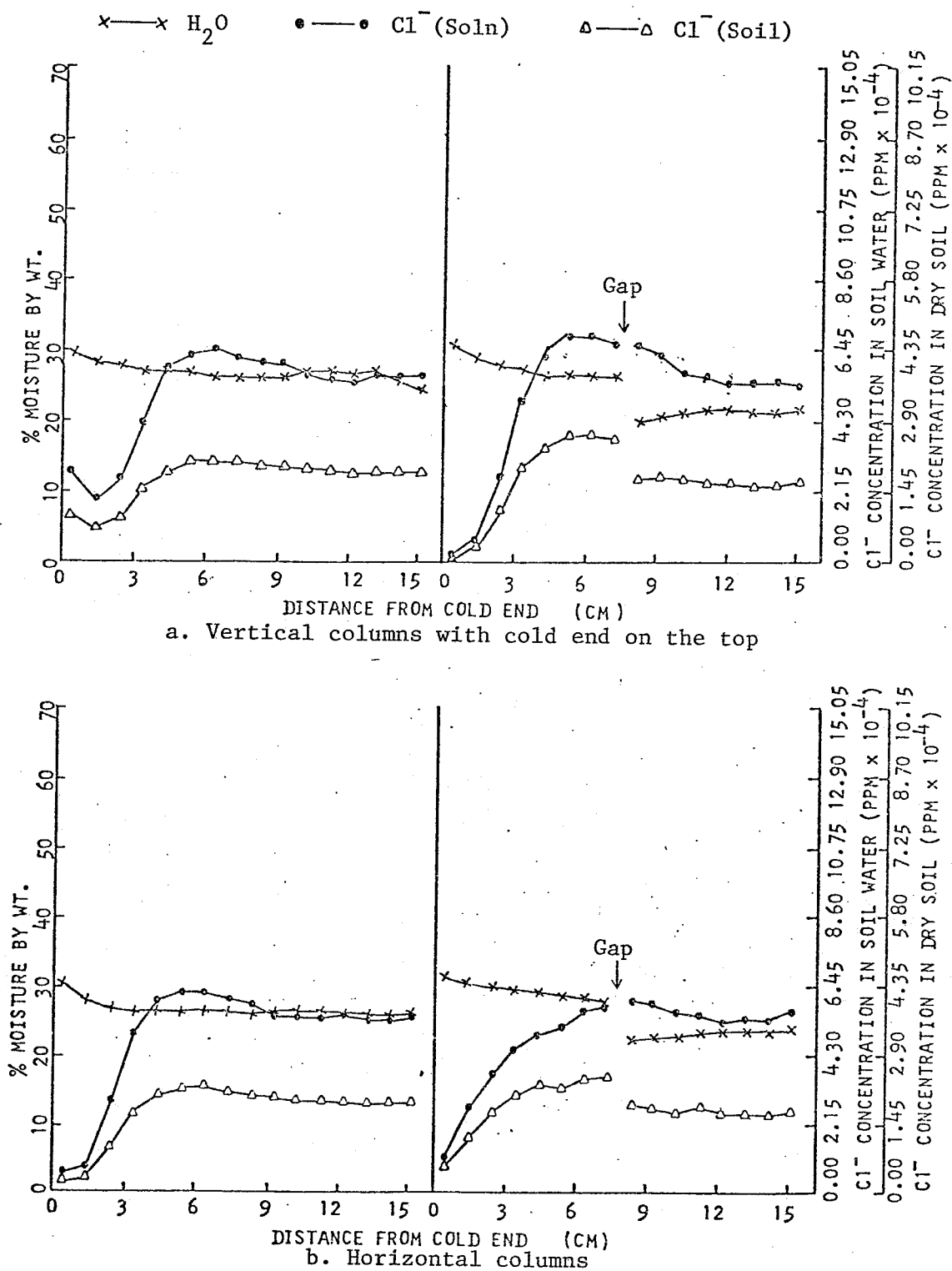
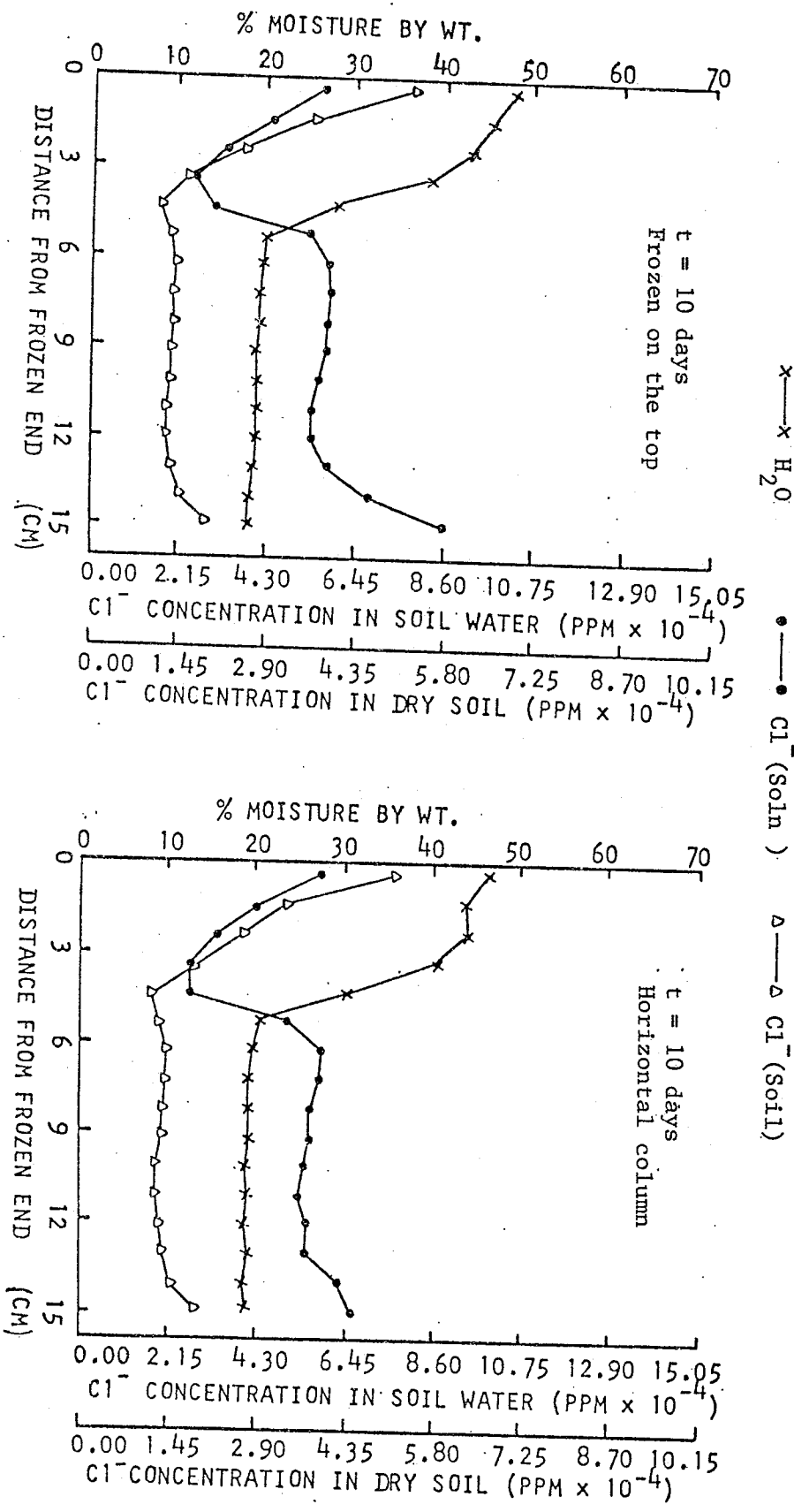


Fig. 28. Moisture and Cl^- distribution in vertical and horizontal columns after 10 days of thermal treatment (initial $\text{H}_2\text{O} = 27\%$ and $\text{KCl} = 10\%$).

with cold end on the bottom and the horizontal column. This provided evidence that the possible liquid circulation in a horizontal column, if there was any, could be similar to that of the stable configuration. However, in the soil column with cold end on the top the Cl^- distribution was different from the others. The minimum in Cl^- concentration was found 1.5 cm from the coldest end for the continuous vertical column with cold side on the top (Fig. 28). Forces responsible for the above distribution of Cl^- were not apparent by the instability of its geometric configuration. For the discontinuous vertical soil columns with the cold end on the top there was no Cl^- concentration gradient in the warmer half of the column. There was also no Cl^- concentration gradient (Fig. 19 and 28) in the warmer half of the horizontal column. In the colder half of the column the Cl^- concentration gradient was greater in the discontinuous column with cold end on the top than in that with the cold end on the bottom. The greater Cl^- movement in the colder half of the column with the cold side on the top could be attributed to an unstable configuration and an increase in liquid water circulation. The results obtained with the horizontal column were similar to that of the most stable configuration. Behavior of the NO_3^- ion was identical to the behavior of the Cl^- ion. This study clearly showed that differences in geometric configuration affected salt transport. Moisture movement was similar in all the various geometrical configurations.

The moisture distribution was different when the top versus the bottom of a vertical column was frozen (Fig. 26 and 29). The rate of water movement was smaller in the unstable soil columns (cold side on top) than in the stable soil column (cold side on bottom). The depth of frost penetration was smaller in both horizontal and unstable vertical

Fig. 29. Moisture and Cl^- distribution in vertical and horizontal columns with one frozen end (initial $H_2O = 27\%$ and $KCl = 10\%$).



columns than in the stable column. The moisture content was uniform throughout the unfrozen portion of the unstable columns. The salt distribution curves of the vertical column with the freezing end on top and the horizontal column were similar. However, they were different from that of the most stable configuration (Fig. 26 and 29). As noticed before there was a very small salt concentration gradient in the unfrozen zone of the most stable column after 10 days of thermal treatment. Except for the three warmest sections the concentration gradient of salt in unfrozen zone of the soil column with the unstable configuration was smaller than that in the column with a stable configuration. The salt concentration gradient based on dry soil weight in the frozen zone of the unstable soil columns was greater than in the stable columns. This difference indicated that the rate of Cl^- movement in the frozen zone was smaller in the stable column than in unstable columns. The concentration of salt on a soil solution basis in the frozen zone also showed a minimum concentration at the frozen front. The pattern of the salt concentration distribution based on dry soil weight in the unfrozen zone showed that the salt movement had some of the characteristics of a pushing process. This will be discussed later in this chapter.

5.2.4 Effect of Air Gap Length and Position on Mass Transport

The air gap employed for the previous studies was 0.5 cm and always placed in the middle of the column. The temperature gradient in the warmer half of the soil column was very small (Fig. 16). An experiment was therefore conducted to maintain a substantially larger thermal gradient in the warmer part of the soil column by placing air gaps of various sizes at various positions to stop the return flow of liquid water. The distribution curves of moisture, Cl^- and temperature for a column open on the

top end and with an air gap placed at the ice-water phase boundary are shown in Fig. 30. In the colder part of the column, the highest moisture content was found near the gap. This indicated that transport of the unfrozen liquid and vapor within the frozen zone was smaller than the rate of condensation of vapor at the frost front. Liquid transfer within the frozen soil could be observed by the fact that there was an unequal Cl^- distribution within the frozen zone. Some Cl^- was transported from the warmer portion to the colder portion within the frozen zone. There was a great moisture gradient in the unfrozen portion with a maximum in moisture content located near the gap. This moisture redistribution was caused by a greater rate of moisture movement from warm to cold end than that of vaporization and transportation to the freezing front through the gap. In the unfrozen portion of the column, Cl^- was depleted in the colder portion and transported to the warmer region (Fig. 30). The phenomena was characteristic of a pushing process. If only the salt was pushed toward the warm end the concentration of the salt at the warm end would increase resulting in depletion of salt at the cold end. The concentration of salt in the middle of the column would remain nearly constant. With prolonged time the concentration gradient would be exponential in form. Due to the great moisture gradient within the unfrozen portion return flow in the liquid phase was possible. However, if a pushing process had occurred the Cl^- distribution curve indicated that the process was in its relatively early stage.

The results obtained by changing the position and length of air gap and using air dry soil in the cold compartment indicated that the moisture accumulated near the gap at the colder region and only a very small amount of water moved toward the coldest end (Fig. 31). Vapor movement

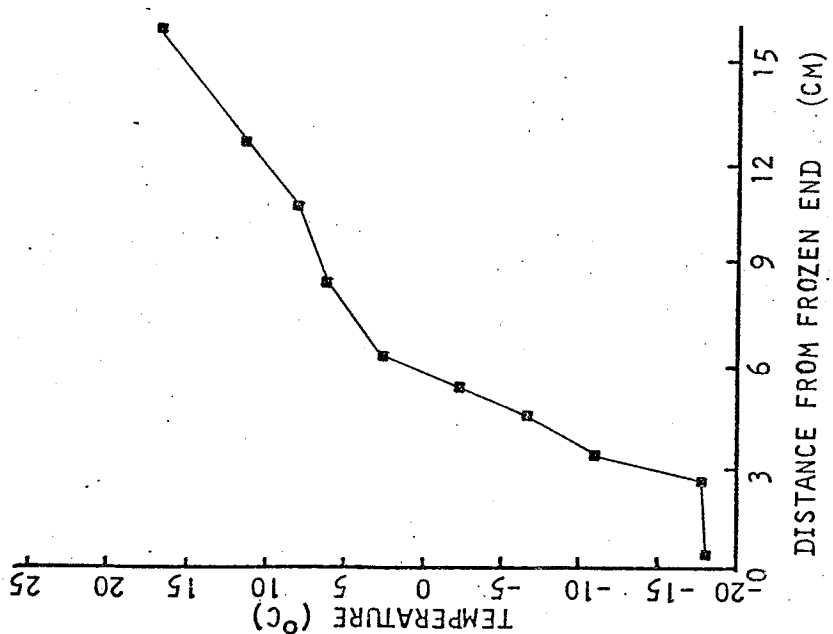
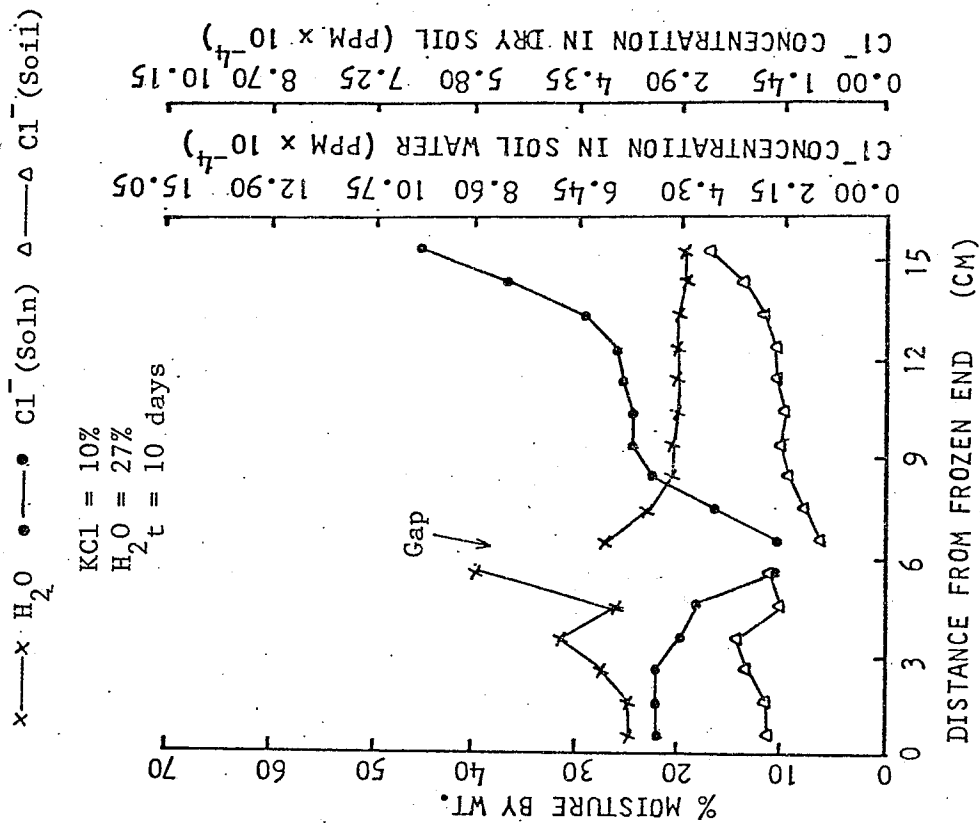


Fig. 30. Moisture, Cl^- and temperature distribution in soil column with an open and frozen top end and with 0.5 cm air gap.

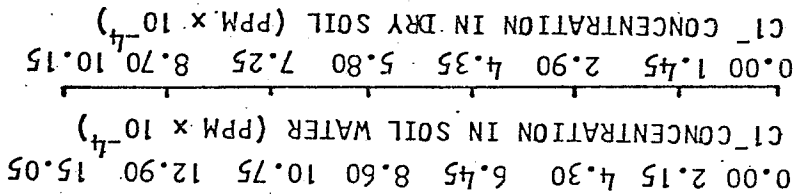
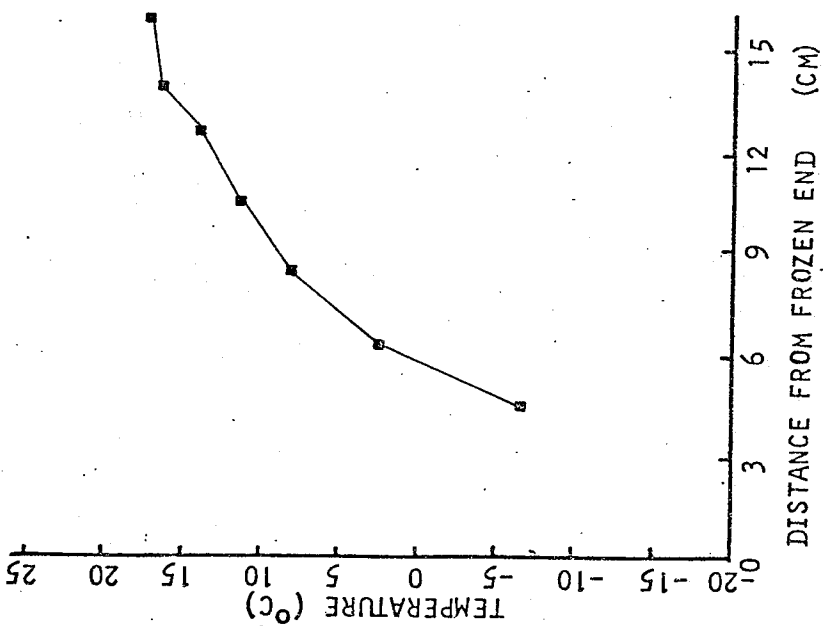
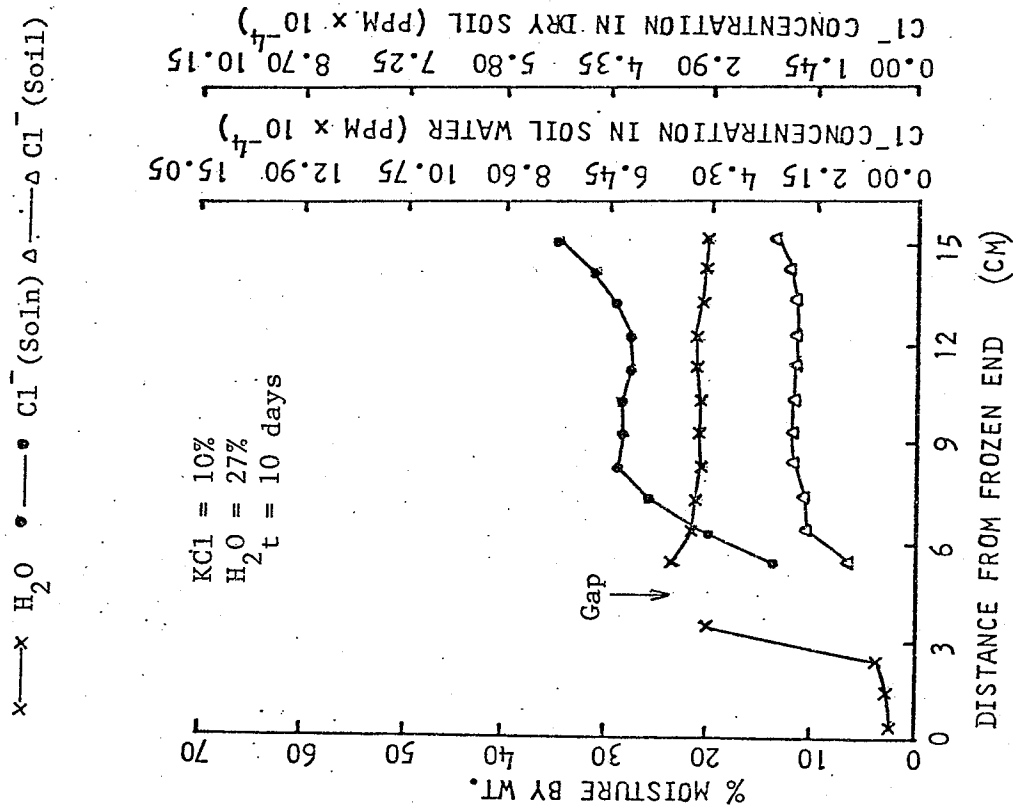


Fig. 31. Temperature, moisture and Cl⁻ distribution in a discontinuous column with one frozen end and an 1-cm air gap (4 sections of dry soil).

within the frozen zone was negligible even though the porosity was not limiting vapor transport. This confirmed the finding that in a soil column subjected to a thermal gradient, moisture transport does not take place directly from the warmest end to the coldest end. The transport was a sequence of vaporization and condensation processes occurring between the nearest neighbor volume elements. The moisture gradient in this case was smaller in the warmer portion than that observed in Fig. 30. Evidence of the pushing process in salt movement was also quite pronounced (Fig. 31). Again return flow of liquid water was possible due to the relatively high moisture gradient. A comparison of the relative magnitude of movement of moisture and salt between the different set-up was not feasible because the conditions of every column were different. The increase in moisture content and no detectable presence of Cl^- in the colder region of the column (Fig. 31) showed that only vapor moved across the air gap.

For the third study a 1-cm air gap was used but different thermal gradients were employed. The thermal gradient became steady 3 days after the application of thermal treatment. The steady state temperature and mass distribution are shown in Fig. 32. The soil on the cold side of the gap was frozen and that on the warm side was not frozen. There was no detectable amount of water in the gap. The water content of the soil on the cold side of the gap was lower than on the warmer side of the gap. This indicated that the rate of water transport in the colder region (frozen zone) was greater than that of vapor transport across the air gap as evidenced by the transport of Cl^- , based on soil weight, from the warmer part of the frozen zone to the coldest region. The high demand for water in the colder side could prevent the accumulation of water

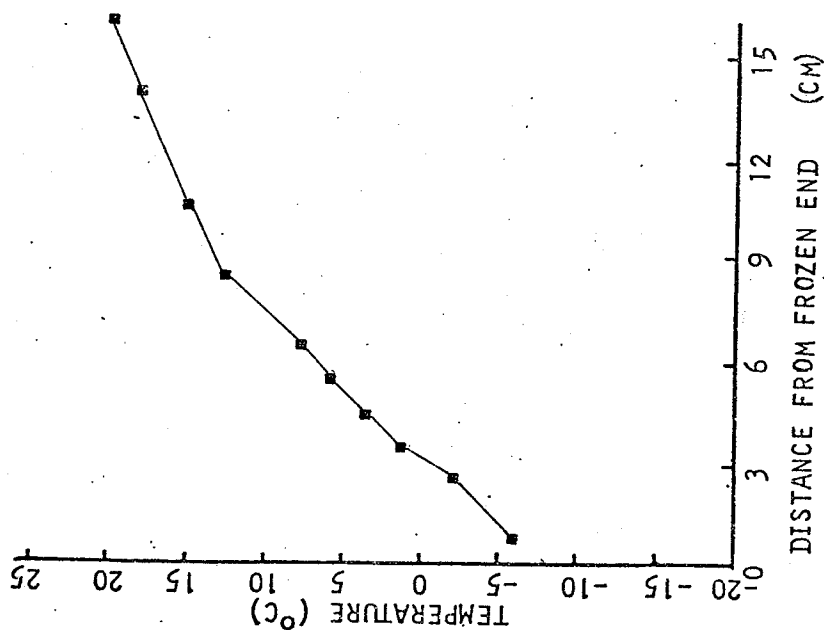
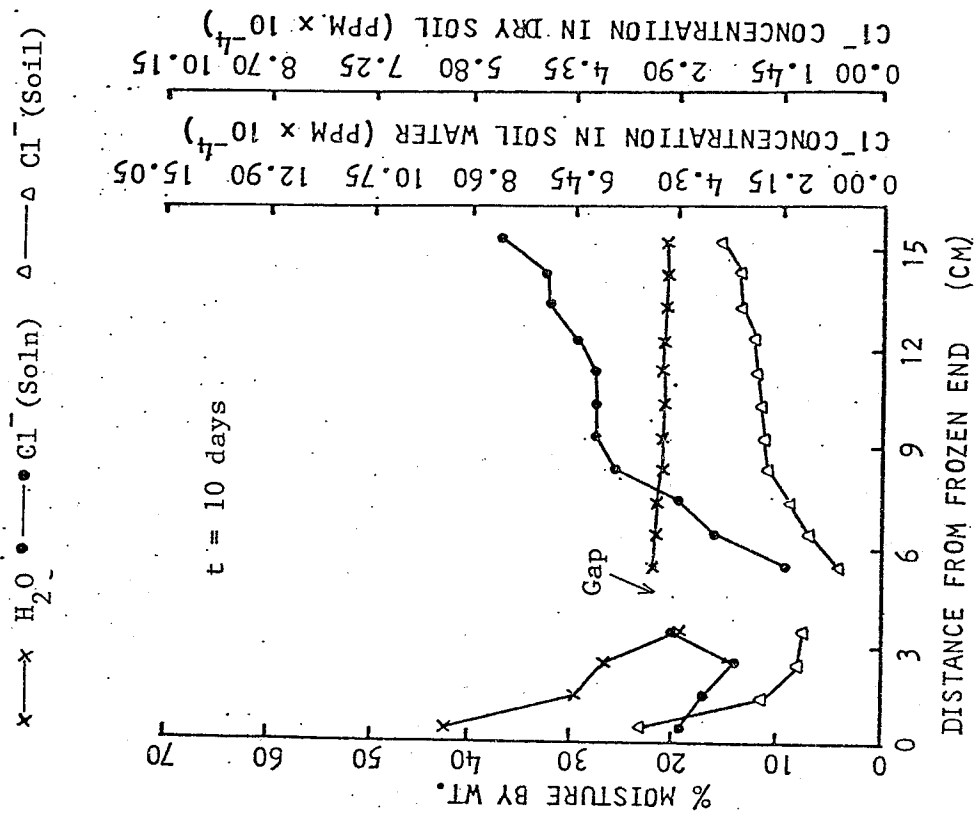


Fig. 32. Temperature, moisture and Cl⁻ distribution in soil column with an 1-cm air gap and frozen bottom end. (initial H₂O = 27% and KCl = 10%).

which could create the moisture gradient to cause liquid moisture return flow in the warmer part of soil column.

The moisture gradient in the warmer region was very small or negligible. The difference in moisture content between the cold side and the warm side of the unfrozen region was slightly over 1% (Fig. 32). The moisture in the warmer region was under about 1738 cm-H₂O suction. The liquid water flux due to this moisture gradient under isothermal condition could be calculated using the relationship between hydraulic conductivity and pF relationship shown in Fig. 33. The value was found to be around 0.0141 cm³/day cm² i.e. 0.0448 cm/day linear velocity. The liquid water flux against the thermal gradient was expected to be smaller than the calculated value.

If the average distance of Cl⁻ depletion was chosen as 2.5 cm (from 5 cm to 7.5 cm distance from the frozen end in Fig. 32) and it is assumed this was due to return liquid water movement, the flux and the linear velocity of water would be $2.5 \times 0.225 \times 1.4 \times 1/10 = 0.0788 \text{ cm}^3/\text{day cm}^2$ for flux and $2.5 \times 10^{-1} = 0.25 \text{ cm/day}$ for linear velocity. In the calculation the moisture content was assumed to be 22.5% and the bulk density to be 1.4 during the 10 day period. Thus the Cl⁻ exclusion of approximately 2.5 cm from the air gap during the 10 day period could not have been caused solely by the liquid water flow which was initiated by the moisture gradient. The Cl⁻ concentration distribution curve seemed to be the result of a pushing process in the closed column due to the thermal gradient. The pushing process of salt movement in a closed solution system has been described by de Groot (1942) and Cho (1975)*. The pushing process is diagrammatically shown in Fig. 34. The salt content was initially uniform throughout the whole column (Fig. 34a). If the

* C. M. Cho, unpublished work.

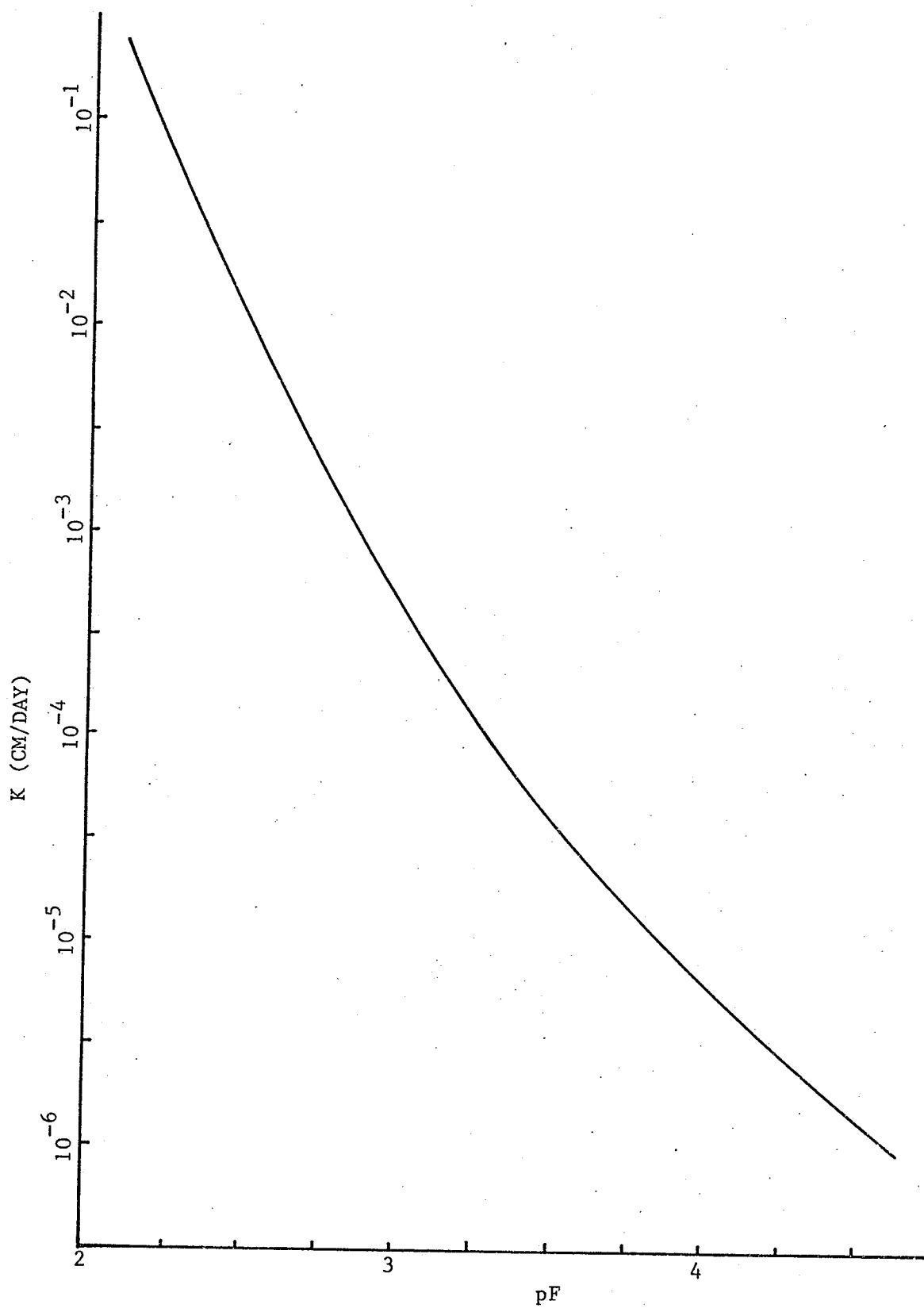


Fig. 33. Hydraulic conductivity (K) and pF relation curve of Wellwood clay loam.

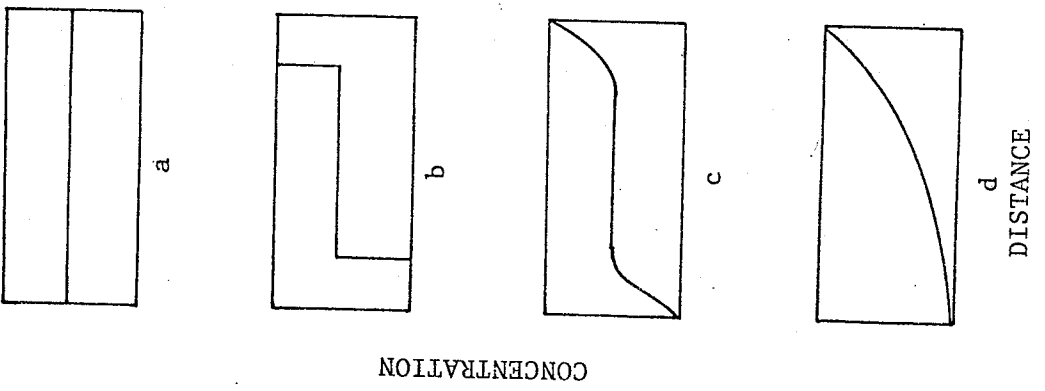
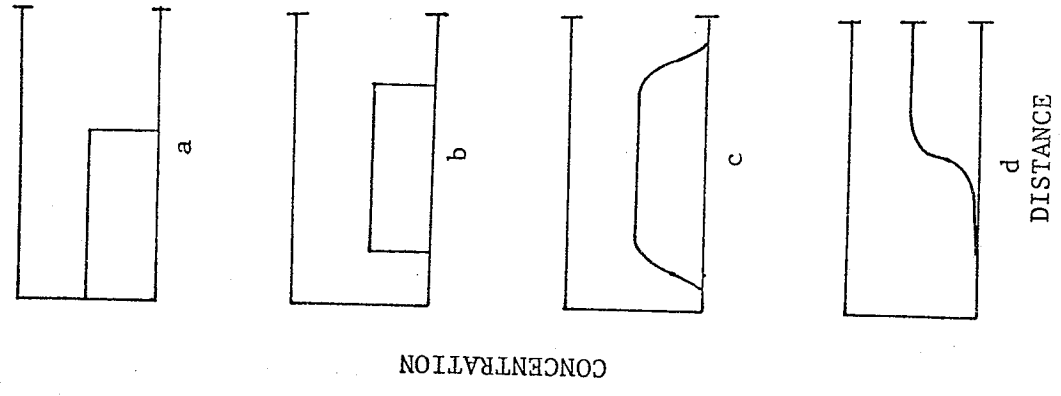


Fig. 34. Pushing process in a closed system. Fig. 35. Pushing process in an open system.

pushing process due to an external force took place without diffusion the salt distribution would be similar to that shown in Fig. 34b. If the salt movement were due to a pushing process along with diffusion the salt concentration curve should be like that shown in Fig. 34c. Finally the steady state concentration profile depicted in Fig. 34d would result. It is noticed that the concentration would increase exponentially from the cold to the warm end. If the system was open on the warmer end the distribution of salt would be completely different (Fig. 35). There would be no reflection of the transported salt at the warmest end since there was no wall. As was mentioned before some of the previous results showed a pattern of distribution of salt similar to that of Fig. 34c. It was thus assumed that the pushing process was operative. As the rate of return flow in the liquid phase decreased in the unfrozen zones (Fig. 30, 31 and 32) the characteristics of pushing process became pronounced. In the results shown in Fig. 32 liquid flow to the warmest end was unlikely, and hence, the Cl^- distribution was probably the result of a pushing process.

In the fourth study the length of the air gap was increased to 2 cm and placed in between the 2nd and 3rd sections from the coldest end. The coldest section was filled with air dry Wellwood soil acting as a water sink. There was moisture transport across the air gap into the dry soil (Fig. 36) as was observed in Fig. 31. Moisture transfer across a 1-cm air gap (Fig. 31) was almost equal to that across a 2-cm air gap (Fig. 36). Evidently the length of an air gap did not play an important role in the vapor transport across the gap. The moisture gradient in the unfrozen zone was very small (Fig. 36). The return flow, if any, to the warmest end would be very small. The Cl^- distribution pattern showed a

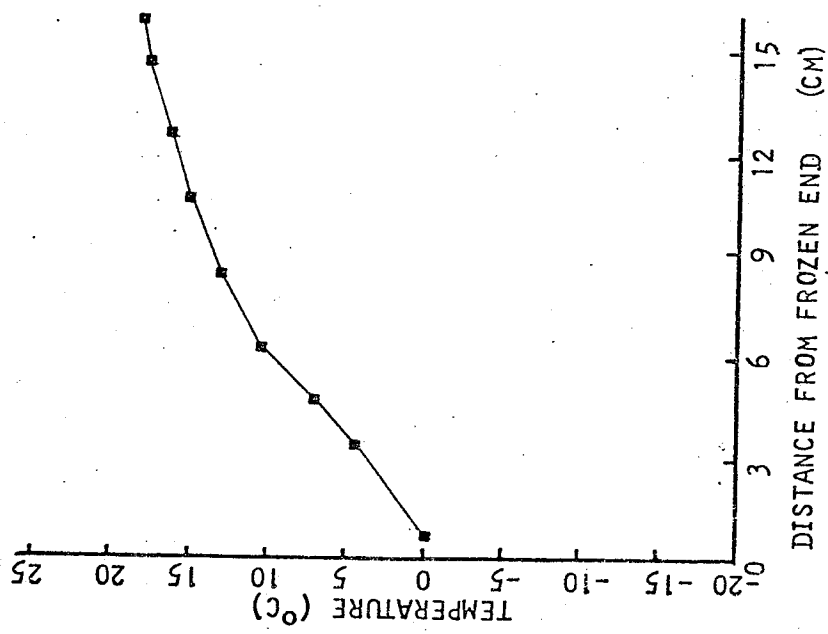
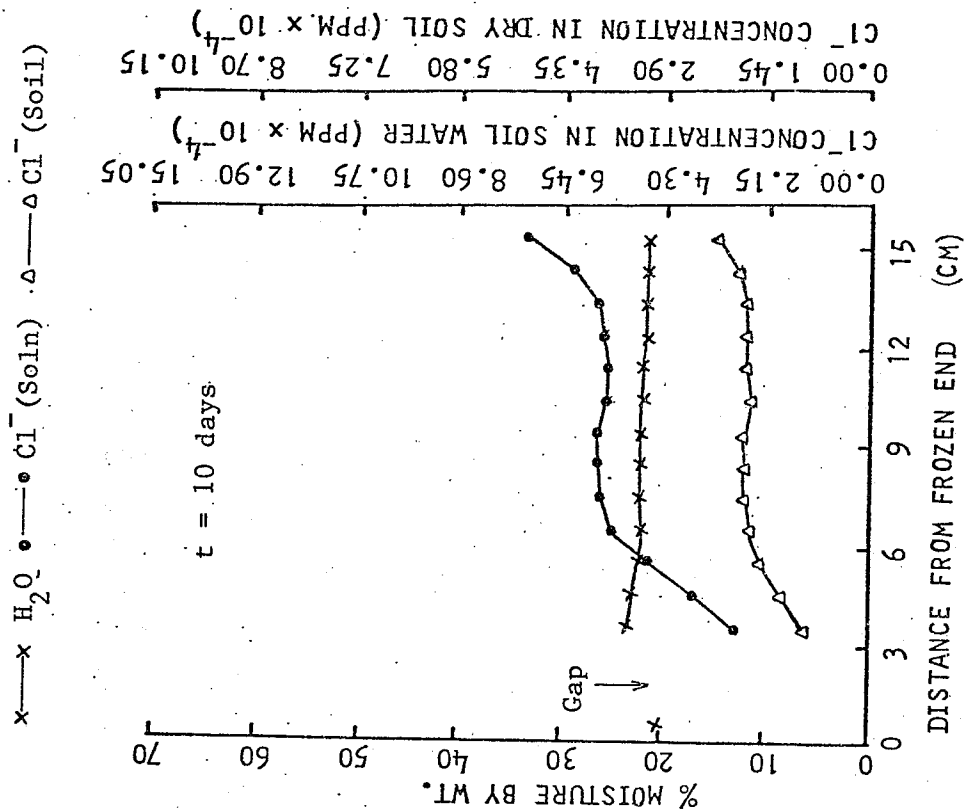


Fig. 36. Temperature, moisture and Cl⁻ distribution in soil column with a 2-cm air gap and a frozen bottom end (initial H₂O = 27% and KCl = 10%).

typical pushing process combined with diffusion as was observed in the result using uniformly wet soil (Fig. 32).

The study revealed that salt movement under a thermal gradient might be due to both convection and segregation, or a pushing process. Thus, the use of Cl^- as a tracer of liquid flow under a thermal gradient should be carried out with great caution.

The behavior of NO_3^- was similar to that of Cl^- as was observed previously. There was no denitrification during the experimental period and this could be due to the sterilizing or inhibiting effect of the high salt concentration upon soil micro-organisms. The recovery of added NO_3^- varied from 95 to 100%. If NO_3^- was subjected to some chemical reaction the behavior of NO_3^- would be expected to be different from that of Cl^- .

5.2.5 Simulation of Natural Conditions

The steady state temperature distribution throughout soil columns subject to simulated conditions for the first and second 10 days were slightly different. The temperature distribution during the first 10 days was identical to that shown in Fig. 25. The temperature curve for the 2nd 10 days is shown in Fig. 37. The resulting distribution of moisture and Cl^- after 20 days of reversed thermal treatments are shown in Fig. 37. The results obtained from this soil column were different from that of the soil column with only the bottom end frozen for 10 days (Fig. 26). The depth of frost penetration was less and a smaller amount of water moved to the frozen zone in this soil column. When the bottom of the column started to freeze after the reversal of the thermal treatment the top end was still frozen. Therefore the moisture content was not uniform and the amount of moisture available for movement was considerably reduced. Also the changes in temperature gradient during the 2nd 10 days were

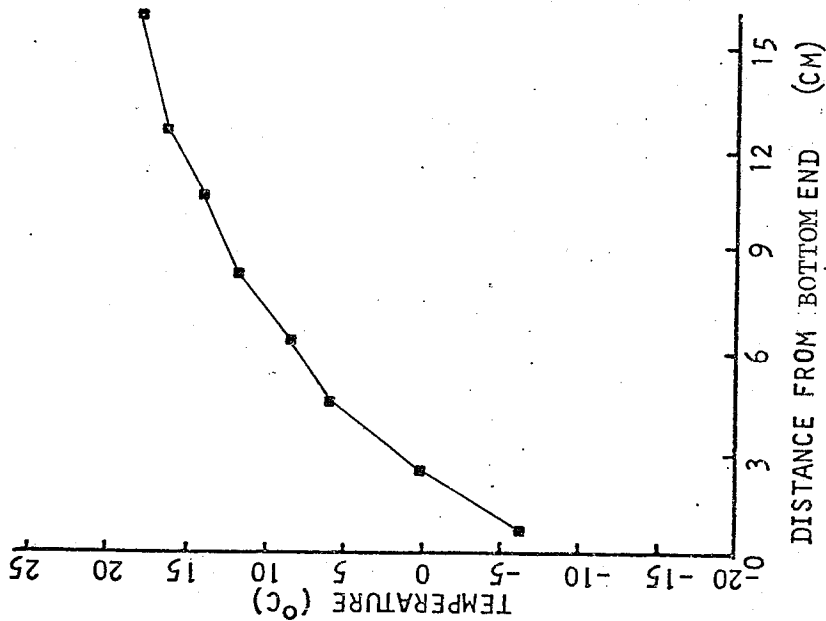
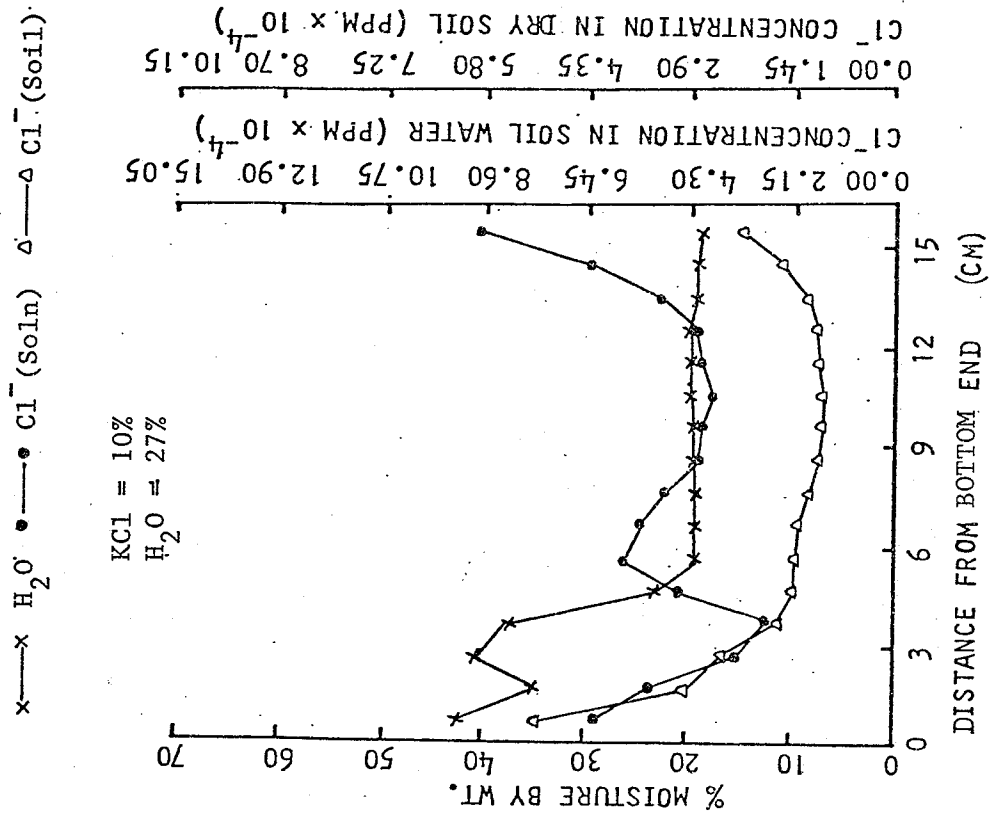


Fig. 37. Temperature, moisture and Cl⁻ distribution in soil column with frozen top end for first 10 days and frozen bottom end for second 10 days of thermal treatment.

complicated and different from that of the soil column with only the bottom end frozen. All of these factors could account for the difference in the moisture movement between these two kinds of treatment. However, the shape of the moisture distribution curves were similar in these two different treatments. There was no moisture gradient in the unfrozen zone.

The Cl^- distribution curve (Fig. 37) showed that there were two maximum points with one located at each end of the column. This distribution was not observed when only the bottom of the column was frozen (Fig. 26). The cold end at the termination of the experiment corresponded to the warmest end at the termination of first 10 days of thermal treatment. The Cl^- which accumulated during the first 10 days at the warm end was evidently partially trapped and remained there during the second 10 days of thermal treatment.

Changing the direction of the thermal gradient had a great effect on mass transport in a closed soil column. This suggests that the temperature change from winter to spring also results in a redistribution of soil moisture and salts in the soil profile.

5.2.6 Open System

All the experiments except one result shown in Fig. 30 were conducted in a closed system in which energy but not mass could be transported into or out of the system. In this study the soil columns with an open top were used. The temperature distribution curve of the soil column with an open top at the end of a 10 day thermal treatment is shown in Fig. 38. The temperature of the cold side on the top was above freezing. The temperature gradients were smaller in the first 3 cm than in the rest of the column.

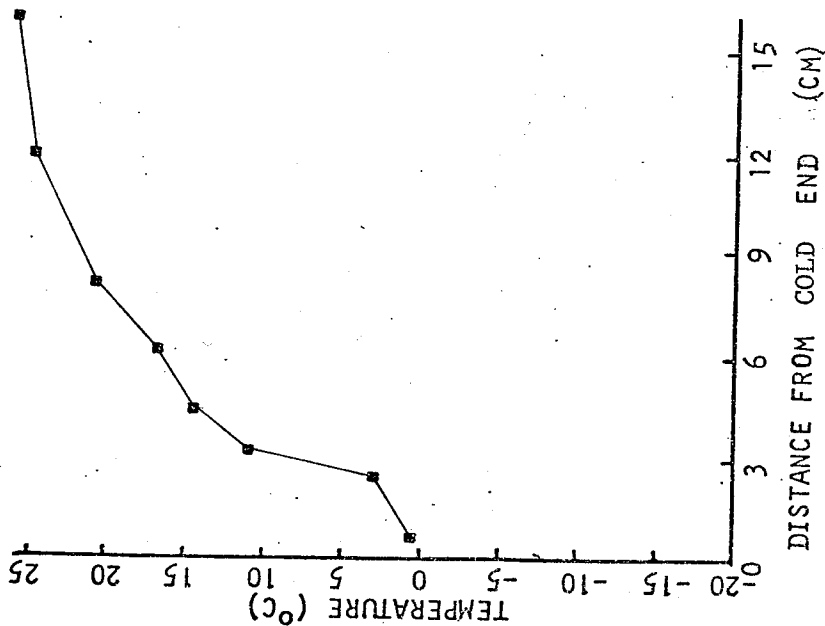
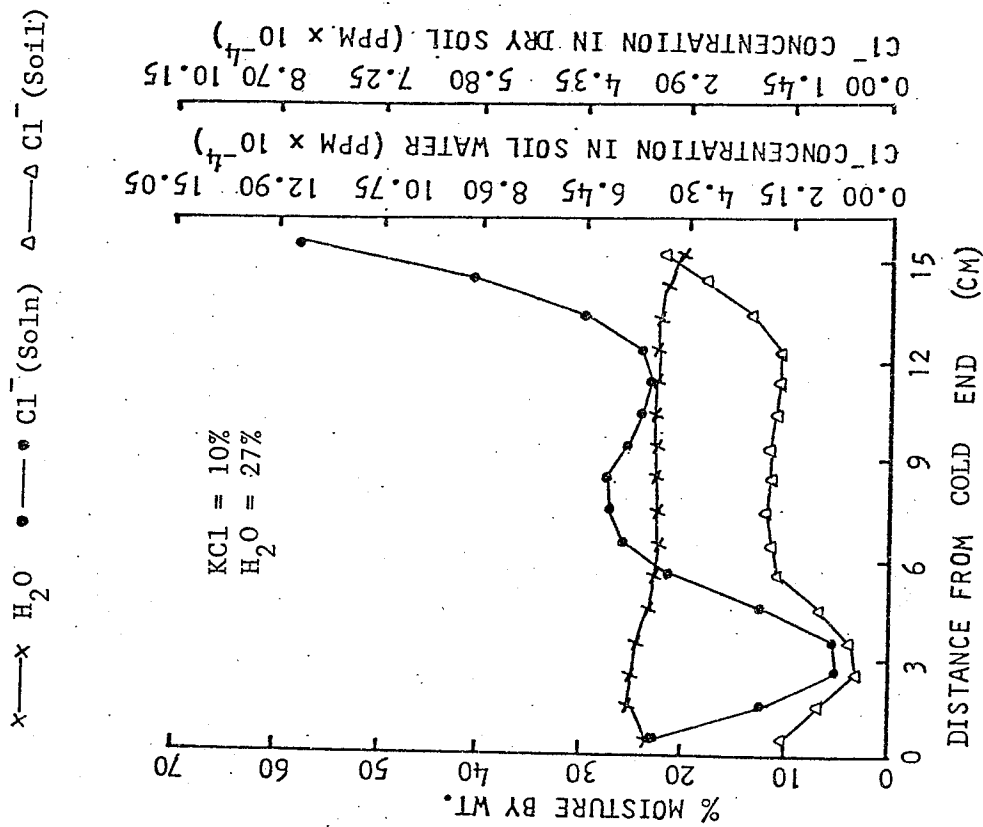


Fig. 38. Temperature, moisture and Cl⁻ distribution in soil column with an open top after 10 days of thermal treatment.

The moisture content increased slightly from the warm end to the cold end except for the surface section. The drop of moisture content on the surface was probably due to water vaporization from the soil surface. There was a net loss of soil water from the system.

The Cl^- distribution showed that there was a minimum concentration near the 3rd and 4th sections (cm) from the top. The distribution curve below this point was very similar to those obtained in Fig. 28 and 29 with the exception that the degree of "pushing" was greater for the results shown in Fig. 38. Opening the top in order for vapor to escape evidently did not have much effect upon condensation and possible return of liquid flow as compared to the closed system. The decreased Cl^- concentration within the top 3 cm could have been due to dilution and diffusion of Cl^- from this zone to the position of minimum Cl^- concentration where the maximum temperature gradient existed.

As the temperature on the top end was decreased to below the freezing point the top 3 cm of soil froze simultaneously and the temperature gradient for this 3 cm of soil was very small (Fig. 39). At the end of the 10 day treatment the frost penetrated 8 cm. The surface soil moisture content was smaller than the initial water content due to vapor loss from the surface. It was evident that the rate of moisture movement to the surface was smaller than the vapor loss from the surface as there was accumulation of water within the frozen zone. Because the top 3 sections were frozen simultaneously and the gradient was small the water movement in the top 3 cm was small. The moisture accumulated at the 4th section. The moisture gradient on the unfrozen zone was very small. The Cl^- concentration curve (Fig. 39) showed that there was no Cl^- movement into or out of the top 2 sections. In other words the liquid water

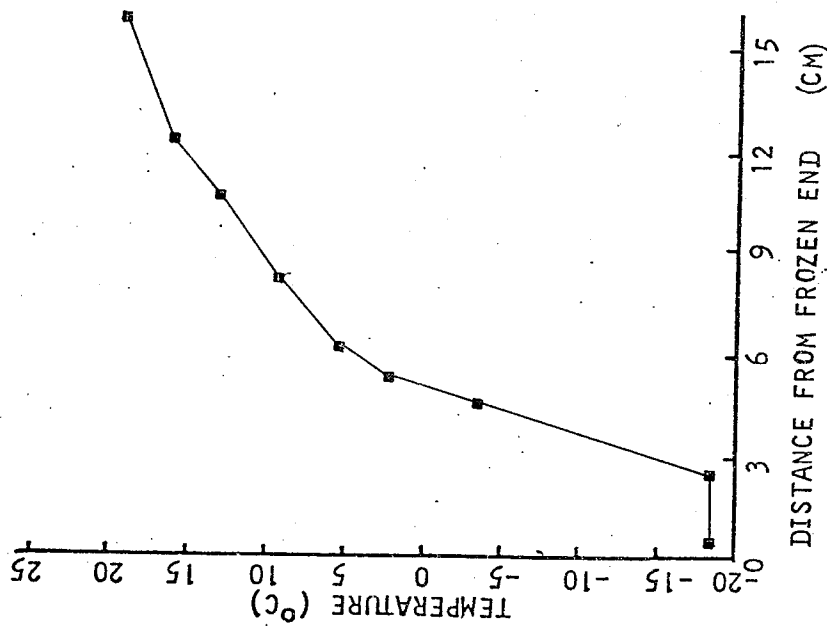
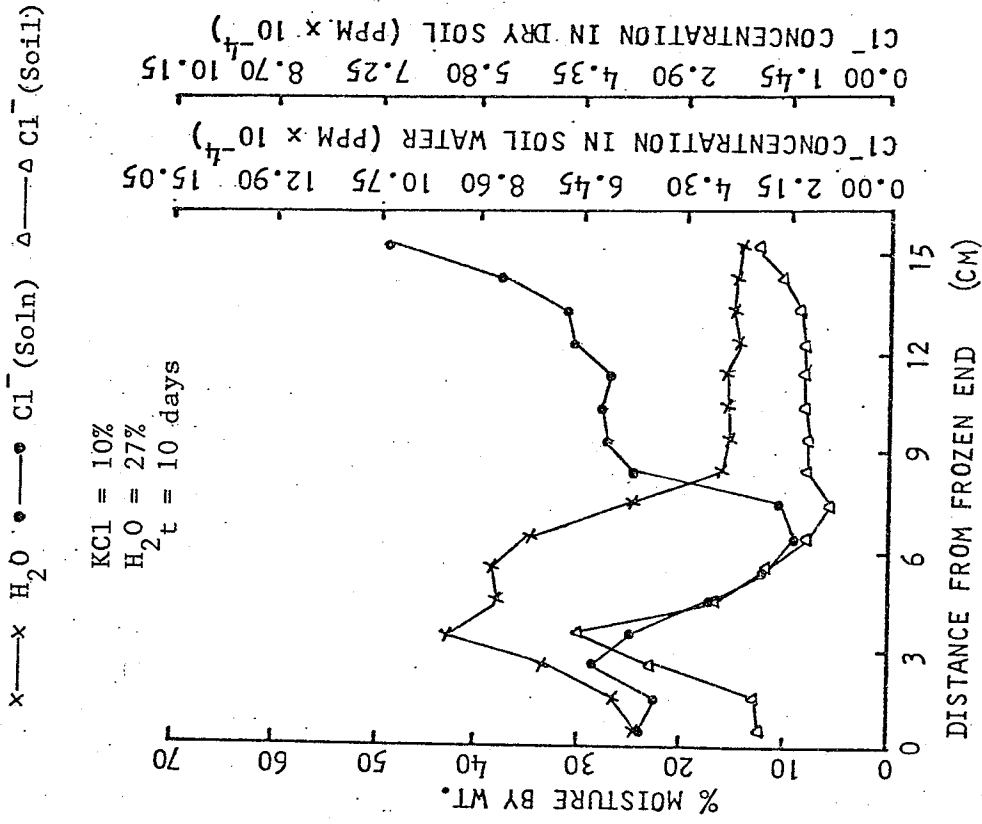


Fig. 39. Temperature, moisture and Cl^- distribution in soil column with a frozen top end and open.

flow was very small within these sections. Both higher moisture content and Cl^- concentration in the 4th section than in 3rd section from the top indicated that the vapor and unfrozen liquid water flow toward the 4th section took place during and/or after the freezing process. The patterns of moisture content and Cl^- concentration distribution from 4 cm down to the bottom end were similar to the result of a closed frozen system (Fig. 26).

5.2.7 General Discussion

The results obtained indicated that moisture and salt transport took place due to imposed thermal gradient. Moisture always accumulated at the colder region as a result of movement from the warm region. The quantity or the rate of transport of moisture was definitely related to the thermal gradient. The rate was greater with a higher gradient. It seemed, however, the moisture distribution might not be directly related to the water flux because of the internal circulation of soil moisture.

The steady state moisture distribution in a closed soil system under nonisothermal conditions could be obtained if there was no flow of water or if fluxes due to various forces were equal in magnitude but opposite in directions. With a closed continuous soil column with the cold end at a temperature above freezing a steady state moisture distribution was obtained 5 days after thermal treatment. To observe the mechanism of causing the steady state moisture distribution, an air gap was used for blocking liquid water flow. In addition various salt concentrations were used to decrease the vapor pressure. The changes in the salt distribution was used as an indicator of liquid water flow. Under a thermal gradient Cl^- in the cold end moved towards the warm end. The redistribution of moisture in the discontinuous soil column and Cl^-

concentration in both continuous and discontinuous soil column indicated that steady state conditions for both moisture and Cl^- were not attained in 20 days. The results suggested that vapor movement from warm end to cold end was an important transport mechanism and that a circular water movement as a result of vapor moving to the cold end and liquid water returning to the warm end, might result in a steady state moisture distribution in a closed soil system. This conclusion was based on the assumption that Cl^- moved only with liquid water. Chloride movement under a thermal gradient in aqueous solutions is well known and is caused by the Soret effect. A part of the Cl^- movement in the soil system under a thermal gradient might have been due to the Soret effect the extent of which was not known. When the liquid return flow was blocked by the air gap, a uniform concentration of Cl^- was observed in the warmer half of the column. Such distribution did not exclude the possibility of the presence of the Soret effect since thermal gradient in the warmer half of the column was also very small.

A large thermal gradient and no moisture gradient in a soil column were needed in order to distinguish Cl^- movement due to the Soret effect from flow with liquid water. Therefore a combination of several techniques such as an air gap with the colder region frozen, an air gap with the colder region frozen and opened, changing the air gap length and an air gap with one side filled with dry soil below freezing temperature were used. The air gap was used to block the liquid water flow and the freezing process served as a water sink. By using these techniques a larger thermal gradient was obtained. The moisture gradient was very small in the unfrozen portion of the column. The Cl^- redistribution curve in the unfrozen zone showed the characteristic of the pushing

process along with the diffusion process. Calculations on rate of water flow due to the small moisture gradient and rate of movement of Cl^- indicated that the Cl^- movement was greater than that due to liquid water flow alone. An additional mechanism such as the thermal diffusion of salt or the Soret effect might be operative.

In Manitoba the direction of thermal gradients along with the position of frost in the soil profile changes from winter to spring. In the laboratory, a change in the freezing directions was simulated. The top end of a soil column was frozen first then the bottom end was frozen with thawing of the top. The results showed that the rate of Cl^- movement to both ends was greater than movement in soil columns with only one end frozen. The soil column with open top end was used as an open system where both energy and water could enter or leave the column. The moisture content of the soil column increased with decreasing temperature except the open end and Cl^- concentration distribution showed that a minimum concentration of Cl^- appeared at 3 and 4 cm from surface in the unfrozen soil column. For the soil column with one end frozen the moisture content distribution also showed the surface evaporation and the maximum moisture content and Cl^- concentration were located at 4 cm from the surface. The results could not be compared with the closed system because the thermal gradients were different between the two systems.

The effects of the stability configuration of soil column under a thermal gradient were studied. The redistribution of moisture and Cl^- were affected by the stability of the column configuration. In the unfrozen soil column with the cold end on the top a minimum Cl^- concentration was found at a distance from the top but in the stable soil column it was located at the coldest end. There was a greater amount of Cl^-

moving to the warmer end in the unstable soil columns than in the stable soil column with one end frozen. The frost penetrated deeper in the stable soil column than in unstable soil columns. The effects of salt concentration upon moisture movement were also investigated. It was found that salt concentration had very small or no effects upon the moisture movement under a thermal gradient.

6 SUMMARY AND CONCLUSIONS

The field experiment was designed to determine the magnitude of transport of surface-applied NO_3^- and Cl^- in two Manitoba soils. Calcium nitrate and CaCl_2 were applied on the surface of Almasippi loamy sand at the rate of 1681.5 Kg N or Cl / ha and on Oct. 5, 1973 and July 3, 1974, on Red River clay on Nov. 2, 1973. The distribution of temperature, moisture, NO_3^- and Cl^- were determined at various time intervals throughout this study. Chloride was used to serve as a tracer of liquid water moving through the soil profile.

The results showed that the seasonal variation in soil temperature at the fixed depth was a typical cosine function. The surface soil temperature was higher than that of subsurface soil in spring and summer, however, the thermal gradient was reversed in fall and winter. The distribution of soil moisture was found to vary with the seasons. It was generally observed that when the temperature of surface soil was higher than that of subsurface soil, the surface soil moisture content was lower than the subsurface soil moisture content. On the other hand when the surface soil temperature was lower than the subsurface soil temperature, the moisture content of the surface soil was higher than that of the subsurface soil.

The movement of surface-applied NO_3^- and Cl^- was found to be governed by the climatic conditions but also by soil characteristics. In the Almasippi sandy soil the rate of downward movement of NO_3^- and Cl^- was found to be very small in summer, fall and winter periods. Appreciable downward movement of surface applied NO_3^- and Cl^- took place during the period of spring-thaw. The depth of NO_3^- and Cl^- penetration into the soil profile during this period was greater than could be affected

by melting snow alone.

In the clay soil the downward movement of surface-applied NO_3^- was very small throughout a whole year. The amount of NO_3^- remaining in the soil decreased with time. However, the majority of the remaining NO_3^- stayed near the surface. Denitrification and immobilization were two possible causes for the decrease in applied NO_3^- . The initially high Cl^- concentration in the soil made applied Cl^- ineffective as a tracer of liquid water movement.

Six experiments were conducted in the laboratory in order to investigate the relative speed and direction of liquid and vapor flow and the movement of dissolved salt under a thermal gradient in a soil column. The effects of moisture content, salt concentration, stability of soil column and freezing process on the mass transport were also studied.

The results indicated that the moisture always accumulated at the colder region of the column. Chloride ion, on the other hand, accumulated at the warmer region of the column. The results seemed to indicate that a circular convection of soil moisture as the result of vapor moving to the cold end and the liquid water, formed by condensation of vapor, returning to the warm end might be an important transport mechanism in a closed soil column. The salt movement due to thermal diffusion, the Soret effect, could not be investigated in an unsaturated continuous soil column.

The steady state moisture distribution in a continuous soil column was attained within 5 days after the thermal treatment. The amount of moisture transported under a similar thermal gradient was the highest when the initial moisture content was 27% as compared to 23 and 32%. The Cl^- distribution in a continuous column changed with time indicating a

steady state with respect to Cl^- was not attained. Analysis of moisture and Cl^- distribution in a discontinuous soil column indicated that the steady state was not attained within experimental period, 20 days.

In order to distinguish Cl^- movement due to the Soret effect from convective flow, several techniques such as combining air gap length and position with freezing process were employed. The primary purpose of the use of these techniques was to block the return flow of liquid water that was formed by condensation of vapor at the colder region. The results indicated that the Cl^- ions were depleted at the colder region and accumulated at the warmer region. The characteristics of the Cl^- distribution curve resembled the compressed box function against a wall due to pushing process. The comparison between the calculated rate of moisture flow due to moisture gradient and the measured rate of Cl^- flow indicated that the Cl^- movement was greater than moisture movement. It seemed possible that the thermal diffusion of salt was operative.

The freezing process at one end of a soil column retained whatever transported to that region. In the frozen zone the Cl^- concentration based on dry soil weight was higher than the initial value, however, the Cl^- concentration based on soil solution was lower than the initial concentration. The results indicated that water moved to the frozen zone in both liquid and vapor phases and the vapor transport was the dominant mechanism.

The stability configuration of a soil column had some effects on the final distribution of soil moisture, NO_3^- and Cl^- after thermal treatment. The minimum in Cl^- concentration was located at 1.5 cm from the coldest end in continuous unstable-configuration vertical column without a frozen end. The rate of Cl^- movement in the cold region of a

discontinuous vertical column without a frozen end was greater in an unstable configuration than in a stable configuration. The rate of water movement was smaller in the columns with a frozen top end than that in the soil column with a frozen bottom end. The results showed that the liquid water circulation took place in the unstable-configuration soil column.

The results obtained by reversing the thermal gradient of a soil column with time in order to simulate the natural freezing conditions indicated the Cl^- movement was enhanced. The amount of Cl^- movement to both the frozen and warm ends in these columns was greater than that in the soil columns with only one frozen end.

In one experiment, the top end of the soil column was cold and opened in order to let the vapor move out from soil to atmosphere. The results showed the maximum in water content and the minimum in Cl^- concentration were not at the coldest frozen end of an open soil column. The rate of Cl^- movement to the warm end in a soil column without a frozen end was greater in the open system than in the closed system.

Mathematical formulation of vapor and liquid transport in soil under thermal gradient was attempted. The formulation differed from the previous analyses (Philip and de Vries 1957; Taylor and Cary 1964). In obtaining the formulation it was assumed that there was no cross interaction between substances of different phases. Thus it was assumed that the vapor flux was independent of soil moisture content and vice versa. An interaction term between vapor and moisture content arose because of the production term i.e. rate of vaporization or condensation. The equations were non-homogeneous, nonlinear simultaneous partial differential equations of parabolic type. No solution, either analytic or numerical, could be found. Thus, no attempt was made to compare theoretical distribution curves with those obtained experimentally.

BIBLIOGRAPHY

- Abd-El-Aziz, M. H. and Taylor, S. A. 1965. Simultaneous flow of water and salt through unsaturated porous media. I Rate equations. *Soil Sci. Soc. Amer. Proc.* 29:141-143.
- Anderson, D. M. 1966. Phase composition of frozen montmorillonite-water mixtures from heat capacity measurements. *Soil Sci. Soc. Amer. Proc.* 30:670-675.
- Anderson, D. M. 1967. The interface between ice and silicate surfaces. *J. Colloid Interface Sci.* 25:174-191.
- Anderson, D. M., Tice, A. R. and Banin, A. 1973. The water-ice phase composition of clay-water systems: I. The kaolinite water system. *Soil Sci. Soc. Amer. Proc.* 37:819-822.
- Anderson, D. M. and Linville, A. 1962. Temperature fluctuations at a wetting front: I. Characteristic temperature time curves. *Soil Sci. Soc. Amer. Proc.* 26:14-18.
- Berg, W. A. and Thomas, G. W. 1959. Anion elution patterns from soil and clay. *Soil Sci. Soc. Amer. Proc.* 23:348-350.
- Biggar, J. W. and Nielsen, D. R. 1967. Leaching and miscible displacement. in R. M. Hagan, H. E. Haise and T. W. Edminister eds., *Irrigation of agricultural lands*, American Soc. Agron. Monograph No.11, Madison, Wis.
- Black, T. A., Gardner, W. R. and Thurtell, G. W. 1969. The prediction of evaporation, drainage and soil water storage for a bare soil. *Soil Sci. Soc. Amer. Proc.* 33:655-660.
- Bolt, G. H. and Groenevelt, P. H. 1967. Thermostatics and thermodynamics of soil water. *Int. Soil Water Symp. (ICID), Prague, Discussions (I)* p. 71-97.
- Bouyoucos, G. J. 1915. The effect of temperature on some of the most important physical processes in soils. *Michigan Agr. Sta. Tech. Bull.* 22.
- Bouyoucos, G. J. 1916. The freezing point method as a new means of measuring the concentration of the soil solution directly in the soil. *Michigan Agr. Sta. Tech. Bull.* 24:1-44.
- Bresler, E. 1973. Simultaneous transport of solutes and water under transient unsaturated flow conditions. *Water Resour. Res.* 9:975-986.
- Brown, D. A. 1953. Cation exchange in soils through the moisture range, saturation to the wilting percentage. *Soil Sci. Soc. Amer. Proc.* 17:92-96.
- Carslaw, H. S. and Jaeger, J. C. 1959. *Conduction of heat in solids.* Oxford Univ. Press, London.

- Carter, J. N., Bennett, O. L. and Pearson, R. W. 1967. Recovery of fertilizer nitrogen under field conditions using nitrogen-15. *Soil Sci. Soc. Amer. Proc.* 31:50-56.
- Cary, J. W. 1963. Onsager's relation and the nonisothermal diffusion of water vapor. *J. Phys. Chem.* 67:126-129.
- Cary, J. W. 1964. An evaporation experiment and its irreversible thermodynamics. *Int. J. Heat and Mass Transfer* 7:531-538.
- Cary, J. W. 1965. Water flux in moist soil: Thermal versus suction gradients. *Soil Sci.* 100:168-175.
- Cary, J. W. 1966. Soil Moisture transport due to thermal gradients: Practical aspects. *Soil Sci. Soc. Amer. Proc.* 30:428-433.
- Cary, J. W. and Mayland, H. F. 1972. Salt and water movement in unsaturated frozen soil. *Soil Sci. Soc. Amer. Proc.* 37:549-555.
- Cary, J. W. and Taylor, S. A. 1962a. The interaction of the simultaneous diffusion of heat and water vapor. *Soil Sci. Soc. Amer. Proc.* 26:413-416.
- Cary, J. W. and Taylor, S. A. 1962b. Thermally driven liquid and vapor phase transfer of water and energy in soil. *Soil Sci. Soc. Amer. Proc.* 26:417-420.
- Cassel, D. K., Nielsen, D. R. and Biggar, J. W. 1969. Soil-water movement response to imposed temperature gradients. *Soil Sci. Soc. Amer. Proc.* 33:493-500.
- Childs, E. C. 1945. The water table, equipotentials, and streamlines in drained land:III. *Soil Sci.* 59:405-415.
- Childs, E. C. and Collis-George, N. 1950. The permeability of porous materials. *Proc. Royal soc., London* 201A:392-405.
- Cho, C. M. 1971. Convective transport of ammonium with nitrification in soil. *Can. J. Soil Sci.* 51:339-350.
- Crank, J. 1967. *The mathematics of diffusion.* Oxford Univ. Press, London.
- Darcy, H. 1856. *Les Fontaines Publique de la Ville de Dijon,* Victor Dalmont, Paris.
- Davidson, J. M., Stone, L. R., Nielsen, D. R. and LaRue, M. E. 1969. Field measurement and use of soil-water properties. *Water Resour. Res.* 5:1312-1321.
- Day, P. R. 1956. Dispersion of a moving salt-water boundary advancing through a saturated sand. *Trans. Amer. Geophys. Union* 37:595-601.
- Day, P. R. and Forsythe, W. M. 1957. Hydrodynamic dispersion of solutes in the soil moisture stream. *Soil Sci. Soc. Amer. Proc.* 21:477-480.

- Day, P. R. and Luthin, J. N. 1956. A numerical solution of the differential equation of flow for a vertical drainage problem. *Soil Sci. Soc. Amer. Proc.* 20:443-447.
- de Grood, S. R. 1942. Theorie phenomenologique de l'effect Soret. *Physica* 9:699-708.
- de Groot, S. R. 1952. Thermodynamics of irreversible processes. North-Holland Publishing Co., Amsterdam.
- Dirksen, C. 1969. Thermoosmosis through compacted saturated clay membranes. *Soil Sci. Soc. Amer. Proc.* 33:821-826.
- Dirksen, C. and Miller, R. D. 1966. Closed-system freezing of unsaturated soil. *Soil Sci. Soc. Amer. Proc.* 30:168-173.
- Doering, E. J. 1965. Soil-water diffusivity by the one-step method. *Soil Sci.* 99:322-326.
- Dyer, K. L. 1965. Unsaturated flow phenomena in Panoche sandy clay loam as indicated by leaching of chloride and nitrate ions. *Soil Sci. Soc. Amer. Proc.* 29:121-126.
- Edlefsen, N. E. and Bodman, G. B. 1941. Field measurements of water movement through a silt loam soil. *J. Am. Soc. Agron.* 33:713-731.
- Erh, K. T., Nielsen, D. R. and Biggar, J. W. 1971. Two dimensional heat transfer in porous media with steady-state water flow. *Soil Sci. Soc. Amer. Proc.* 35:209-214.
- Ferguson, H., Brown, P. L. and Dickey, D. D. 1964. Water movement and loss under frozen soil conditions. *Soil Sci. Soc. Amer. Proc.* 28:700-703.
- Field-Ridley, G. 1975. Nitrogen movement in two Manitoba soils. M. Sc. Thesis. Univ. of Manitoba, Winnipeg, Manitoba, Canada.
- Fireman, M. 1944. Permeability measurements on disturbed soil samples. *Soil Sci.* 58:337-353.
- Fitts, D. D. 1962. Nonequilibrium thermodynamics. McGraw Hill Book Co., New York.
- Freeze, R. A. 1969. The mechanism of natural ground water recharge and discharge. I. One dimensional vertical, unsteady, unsaturated flow above a recharging or discharging ground-water flow system. *Water Resour. Res.* 5:153-171.
- Gardner, W. R. 1962. Approximate solution of a non-steady-state drainage problem. *Soil Sci. Soc. Amer. Proc.* 26:129-132.
- Gardner, W. R. 1969. Water movement below the root zone. 8th Int. Congr. Soil Sci. Bucharest, Romania, 2:63.

- Gardner, W. R. and Hillel, D. I. 1962. The relation of external evaporation conditions to the drying of soils. *J. Geophys. Res.* 67:4319-4325.
- Gardner, W. R. and Mayhugh, M. S. 1958. Solutions and tests of the diffusion equation for the movement of water in soil. *Soil. Sci. Soc. Amer. Proc.* 22:197-201.
- Globus, A. M. 1962. Mechanisms of soil and ground moisture migration and of water movement in freezing soils under the effect of thermal gradients. *Soviet Soil Sci.* 2:130-139.
- Graham-Bryce, I. J. 1963. Self-diffusion of ions in soil II. Anions. *J. Soil Sci.* 14:188-200.
- Green, R. E. and Corey, J. C. 1971. Calculation of hydraulic conductivity: A further evaluation of predictive methods. *Soil Sci. Soc. Amer. Proc.* 35:3-8.
- Groenevelt, P.H. and Kay, B. D. 1974. On the interaction of water and heat transport in frozen and unfrozen soils: II. The liquid phase. *Soil Sci. Soc. Amer. Proc.* 38:400-404.
- Gurr, C. G., Marshall, T. J. and Hutton, J. T. 1952. Movement of water in soil due to a temperature gradient. *Soil Sci.* 74:335-345.
- Hallaire, M. 1958. in 'Water and its conduction in soils' Spec. Rept. 40:88-105. Highway Res. Branch, Washington D. C.
- Hanks, R. J. and Bowers, S. A. 1962. Numerical solution of the moisture flow equation for infiltration into layered soil. *Soil Sci. Soc. Amer. Proc.* 26:530-534.
- Harlan, R. L. 1973. Analysis of coupled heat-fluid transport in partially frozen soil. *Water Resour. Res.* 9:1314-1323.
- Hillel, D. 1971. *Soil and water: Physical principles and processes.* Academic Press Inc., New York and London.
- Hoekstra, P. 1966. Moisture movement in soils under temperature gradients with the cold side temperature below freezing. *Water Resour. Res.* 2:241-250.
- Hoekstra, P. 1969. Water movement and freezing pressures. *Soil Sci. Soc. Amer. Proc.* 33:512-518.
- Hoekstra, P. and Chamberlain, E. 1964. Electro-osmosis in frozen soil. *Nature* 203:1406-1407.
- Hornberger, G. M., Remson, I. and Fungaroli, A. A. 1969. Numeric studies of a composite soil moisture groundwater system. *Water Resour. Res.* 5:313-352.

- Hutcheon, W. L. 1955. Moisture flow induced by thermal gradients within unsaturated soils. Ph. D. thesis, Univ. of Minnesota, Minnesota, U. S. A.
- Hutcheon, W. L. 1958. Moisture flow induced by thermal gradients within unsaturated soils. Special Report 40. Highway Res. Branch, Washington D. C.
- Jackson, R. D. 1964a. Water vapor diffusion in relatively dry soil. I. Theoretical considerations and sorption experiments. Soil Sci. Soc. Amer. Proc. 28:172-176.
- Jackson, R. D. 1964b. Water vapor diffusion in relatively dry soil. III. Steady-state experiments. Soil Sci. Soc. Amer. Proc. 28:467-470.
- Jackson, R. D. 1973. Diurnal changes in soil-water content during drying. in 'Field soil water regime! Soil Sci. Soc. Amer. Special Publ. No.5.
- Jackson, R. D., Kimball, B. A., Reginato, R. J. and Nakayama, F. S. 1973. Diurnal soil-water evaporation: Time-depth-flux patterns. Soil Sci. Soc. Amer. Proc. 37:505-509.
- Jackson, R. D., Reginato, R. J. and van Bavel, C. H. M. 1965. Comparison of measured and calculated hydraulic conductivities of unsaturated soil. Water Resour. Res. 1:375-380.
- Joffe, J. S. 1949. Pedology. New Brunswick, N. J., Pedology Publications.
- Jones, H. E. and Kohnke, H. 1952. The influence of soil moisture tension on vapor movement of soil water. Soil Sci. Soc. Amer. Proc. 16:245-248.
- Joshua, W. D. 1971. Soil moisture movement under temperature gradients. Ph. D. thesis, Univ. of Saskatchewan, Saskatoon, Saskatchewan, Canada.
- Joshua, W. D. and de Jong, E. 1973. Soil moisture movement under temperature gradients. Can. J. Soil Sci. 53:49-57.
- Jost, W. 1952. Diffusion in solids, liquids, gases. Academic Press, Inc., New York.
- Kamphake, L. J. Hannah, S. A. and Cohen, J. M. 1967. Automated analysis for nitrate by hydrazine reduction. Water Res. 1:205-216.
- Kay, B. D. and Groenevelt, P. H. 1974. On interaction of water and heat transport in frozen and unfrozen soils. I. Basic theory; The vapor phase. Soil Sci. Soc. Amer. Proc. 38:395-400.
- Kemper, W. D. 1960. Water and ion movement in thin films as influenced by the electrostatic charge and diffuse layer of cations associated with clay mineral surfaces. Soil Sci. Soc. Amer. Proc. 24:10-16.

- Kemper, W. D., Maasland, D. E. L. and Porter, L. K. 1964. Mobility of water adjacent to mineral surfaces. *Soil Sci. Soc. Amer. Proc.* 28:164-167.
- Kirkham, D. and Power, W. L. 1972. *Advanced soil physics*. Wiley-Interscience, New York.
- Kissel, D. E. Ritchie, J. T. and Burnett, E. 1973. Chloride movement in undisturbed swelling clay soil. *Soil Sci. Soc. Amer. Proc.* 37:21-24.
- Klute, A. 1952. A numerical method for solving the flow equation for water in unsaturated materials. *Soil Sci.* 73:105-116.
- Klute, A. 1965. Water capacity. in 'Methods of soil analysis,' Part I. *Agronomy* 9:273-278.
- Klute, A. 1973. Soil water flow theory and its application in field situations. in 'Field soil water regime!' *Soil Sci. Soc. Amer. Special Publ. No. 5*.
- Klute, A. and Letey, J. 1958. The dependence of ionic diffusion on the moisture content of nonadsorbing porous media. *Soil Sci. Soc. Amer. Proc.* 22:213-215.
- Krupp, H. K., Biggar, J. W. and Nielsen, D. R. 1972. Relative flow rates of salt and water in soil. *Soil Sci. Soc. Amer. Proc.* 36:412-417.
- Kunze, R. J., Uehara, G. and Graham, K. 1968. Factors important in the calculation of hydraulic conductivity. *Soil Sci. Soc. Amer. Proc.* 32:760-765.
- Lai, T. M. and Mortland, M. M. 1961. Diffusion of ions in bentonite and vermiculite. *Soil Sci. Soc. Amer. Proc.* 25:353-356.
- Lapidus, L. and Amundson, N. R. 1952. Mathematics of adsorption in beds: VI. The effect of longitudinal diffusion in ion exchange and chromatographic columns. *J. Phy. Chem.* 56:48-49.
- Lebedeff, A. F. 1927. The movement of ground and soil water. *First Int. Congr. Soil Sci. Proc.* I:459-494.
- Low, P. F. 1960. Viscosity of water in clay system. *Clays and Clay Minerals*, vol. 8:170-182.
- Low, P. F. 1961. Physical chemistry of clay-water interaction. *Advances in Agronomy*, vol. 13:269-327.
- Lutz, J. F. and Kemper, W. D. 1959. Intrinsic permeability of clay as affected by clay-water interaction. *Soil Sci.* 88:83-90.

- MacLean, D. J. and Watkin, P. M. G. 1946. Moisture movement occurring in soil due to the existence of a temperature gradient. Road Research Lab. D. S. I. R. England. Note RN/761.
- Marshall, T. J. 1958. A relation between permeability and size distribution of pores. *J. Soil Sci.* 9:1-8.
- Martin, R. T. 1962. Adsorbed water on clay - a review. *Clays and Clay Minerals*. Vol. 9:28-70.
- Matthes, R. K. and Bowen, H. D. 1963. Water vapor transfer in soil by thermal gradients and its control. *Trans. Amer. Soc. Agr. Eng.* 6:244-250.
- McNeal, B. L. and Coleman, N. T. 1966. Effect of solution composition on soil hydraulic conductivity. *Soil Sci. Soc. Amer. Proc.* 30:308-312.
- Meek, B. D., Grass, L. B., Willardson, L. S. and Mackenzie, A. J. 1970. Nitrate transformations in a column with a controlled water table. *Soil Sci. Soc. Amer. Proc.* 34:235-239.
- Michaels, A. S. and Lin, C. S. 1954. Permeability of kaolinite. *Ind. Eng. Chem.* 46:1239-1246.
- Michaels, A. S. and Lin, C. S. 1955. Effects of counter-electro-osmosis and sodium ion exchange on permeability of kaolinite. *Ind. Eng. Chem.* 47:1249-1253.
- Miller, R. J. and Low, P. F. 1963. Threshold gradient for water flow in clay systems. *Soil Sci. Soc. Amer. Proc.* 27:605-609.
- Miller, E. E. and Miller, R. D. 1956. Physical theory for capillary flow phenomena. *J. Appl. Phys.* 27:324-332.
- Miller, R. J., Overman, A. R. and Peverly, J. H. 1969. The absence of threshold gradients in clay - water systems. *Soil Sci. Soc. Amer. Proc.* 33:183-187.
- Millington, R. J. and Quirk, J. P. 1959. Permeability of porous media. *Nature* 183:387-388.
- Millington, R. J. and Quirk, J. P. 1961. Permeability of porous solids. *Trans. Faraday Soc.* 57:1200-1207.
- Mitchell, J. K. and Younger, J. S. 1967. Abnormalities in hydraulic flow through fine-grained soils, permeability and capillarity of soil. STP417. *A. S. T. M.* 106-139.
- Mokady, R. S. and Bresler, E. 1968. Reduced sodium exchange capacity in unsaturated flow. *Soil Sci. Soc. Amer. Proc.* 32:463-467.
- Mokady, R. S., Ravina, I. and Zaslavsky, D. 1968. Movement of salt in saturated soil columns. *Israel J. Chem.* 6:159-165.

- Moore, R. E. 1940. The relation of soil temperature to soil moisture, pressure potential, retention and infiltration rate. Soil Sci. Soc. Amer. Proc. 5:61-
- Musa, M. M. 1968. Nitrogenous fertilizer transformations in the Sudan Gezira Soil. Plant and Soil 28:413-421.
- Nakayama, F. S. Jackson, R. D., Kimball, B. A. and Reginato, R. J. 1973. Diurnal soil-water evaporation: Chloride movement and accumulation near the soil surface. Soil Sci. Soc. Amer. Proc. 37:509-513.
- Nielsen, D. R. and Biggar, J. W. 1961. Miscible displacement in soils: I. Experimental information. Soil Sci. Soc. Amer. Proc. 25:1-5.
- Nielsen, D. R. and Biggar, J. W. 1962. Miscible displacement in soils: III. Theoretical consideration. Soil Sci. Soc. Amer. Proc. 26:216-221.
- Nielsen, D. R. and Biggar, J. W. 1963. Miscible displacement: IV. Mixing in glass beads. Soil Sci. Soc. Amer. Proc. 27:10-13.
- Nielsen, D. R. and Biggar, J. W. 1973. Analyzing soil water and solute movement under field conditions. in "Soil-moisture and irrigation study II". Int. Atomic Energy Agency, Vienna.
- Nielsen, D. R., Jackson, R. D., Cary, J. W. and Evans, D. D. (ed.) 1972. Soil water. American Soc. of Agronomy and Soil Sci. Soc. Amer. Madison, Wis.
- Oakes, D. T. 1960. Solids concentration effects in bentonite drilling fluids. Clays and Clay Minerals 8:252-273.
- Oddson, J. K., Letey, J. and Weeks, L. V. 1970. Predicted distribution of organic chemicals in solution and adsorbed as a function of position and time for various chemical and soil properties. Soil Sci. Soc. Amer. Proc. 34:412-417.
- Olsen, H. W. 1962. Hydraulic flow through saturated clays. Clays and Clay Minerals. 9:131-161.
- Olsen, H. W. 1965. Deviations from Darcy's law in saturated clays. Soil Soc. Amer. Proc. 29:135-140.
- Olsen, H. W. 1966. Darcy's law in saturated kaolinite. Water Resour. Res. 2:287-295.
- Olsen, S. R., Kemper, W. D. and Jackson, R. D. 1962. Phosphate diffusion to plant roots. Soil Sci. Soc. Amer. Proc. 26:222-227.
- Olsen, S. R., Kemper, W. D. and van Schaik, J. C. 1965. Self-diffusion coefficients of phosphorus in soil measured by transient and steady-state methods. Soil Sci. Soc. Amer. Proc. 29:154-158.
- Olsen, S. R. and Kemper, W. D. 1968. Movement of nutrients to plant roots. Adv. Agron. 20:91-151.

- Olsen, S. R. and Watanabe, F. S. 1963. Diffusion of phosphorus as related to soil texture and plant uptake. *Soil Sci. Soc. Amer. Proc.* 27:648-653.
- Overrein, L. N. 1968. Lysimeter studies in tracer nitrogen in forest soils. I. Nitrogen losses by leaching and volatilization after addition of urea N¹⁵. *Soil Sci.* 106:280-290.
- Overrein, L. N. 1969. Lysimeter studies in tracer nitrogen in forest soils. II. Comparative losses of nitrogen through leaching and volatilization after the addition of urea-, ammonium and nitrate N¹⁵. *Soil Sci.* 107:149-159.
- Parr, J. F. and Bertrand, A. R. 1960. Water infiltration into soils. *Advances in Agron.* 12:311-363.
- Philip, J. R. 1957. Evaporation and moisture and heat fields in the soil. *J. Meteorol.* 14:354-366.
- Philip, R. E. and Brown, D. A. 1964. Ion diffusion: II. Comparison of apparent self and counter diffusion coefficients. *Soil Sci. Soc. Amer. Proc.* 28:758-763.
- Philip, R. E. and Brown, D. A. 1965. Ion diffusion III. The effect of soil compaction on self diffusion of rubidium-86 and strontium-89. *Soil Sci. Soc. Amer. Proc.* 29:657-661.
- Philip, J. R. and deVries, D. A. 1957. Moisture movement in porous materials under temperature gradients. *Trans. Amer. Geophys. Union* 38:222-232.
- Porter, L. K., Kemper, W. D. Jackson, R. D. and Stewart, B. A. 1960. Chloride diffusion in soil as influenced by moisture content. *Soil Sci. Soc. Amer. Proc.* 24:460-463.
- Raats, P. A. C. and Gardner, W. R. 1972. Movement of water in the unsaturated zone near a water table. *Drainage. Amer. Soc. of Agronomy, Madison, Wis.*
- Rawlins, S. L. and Gardner, W. H. 1963. A test of the validity of diffusion equation for unsaturated flow of soil water. *Soil Sci. Soc. Amer. Proc.* 27:501-511.
- Reeve, R. C. 1960. The transmission of water by soils as influenced by chemical and physical properties. *Int. Congr. Agr. Eng. Trans.* 5th (Brussels, Belgium) I:21-32.
- Rhoades, J. D. and Ingvalson, R. D. 1969. Macroscopic swelling and hydraulic conductivity properties of four vermiculitic soils. *Soil Sci. Soc. Amer. Proc.* 33:364-369.
- Richards, L. A. 1931. Capillary conduction of liquids through porous mediums. *Physics* I:318-333.

- Rollins, R. L., Spangler, M. G. and Kirkham, D. 1954. Movement of soil moisture under thermal gradient. Highway Res. Board Proc. 33:492-508.
- Romkens, M. J. M. and Bruce, R. R. 1964. Nitrate diffusivity in relation to moisture content of non-absorbing porous media. Soil Sci. 98:332-337.
- Rose, D. A. 1963a. Water movement in porous material. I. Isothermal vapor transfer. Br. J. Appl. Phys. 14:256.
- Rose, D. A. 1963b. Water movement in porous materials. II. The separation of the components of water flux. Br. J. Appl. Phys. 14:491.
- Rose, D. A. 1965. Water movement in unsaturated porous materials. Bulletin Rilem No. 29:119-124.
- Rose, C. W. 1968a. Water transport in soil with a daily temperature wave. I. Theory and experiment. Aust. J. Soil Res. 6:31-44.
- Rose, C. W. 1968b. Water transport in soil with a daily temperature wave. II. Analysis. Aust. J. Soil Res. 6:45-57.
- Rubin, J. 1968. Theoretical analysis of two dimensional transient flow of water in unsaturated and partially saturated soil. Soil Sci. Soc. Amer. Proc. 32:607-615.
- Rubin, J. and Steinhardt, R. 1963. Soil water relations during rain infiltration: I. Theory. Soil Sci. Soc. Amer. Proc. 27:246-250.
- Rubin, J. and Steinhardt, R. 1964. Soil water relations during rain infiltration: III. Water uptake at incipient ponding. Soil Sci. Soc. Amer. Proc. 28:614-620.
- Sartz, R. S. 1969. Soil water movement as affected by deep freezing. Soil Sci. Soc. Amer. Proc. 33:333-337.
- Scheidegger, A. E. 1954. Statistical hydrodynamics in porous media. J. Appl. Phys. 25:997-1001.
- Scheidegger, A. E. 1963. The physics of flow through porous media. Univ. of Toronto Press, Toronto, Ont.
- Shainberg, I. and Kemper, W. D. 1966a. Conductance of adsorbed alkali cation in aqueous and alcoholic bentonite pastes. Soil Sci. Soc. Amer. Proc. 30:700-706.
- Shainberg, I. and Kemper, W. D. 1966b. Hydration status of adsorbed cations. Soil Sci. Soc. Amer. Proc. 30:707-713.
- Shaykewich, C. F. 1974. in 'The Allocative Conflicts in Water - Resource Management'. Agassiz Center for Water Studies, Univ. of Manitoba.
- Smith, A. 1932. Seasonal subsoil temperature variations. J. Agr. Res. 44:421-428.

- Smith, W. O. 1940. Thermal conductivities in moist soils. *Soil Sci. Soc. Amer. Proc.* 4:32-40.
- Smith, W. O. 1944. Thermal transfer moisture in soils. *Trans. Amer. Geophys. Union, Hydrology Sect.* 511-523.
- Staple, W. J. 1966. Infiltration and redistribution of water in vertical columns of loam soil. *Soil Sci. Soc. Amer. Proc.* 30:553-558.
- Stewart, B. A., Viets, F. G. Jr., Hutchinson, G. L. and Kemper, W. K. 1967. Nitrate and other water pollutants under field feedlots. *Environ. Sci. Tech.* 1: 736-739.
- Swartzendruber, D. 1962. Non-Darcy flow behavior in liquid-saturated porous media. *J. Geophys. Res.* 67:5205-5213.
- Swartzendruber, D. 1963. Non-Darcy behavior and the flow of water in unsaturated soils. *Soil Sci. Soc. Amer. Proc.* 27:491-495.
- Swartzendruber, D. 1966. Soil-water behavior as described by transport coefficients and functions. *Advan. Agron.* 18:327-370.
- Swartzendruber, D. 1968. The flow of water in unsaturated soil. in 'Flow through porous media.' Publ. by Academic Press, New York.
- Taylor, G. I. 1953. Dispersion of soluble matter in solvent flowing slowly through a tube. *Proc. Roy. Soc. (London)* 219:186-203.
- Taylor, S. A. and Cary, 1960. Analysis of the simultaneous flow of water and heat or electricity with the thermodynamics of irreversible processes. 7th Int. Congr. of Soil Sci. *Trans.* 1:80-90.
- Taylor, S. A. and Cary, 1964. Linear equations for the simultaneous flow of matter and energy in a continuous soil system. *Soil Sci. Soc. Amer. Proc.* 28:167-172.
- Taylor, S. A. and Cavazza, L. 1954. The movement of soil moisture in response to temperature gradients. *Soil Sci. Soc. Amer. Proc.* 18:351-358.
- Taylor, G. S. and Luthin, J. N. 1968. Computer methods for transient analysis of water table aquifers. *Water Resour. Res.* 5:144-152.
- Thames, J. L. and Evans, D. D. 1968. Analysis of the vertical infiltration of water into soil columns. *Water Resour. Res.* 4:817-828.
- Thomas, G. W. 1970. Soil and climatic factors which affect nutrient mobility. in 'Nutrient mobility in soils: Accumulation and losses.' SSSA Special Publ. No. 4. *Soil Sci. Soc. Amer.*, Madison, Wis.
- Thomas, G. W. and Swoboda, A. R. 1970. Anion exclusion effects on chloride movement in soils. *Soil Sci.* 110:163-166.

- Topp, G. C. and Miller, E. E. 1966. Hysteretic moisture characteristics and hydraulic conductivities for glass bead media. *Soil Sci. Soc. Amer. Proc.* 30:156-162.
- van Schaik, J. C. and Kemper, W. D. 1966. Contribution of adsorbed cations to diffusion in clay-water system. *Soil Sci. Soc. Amer. Proc.* 30:17-25.
- Weeks, L. V., Richards, S. J. and Letey, J. 1968. Water and salt transfer in soil resulting from thermal gradients. *Soil Sci. Soc. Amer. Proc.* 32:193-197.
- Westcot, D. W. and Wierenga, P. J. 1974. Transfer of heat by conduction and vapor movement in a closed soil system. *Soil Sci. Soc. Amer. Proc.* 38:9-14.
- Whisler, F. D. and Klute, A. 1965. The numerical analysis of infiltration, considering hysteresis, into a vertical soil column at equilibrium under gravity. *Soil Sci. Soc. Amer. Proc.* 29:489-494.
- Williams, P. J. 1964a. Specific heat and apparent specific heat of frozen soils. *Geotechnique* 42:133-142.
- Williams, P. J. 1964b. Unfrozen water content of frozen soils and soil moisture suction. *Geotechnique* 14:231-246.
- Willis, W. O., Carlson, C. W., Alessi, J. and Haas, H. J. 1961. Depth of freezing and spring run-off as related to fall soil moisture level. *Can. J. Soil Sci.* 41:115-123.
- Willis, W. O., Parkinson, H. L., Carlson, C. W. and Haas, H. J. 1964. Water table changes and soil moisture loss under frozen conditions. *Soil Sci.* 98:244-248.
- Winterkorn, H. F. 1947. Fundamental similarities between electro-osmotic and thermo-osmotic systems. *Highway Res. Board Proc.* 27:443.
- Yaron, B. and Thomas, G. W. 1968. Soil hydraulic conductivity as affected by sodic water. *Water Resour. Res.* 4: 545-552.

APPENDIX A*

* Designations for all of the figures are as follows:

●—● NO_3^- (Soln)

△—△ NO_3^- (Soil)

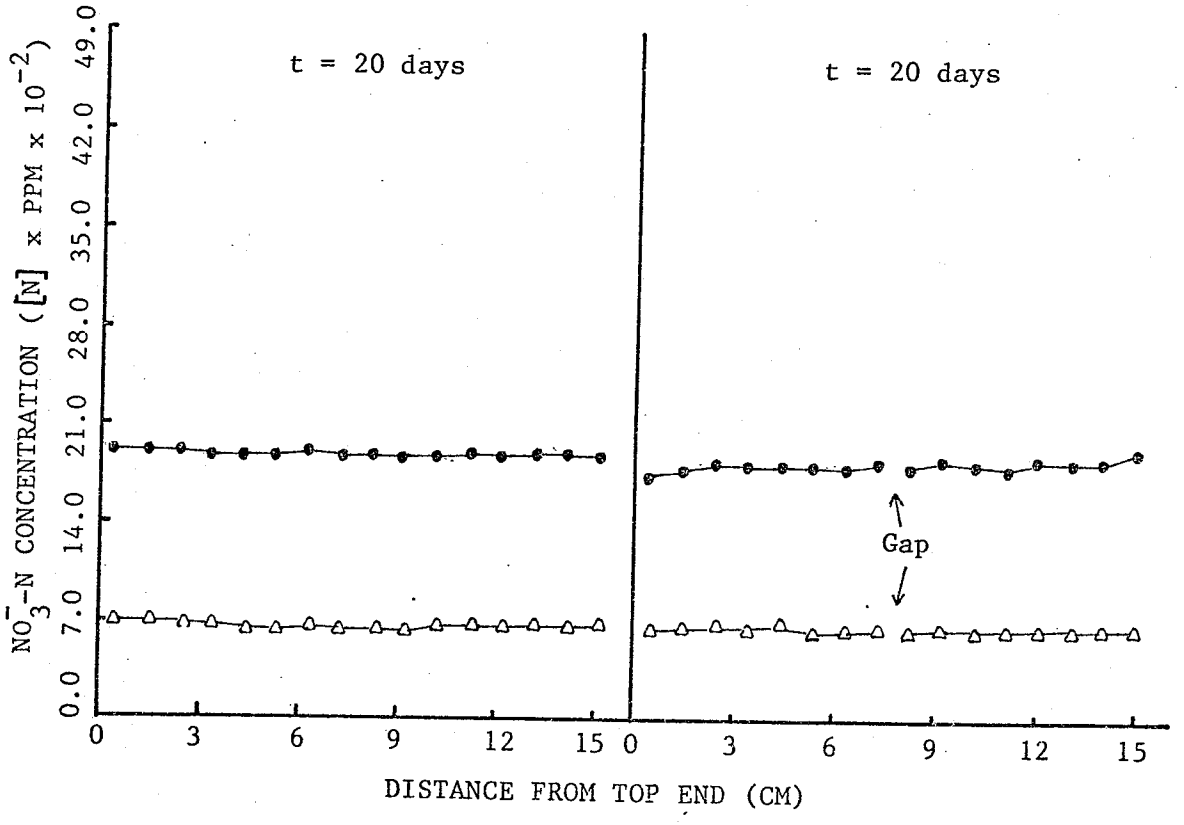
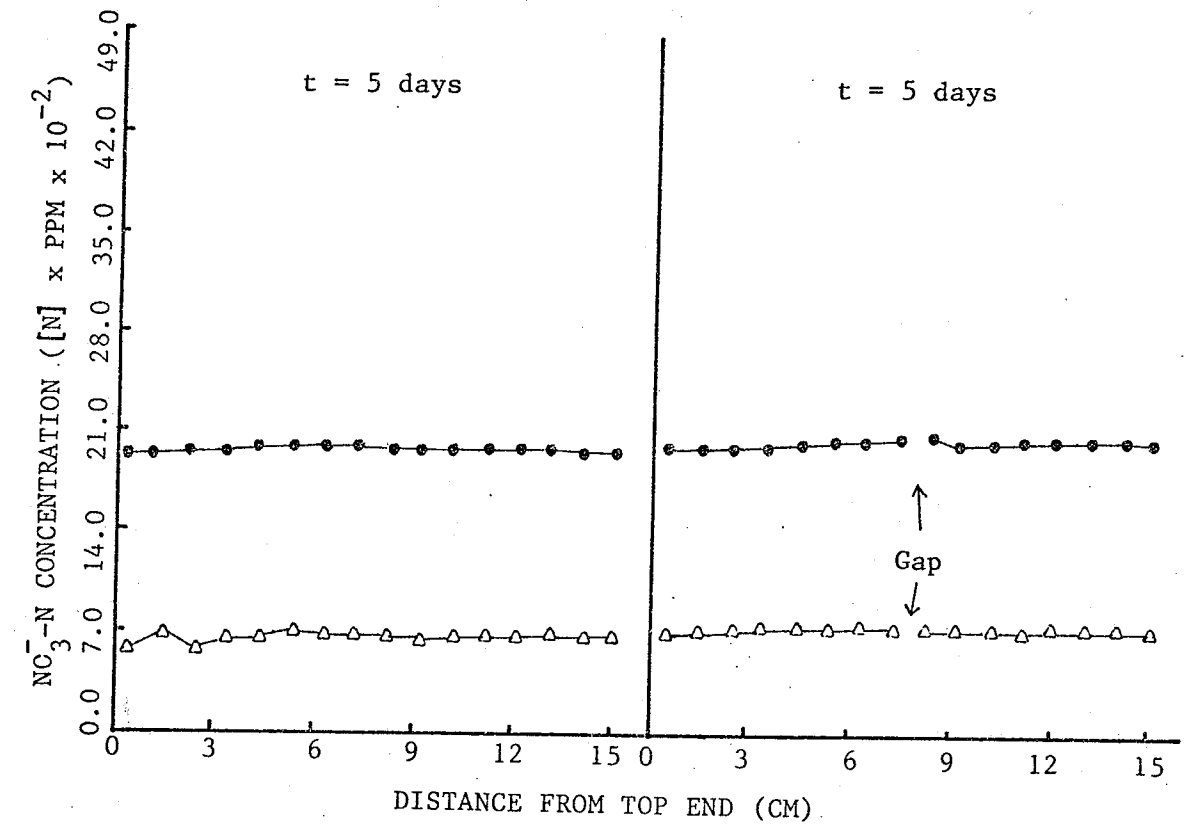


Fig. A1. Nitrate distribution in $\text{Ca}(\text{NO}_3)_2$ and KCl -treated soil columns without temperature gradients (initial $\text{H}_2\text{O} = 27\%$ and $\text{KCl} = 10\%$).

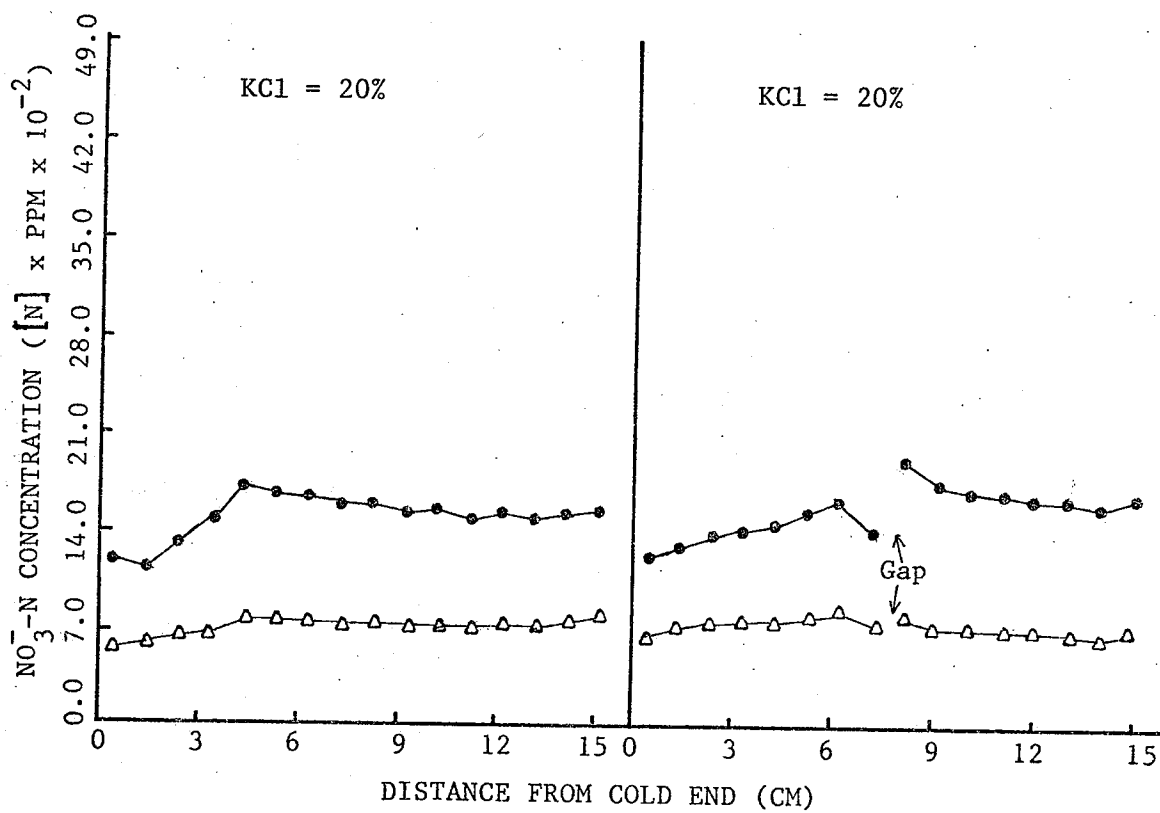
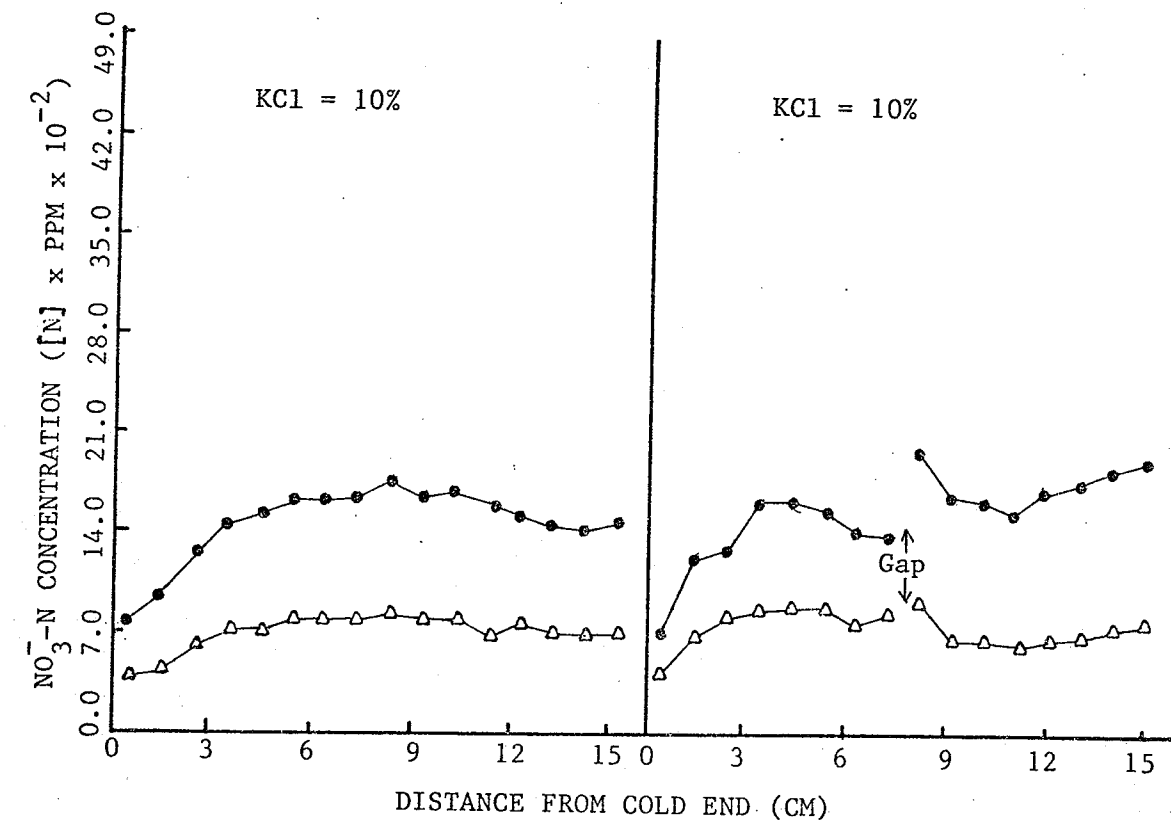


Fig. A2. Nitrate distribution in Ca(NO₃)₂ and KCl-treated soil columns after 10 days of thermal treatment (initial H₂O = 27%)

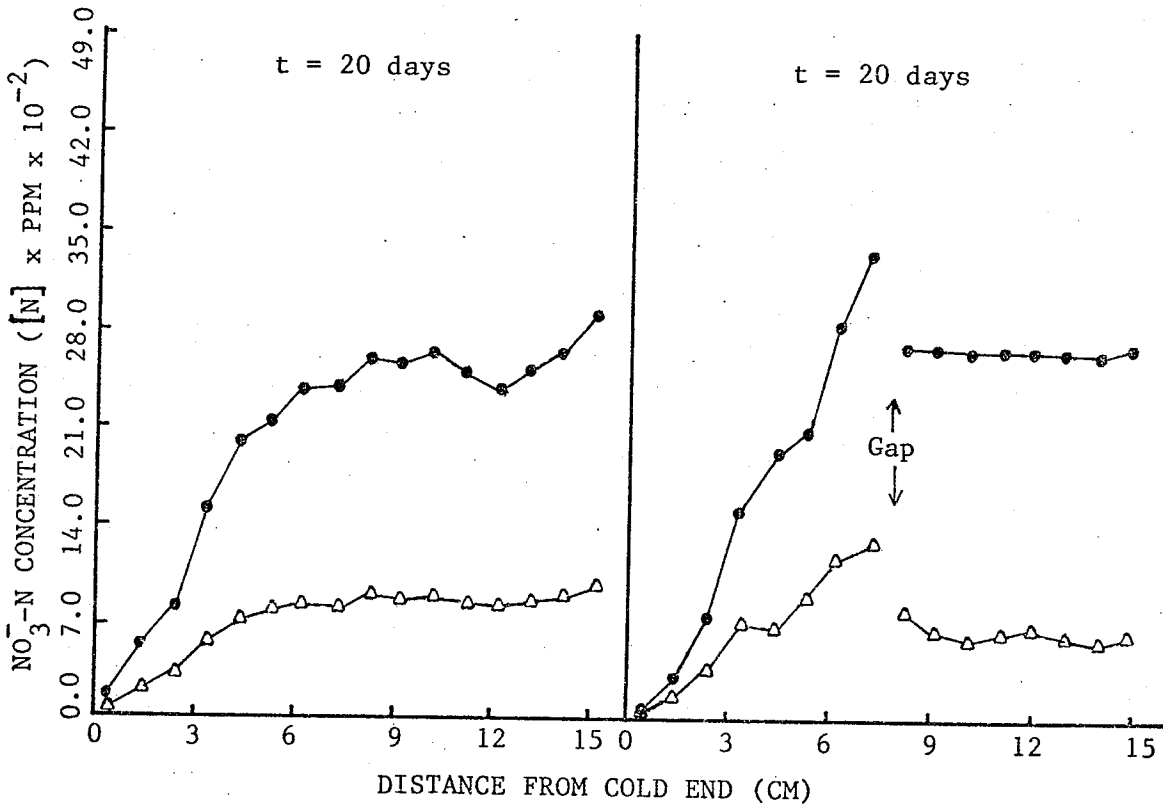
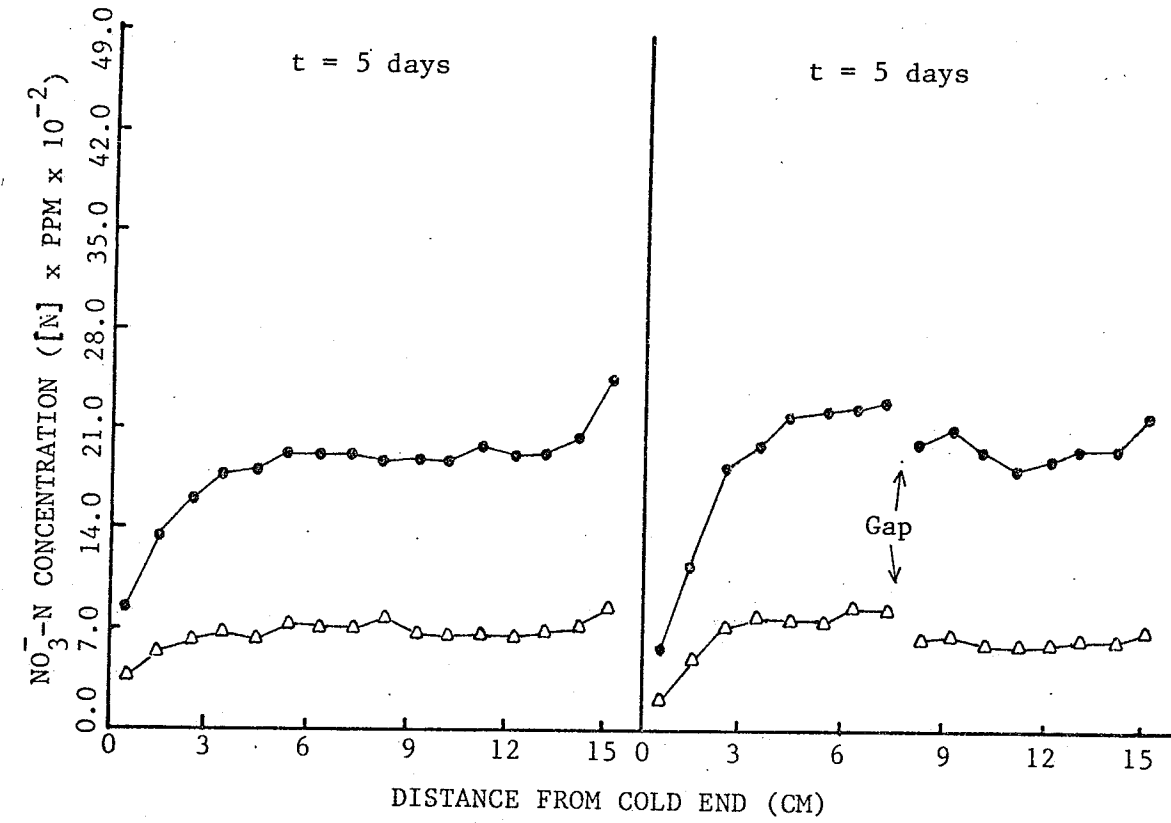


Fig. A3. Nitrate distribution in Ca(NO₃)₂ and KCl-treated soil columns with or without gap after 5 or 20 days of thermal treatment (initial H₂O = 27% and KCl = 10%).

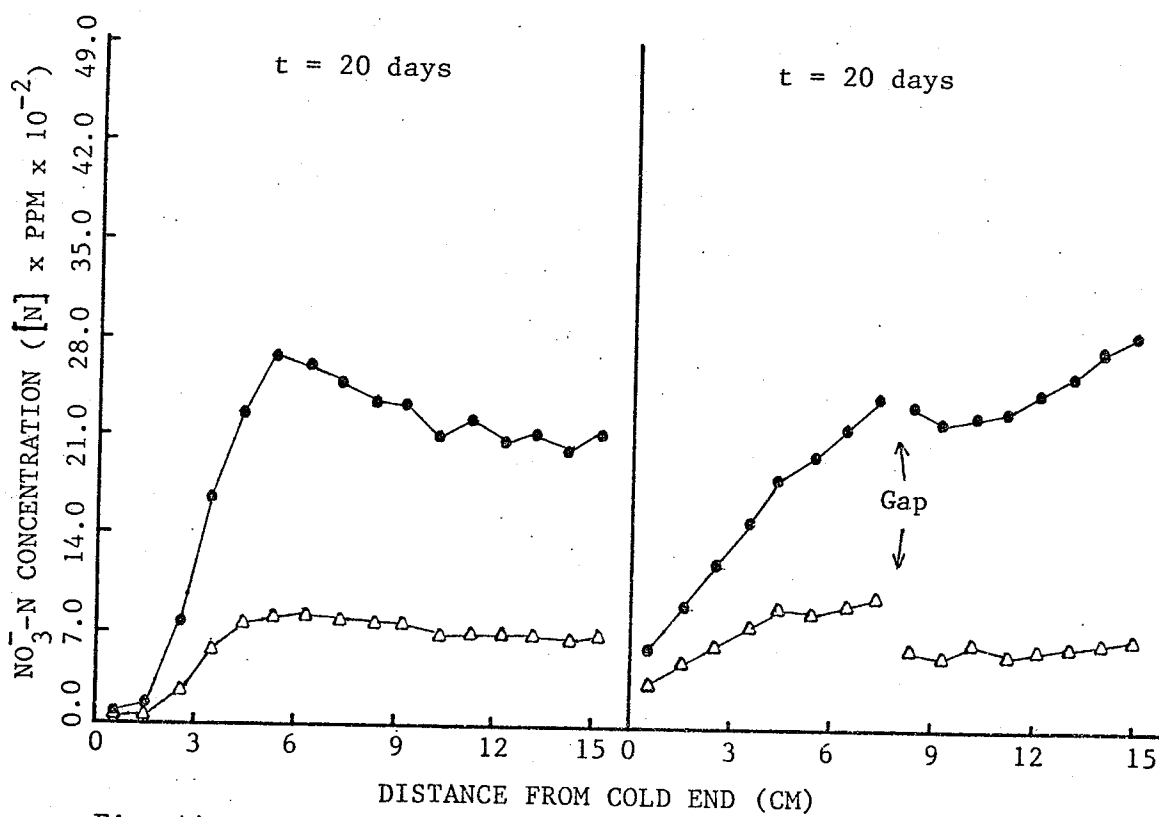
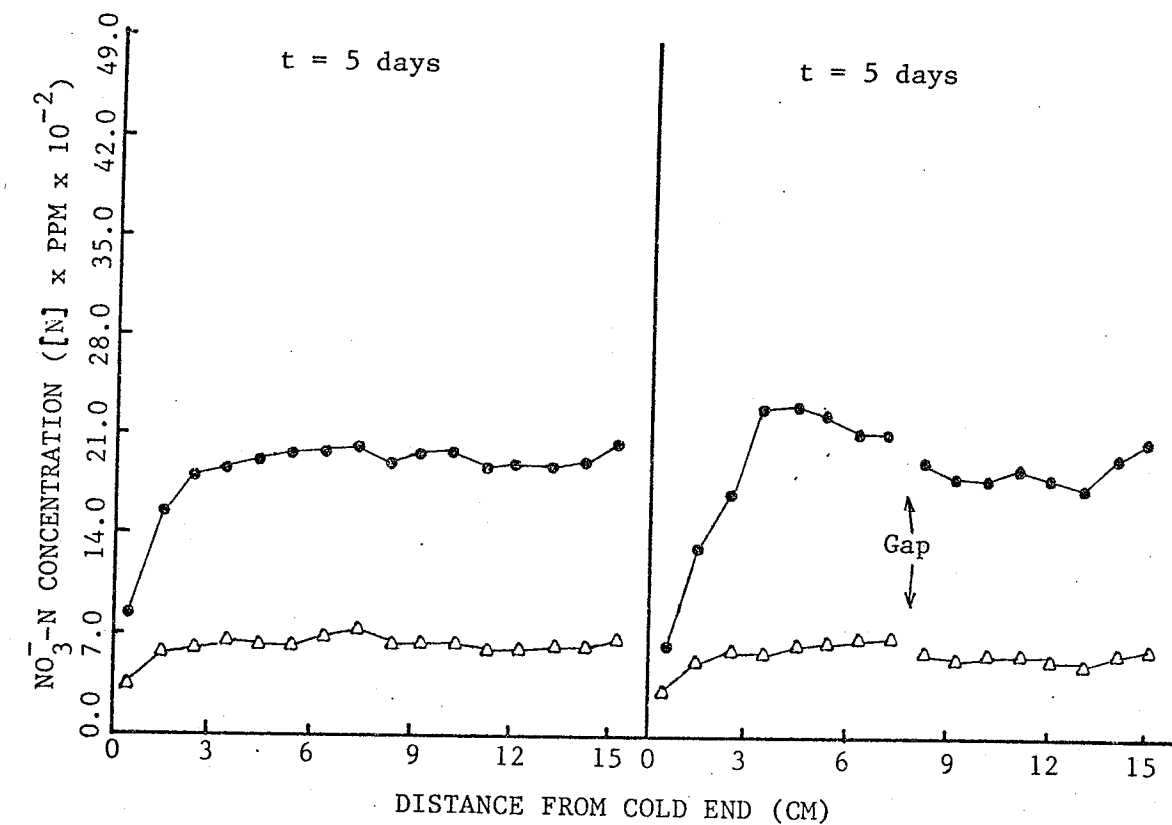


Fig. A4. Nitrate distribution in $\text{Ca}(\text{NO}_3)_2$ and KCl-treated soil columns with or without gap after 5 or 20 days of thermal treatment (initial $\text{H}_2\text{O} = 27\%$ and $\text{KCl} = 20\%$)

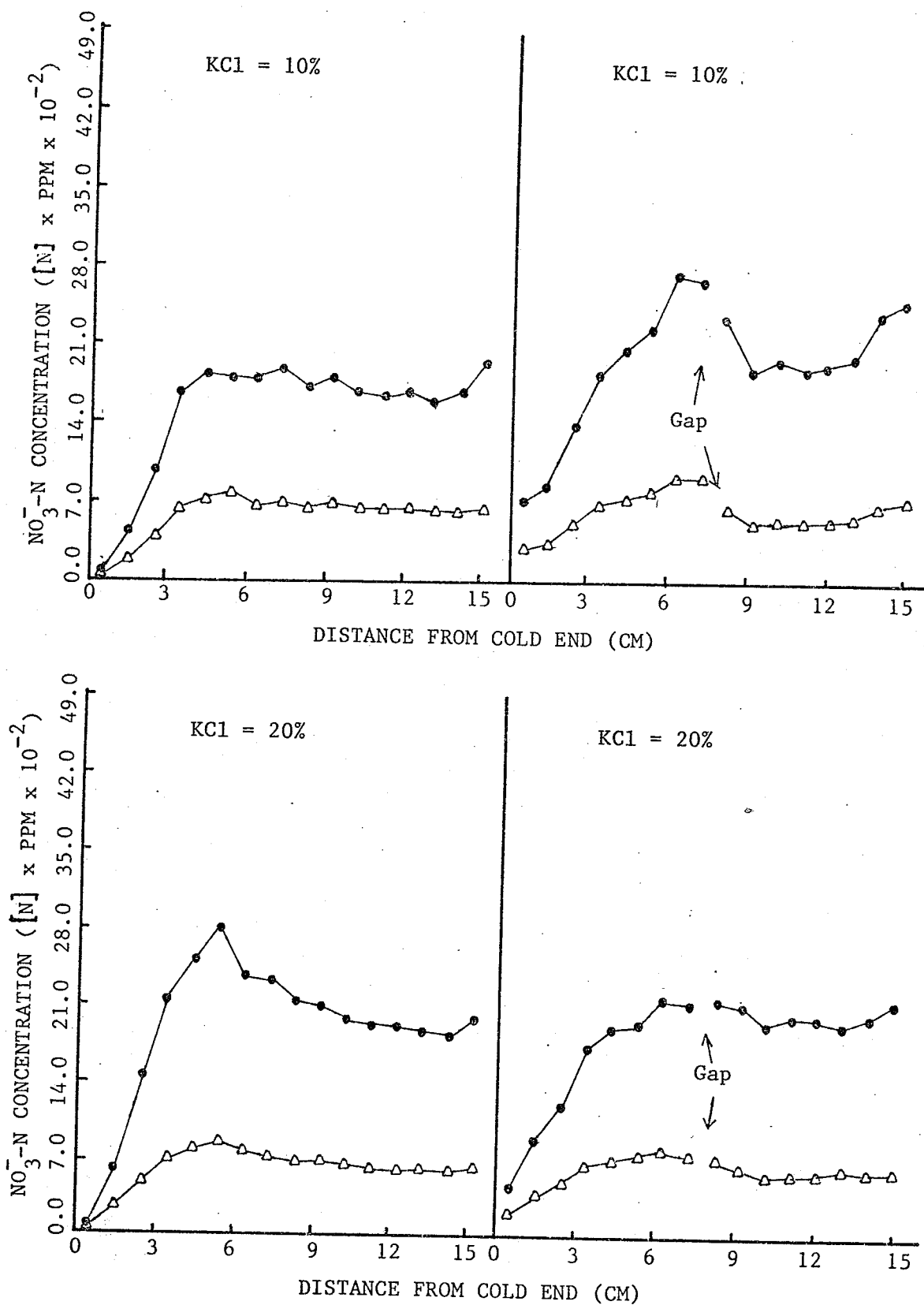


Fig. A5. Nitrate distribution in $\text{Ca}(\text{NO}_3)_2$ and KCl-treated soil columns with or without gap after 10 days of thermal treatment (initial $\text{H}_2\text{O} = 32\%$).

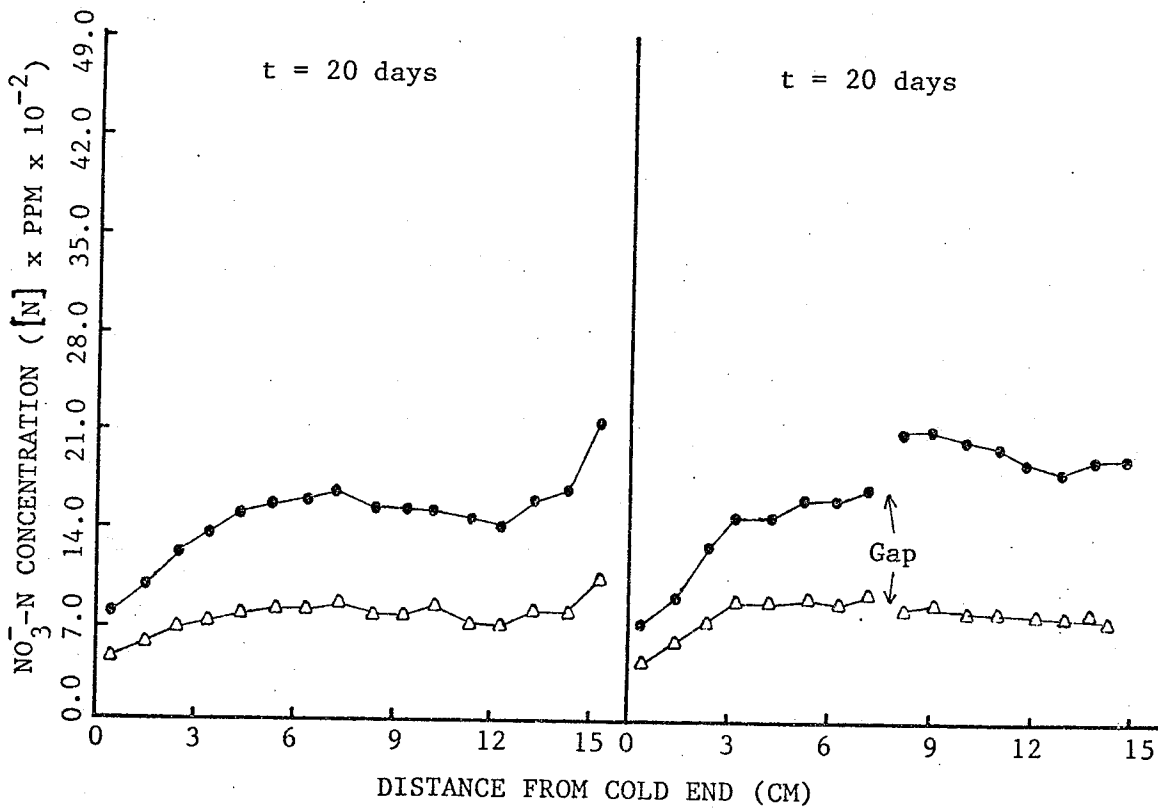
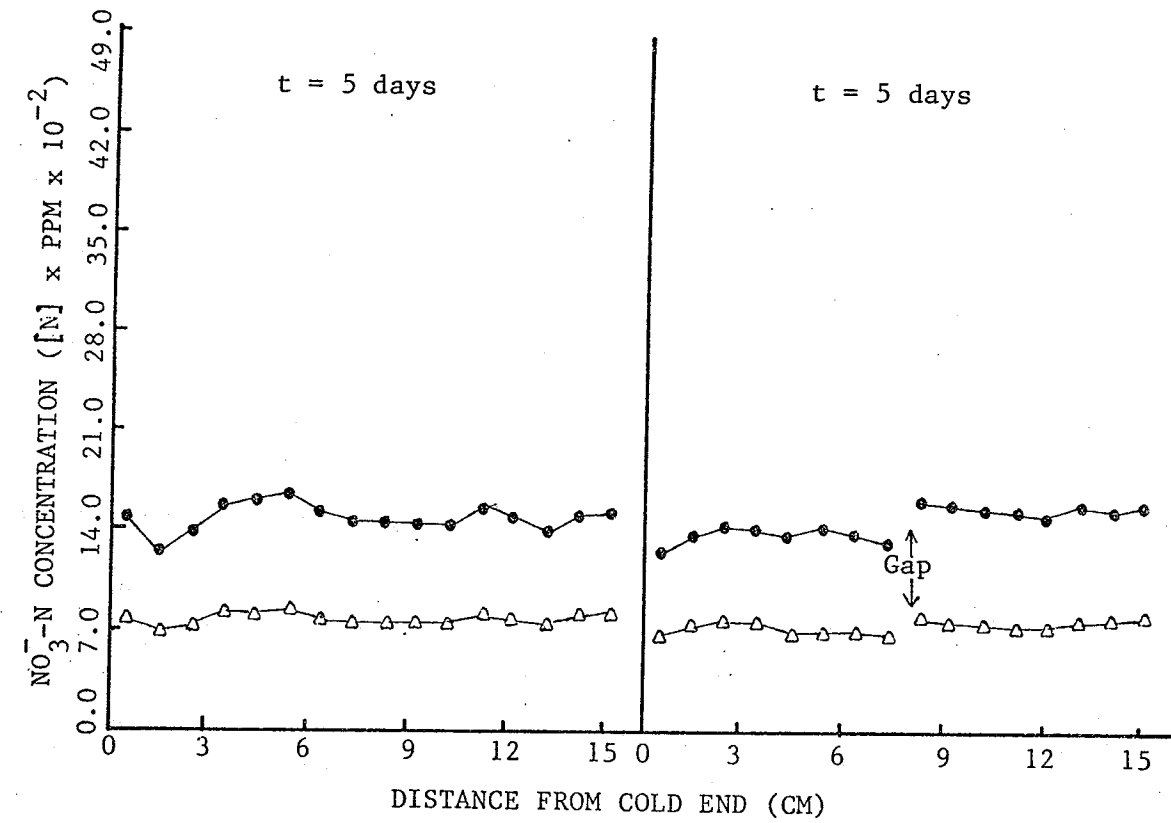


Fig. A6. Nitrate distribution in Ca(NO₃)₂ and KCl-treated soil columns with or without gap after 5 or 20 days of thermal treatment (initial H₂O = 32% and KCl = 10%).

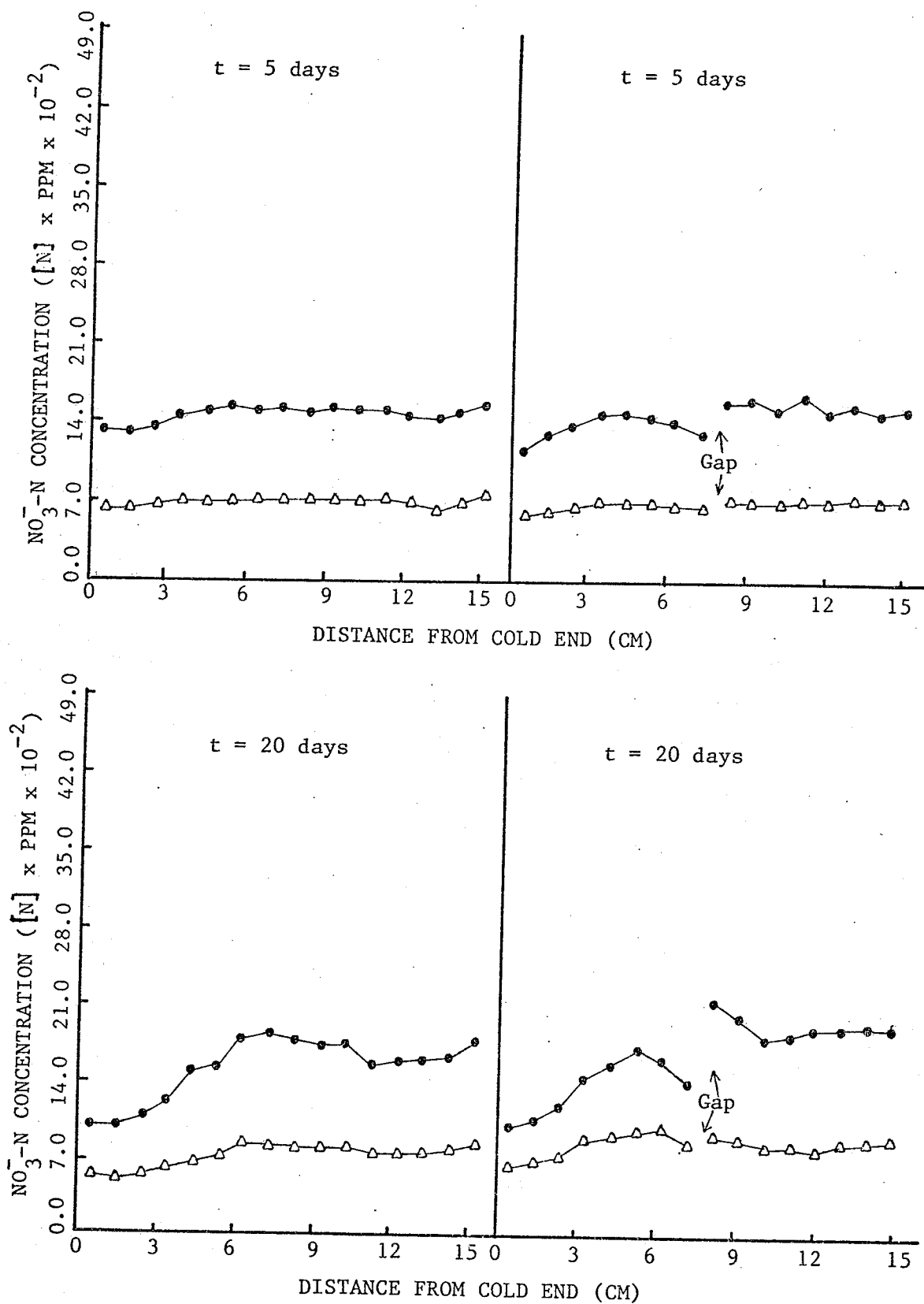


Fig. A7. Nitrate distribution in $\text{Ca}(\text{NO}_3)_2$ and KCl -treated soil columns with or without gap after 5 or 20 days of thermal treatment (initial $\text{H}_2\text{O} = 32\%$ and $\text{KCl} = 20\%$).

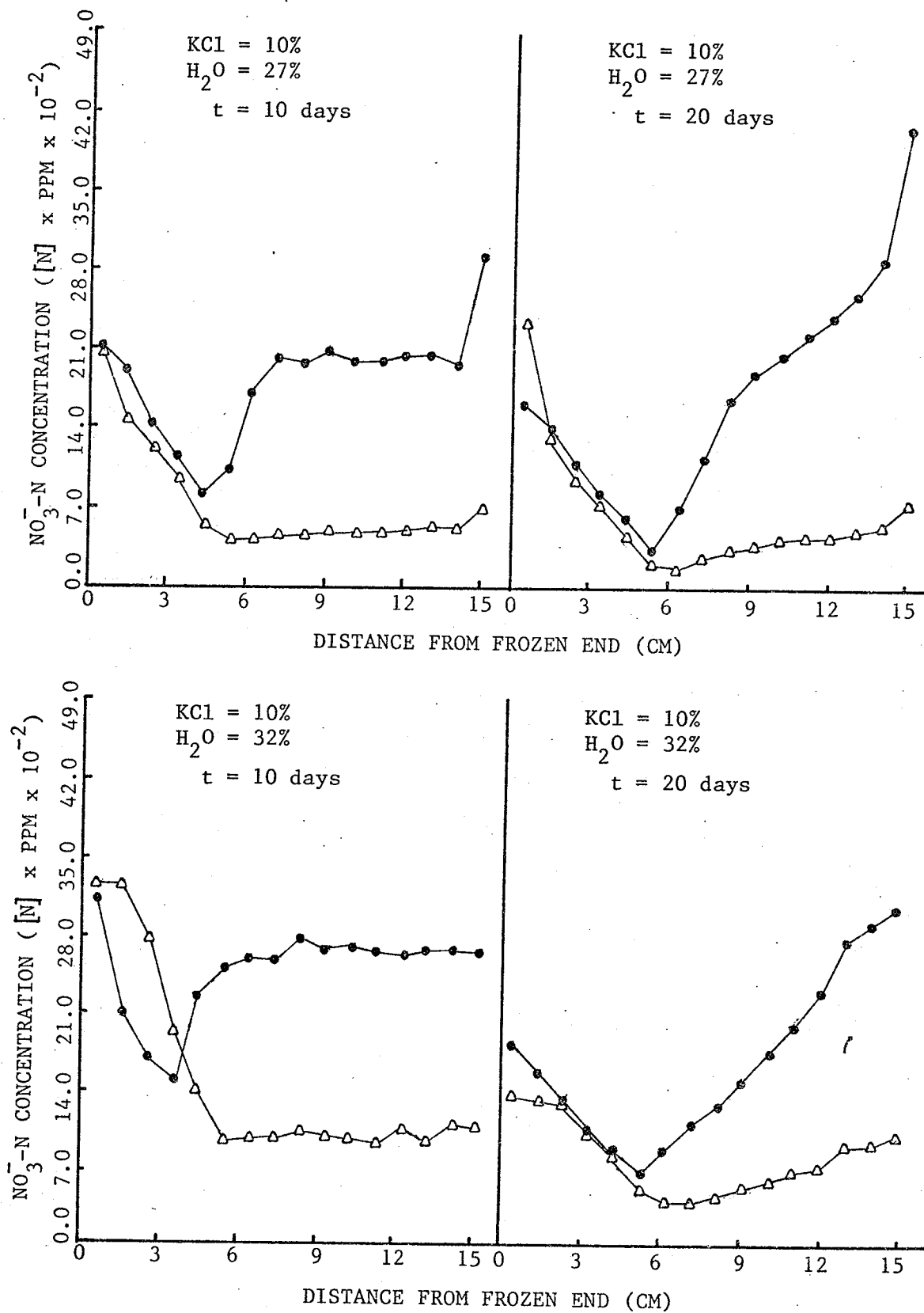


Fig. A8. Nitrate distribution in $\text{Ca}(\text{NO}_3)_2$ and KCl-treated soil columns with a frozen end.

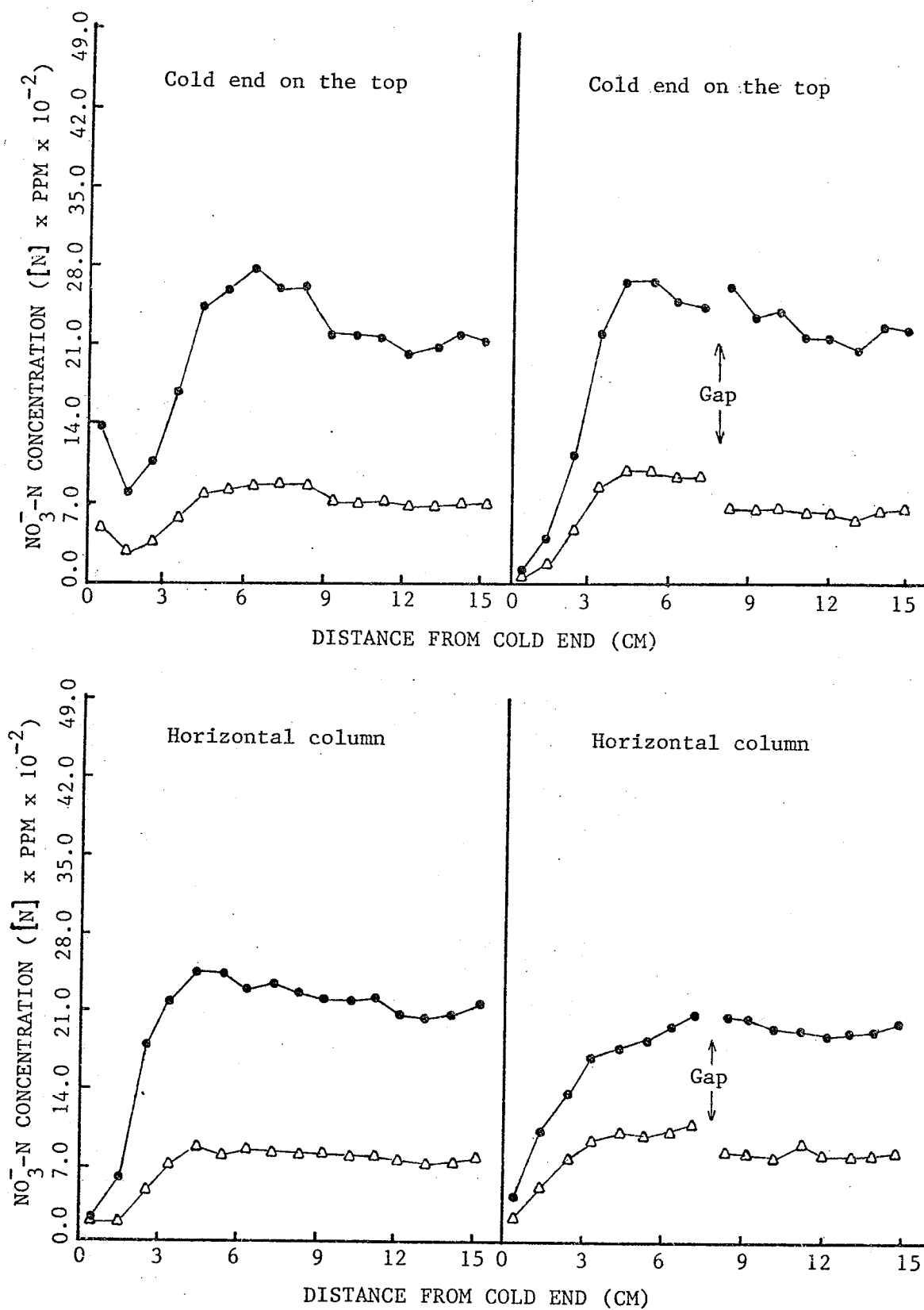


Fig. A9. Nitrate distribution in $\text{Ca}(\text{NO}_3)_2$ and KCl -treated soil columns after 10 days of thermal treatment (initial $\text{H}_2\text{O} = 27\%$ and $\text{KCl} = 10\%$).

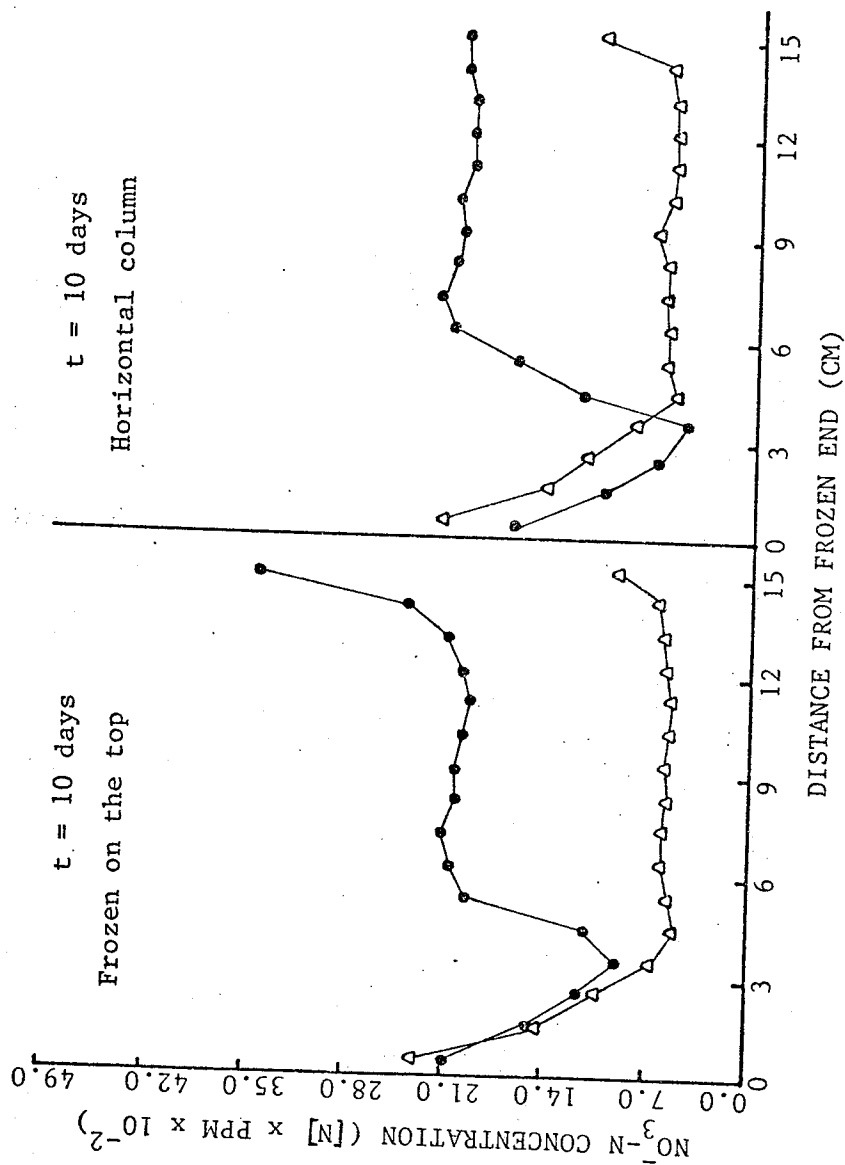


Fig. A10. Nitrate distribution in vertical and horizontal soil columns with one frozen end (initial $\text{H}_2\text{O} = 27\%$ and $\text{KCl} = 10\%$).

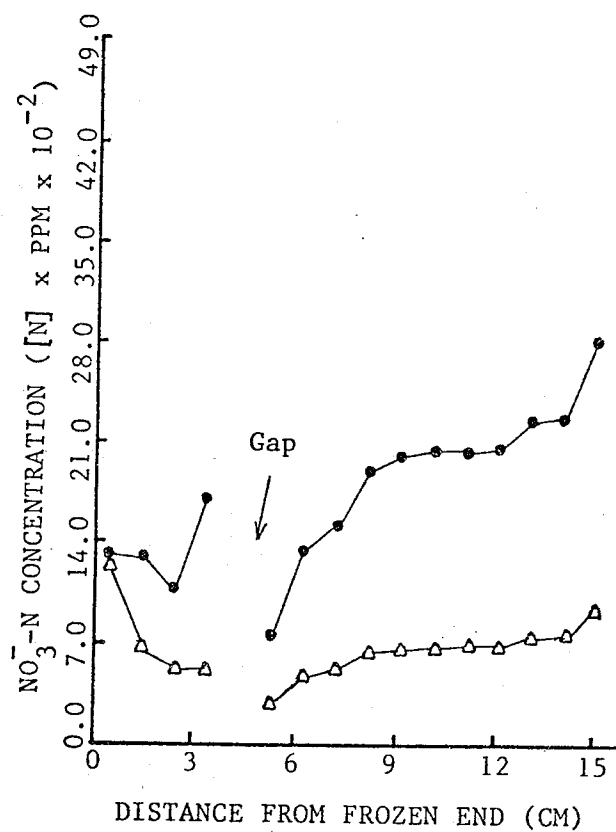


Fig. A11. Nitrate distribution in soil column with an 1-cm air gap and frozen bottom end (initial H₂O = 27% and KCl = 10%).

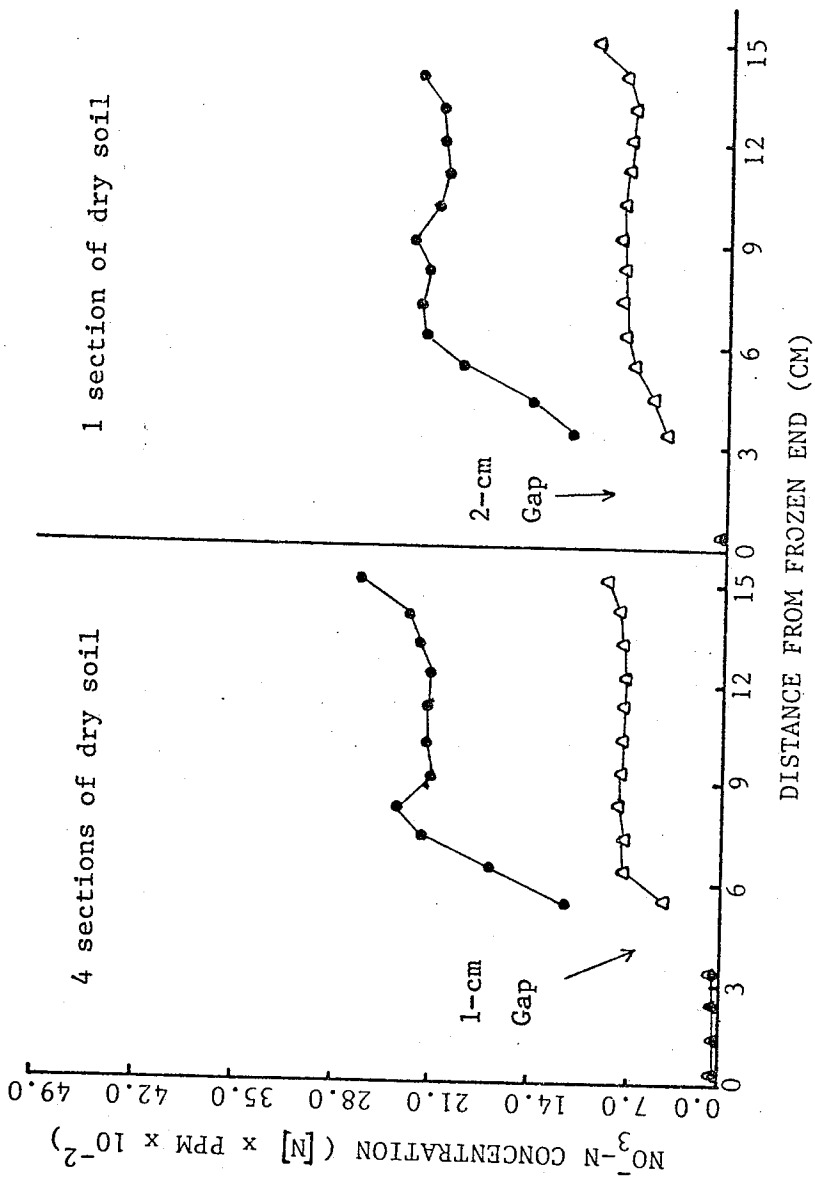


Fig. A12. Nitrate distribution in soil column with a 2-cm or 1-cm air gap and a frozen bottom end (initial H₂O = 27% and KCl = 10%).

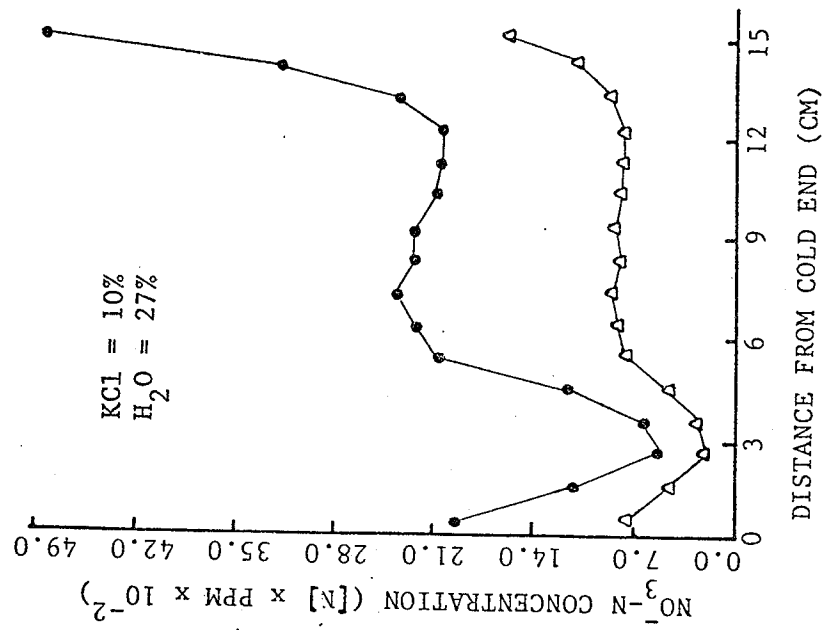


Fig. A14. Nitrate distribution in soil column with an open top after 10 days of thermal treatment.

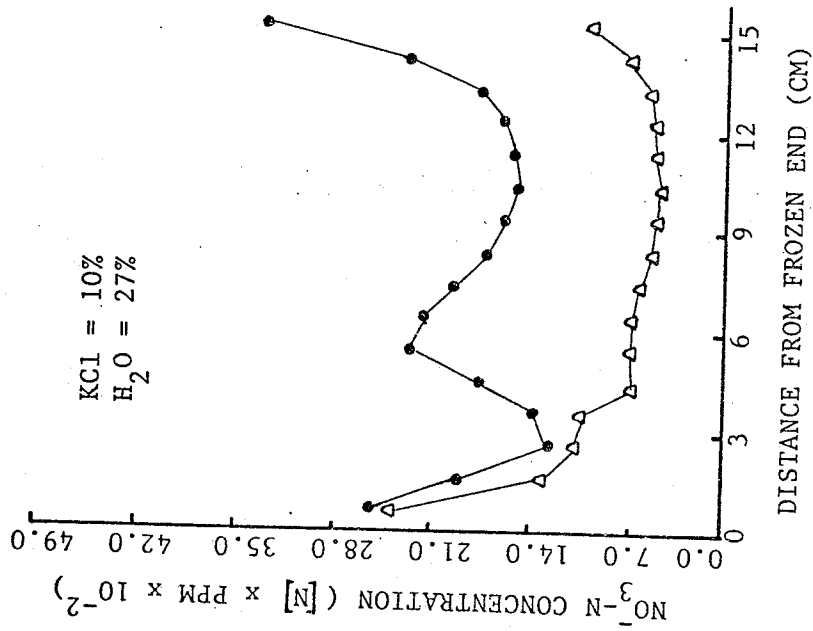


Fig. A13. Chloride distribution in soil column with top end frozen for first 10 days and bottom end frozen for second 10 days of thermal treatments.

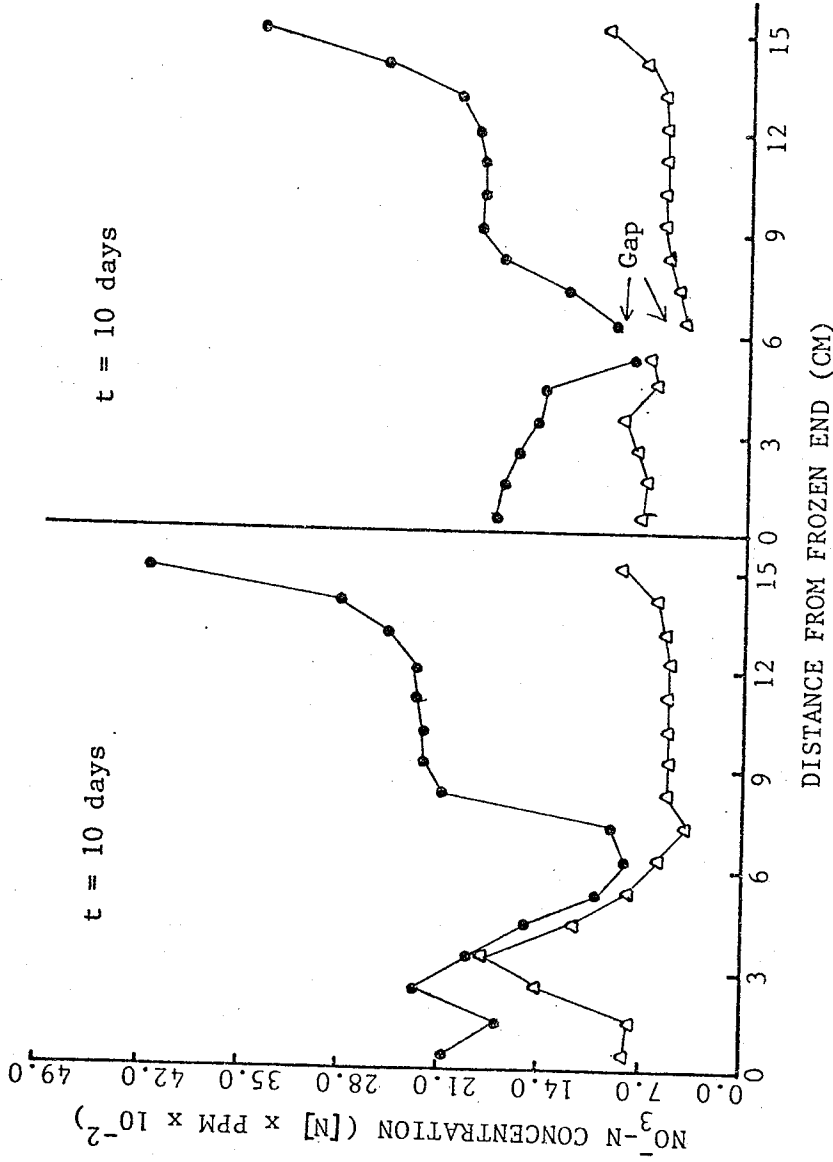


Fig. A15. Nitrate distribution in soil columns with an open and frozen top end and with or without gap (initial H₂O = 27% and KCl = 10%).

APPENDIX B

TABLE B1 DISTRIBUTION OF NO₃-N IN CHECK SOIL PROFILE OF ALMASIPPI LOAMY FINE SAND PLOTS

Date	Concentration (PPM-N)											
	Depth (cm)											
	15.2	30.4	45.6	60.8	76.0	91.2	106.4	121.6	136.8	151.0	166.2	181.2
Oct. 5, 1973	4.4	4.4	4.8	1.4	1.5	1.3	1.3	1.3	*	—	—	—
Mar. 1, 1974	12.6	8.7	2.3	2.4	1.9	2.0	—	—	—	—	—	—
Apr. 17, 1974	6.4	10.2	9.4	5.6	5.8	3.8	1.7	3.5	—	—	—	—
May 28, 1974	5.6	6.3	8.9	9.5	5.4	16.7	14.3	—	—	—	—	—
Jun. 10, 1974	5.7	5.2	3.7	2.7	1.6	1.4	2.3	4.5	7.7	—	—	—
Jul. 3, 1974	3.3	1.8	1.3	1.2	1.3	1.6	7.3	21.3	23.9	20.6	17.1	16.4
Jul. 11, 1974	15.2	6.5	2.1	1.8	1.3	2.0	5.0	8.1	11.0	6.7	9.2	15.8
Jul. 23, 1974	5.8	3.7	2.0	1.7	2.0	2.8	15.1	20.3	23.9	80.2	23.4	23.1
Aug. 26, 1974	7.7	12.4	2.9	1.6	1.5	2.5	9.2	12.8	21.2	64.2	146.8	5.8
Oct. 3, 1974	15.2	11.9	7.8	3.9	1.1	3.9	13.5	11.4	17.9	64.4	102.8	21.9
Oct. 31, 1974	7.7	7.3	4.3	3.9	1.0	3.0	8.5	13.6	18.8	7.8	11.1	261.0
Dec. 19, 1974	12.6	9.8	5.0	1.2	0.4	0.3	0.3	7.5	38.7	120.1	111.5	89.1
Feb. 19, 1975	12.0	5.7	0.8	1.1	1.2	1.8	2.3	2.7	2.3	4.8	4.7	6.2
Apr. 19, 1975	6.2	7.1	8.1	4.3	5.7	4.2	2.3	2.1	—	—	—	—

* No sample

TABLE B2 DISTRIBUTION OF Cl^- IN CHECK SOIL PROFILE OF ALMASIPPI LOAMY FINE SAND PLOTS

Date	Concentration (PPM- Cl^-)														
	Depth (cm)														
	15.2	30.4	45.6	60.8	76.0	91.2	106.4	121.6	136.8	151.0	166.2	181.2			
Oct. 5, 1973	21.1	8.3	18.7	3.8	0.0	0.0	0.0	0.0	*						
Mar. 1, 1974	23.0	13.1	9.6	5.6	5.7	74.8									
Apr. 17, 1974	0.0	15.6	10.5	2.1	2.1	9.8	4.7	26.1							
May 28, 1974	11.4	11.2	10.3	11.0	0.0	0.0	13.9								
Jun. 10, 1974	2.1	0.0	2.1	15.7	6.9	0.0	20.1	5.0	22.1						
Jul. 3, 1974	18.7	13.3	1.9	7.7	13.7	2.1	13.7	13.1	13.2	13.1	10.0	11.2			
Jul. 11, 1974	19.4	20.2	8.0	6.0	16.0	7.3	6.0	18.8	24.4	11.1	13.2	48.6			
Jul. 23, 1974	12.7	17.1	14.5	12.9	16.7	15.4	22.7	27.5	25.2	56.9	25.4	26.6			
Aug. 26, 1974	18.2	17.2	11.3	14.6	12.4	14.6	17.3	22.2	29.3	47.0	111.9	37.3			
Oct. 3, 1974	6.1	7.9	1.9	0.0	0.0	6.2	14.2	11.7	27.3	36.4	59.1	11.1			
Oct. 31, 1974	18.6	12.5	17.1	10.2	12.5	18.5	21.5	17.6	48.1	48.3	76.9	34.6			
Dec. 19, 1974	15.6	15.2	3.7	0.0	8.9	5.2	9.7	13.1	14.2	599.0	137.2	59.6			
Feb. 19, 1975	12.7	9.2	3.6	3.6	1.8	7.1	11.6	6.1	6.2	9.6	11.6	11.0			
Apr. 19, 1975	1.0	8.3	4.2	2.2	1.9	8.8	9.1	18.9							

* No sample

TABLE B3 DISTRIBUTION OF NO_3^- -N IN CHECK SOIL PROFILE
OF RED RIVER CLAY PLOT.

Date	Concentration (PPM-N)		
	15.2	30.4	45.6
	60.8	76.0	91.2
	106.4	121.6	
Nov. 2, 1973	90.5	94.3	119.3
	37.8	20.5	17.3
	13.4	11.3	
May 6, 1974	93.1	48.1	39.8
	44.5	35.8	13.0
	16.2	12.2	
Jun. 10, 1974	59.9	70.7	31.3
	55.0	58.4	37.5
	26.6	20.3	
Jun. 20, 1974	105.4	52.9	14.1
	18.6	9.7	7.5
	8.7	7.6	
Jul. 4, 1974	39.3	27.7	22.1
	22.6	26.6	26.7
	25.2	15.2	
Aug. 7, 1974	23.1	35.7	28.8
	19.4	16.3	19.1
	14.1	11.8	
Aug. 27, 1974	49.9	36.5	25.7
	26.6	34.7	35.7
	29.7	24.1	
Oct. 2, 1974	53.4	41.9	21.9
	16.6	14.0	14.6
	12.9	12.0	
Oct. 31, 1974	51.0	49.4	26.5
	25.4	30.5	24.4
	18.4	21.7	

APPENDIX C

List of Symbols

A	area
a,b	constant
C	volumetric heat capacity of soil
C_i	concentration of component i
D	diffusivity of substances
D_v	diffusivity of vapor
D	diffusivity of liquid water
D_{12}	apparent diffusion coefficient for components 1 and 2
E	internal energy
\bar{E}_i	specific internal energy of component i
F_i	force component
G_i	flux of component i
g	gravitation
H	relative humidity
\bar{H}_i	specific enthalpy of component i
h	hydraulic head of soil water
I	unit tensor
J	total flux of substance
j_E	diffusive energy flux
j_i	diffusion flux of component i
j_s	diffusive entropy flux
j_i^*	diffusion flux of component i with respect to solvent
K	hydraulic conductivity of soil water
L_x	distance between two points
L_e	acute distance between two points
l	height of soil column
P	pressure
Q	volumetric flow rate of fluid
q	heat flux
R	radius of the capillary tube
r	distance from the centre of the tube
S_k	Soret effect coefficient

s	specific entropy
T	temperature
T_o	average yearly temperature of the surface soil
T_1	amplitude of the surface temperature wave
t	time
V	volume
\bar{V}_i	volume of component i
X	weight fraction
x	distance
Z	valence of the ion
α	viscosity factor
β	thermal diffusion coefficient
γ	pore width factor
Γ	matric suction
ϵ	porosity
η	shear viscosity coefficient
κ	constant
λ	thermal conductivity
μ	chemical potential
μ'	chemical potential based on liquid phase
v	center of mass velocity
v_i	linear velocity of component i
v'	velocity of the flow medium
ρ	mass density
ρ_0	saturated vapor pressure
ρ_w	liquid water density
ρ_v	vapor density
σ	stress tensor
τ	temperature difference
ϕ_i	rate of production of component i
ϕ_s	rate of entropy production
ψ	bulk viscosity coefficient
χ	external force
ψ	total water potential
ω	frequency
Λ	thermal diffusivity

θ	volumetric water content
Ω	phenomenological coefficient
∇	gradient operator
∇_T	gradient at uniform temperature
∇^2	Laplacian operator